CHEN, WEI, Ph.D. Spectral Estimation for Random Processes with Stationary Increments. (2018)
Directed by Dr. Haimeng Zhang. 115 pp.

In studying a stationary random process on $\mathbb{R}$, the covariance function is commonly used to characterize the second-order spatial dependency. Through the inversion of Fourier transformation, its corresponding spectral density has been widely used to describe the periodical components and frequencies. When the process is with stationary dth increments, that is, when the resulting process after undertaken dth order of differences is stationary, the notion of structure function is put forward. Through the inversion formula, the spectrum can be represented by the structure function. In this dissertation, we first investigate the properties of the proposed Method of Moments structure function estimator, through which we obtain the spectral density function estimation of the underlying process. In particular, when the process is intrinsically stationary, which is also a process is with stationary increments of order 1, we derive the spectral density functions for commonly used variogram models. Furthermore, our proposed estimation method is applied to estimate the spectral density of power variogram models. All of the above results are supplemented via simulations and a real data analysis. Our results show that the proposed estimation method performs well in recovering the true spectral density function on various processes with stationary increments we considered.

SPECTRAL ESTIMATION FOR RANDOM PROCESSES WITH STATIONARY INCREMENTS

by

Wei Chen

A Dissertation Submitted to
the Faculty of The Graduate School at
The University of North Carolina at Greensboro
in Partial Fulfillment
of the Requirements for the Degree
Doctor of Philosophy

Greensboro
2018

Approved by

_____
Committee Chair

To the people who helped me find hope in the darkest of days!

APPROVAL PAGE

This dissertation written by Wei Chen has been approved by the following committee of the Faculty of The Graduate School at The University of North Carolina at Greensboro.

Committee Chair _____
Haimeng Zhang

Committee Members _____
Sat Gupta

_____
Scott Richter

_____
Greg Bell

_____
Xiaoli Gao

_____
Date of Acceptance by Committee

_____
Date of Final Oral Examination

ACKNOWLEDGMENTS

I do not have adequate words to express my appreciation and gratitude to Dr. Haimeng Zhang, who has been my advisor for almost six years. I was first attracted by his methodical lessons in Mississippi State University, which provided me a solid foundation in statistics. I completed my Masters degree under his patient guidance. After that, I followed Dr. Zhang to University of North Carolina without any doubt. This dissertation would not have been possible without his strong and enduring support. The countless stimulating discussions, his profound knowledge, and his heart-warming encouragement will stay in my memory and influence my future.

I would like to thank my dissertation committee members, Dr. Sat Gupta, Dr. Scott Richter, Dr. Xiaoli Gao and Dr. Greg Bell, for sharing their extremely valuable advices and comments to improve this dissertation. I warmly acknowledge the Department of Mathematics and Statistics for the financial support as a teaching assistant, which provided me a precious opportunity to teach as a lecturer. Especially, I want to thank for all help provided by the department during my pregnancy. Without their sweet arrangements and kindly help, I would be hard to continue on my study as a new mom of the two new born baby girls. Thanks to the support from all faculties, staffs and friends in the department, I have been extremely fortunate for the past four years to spend the most enjoyful and successful period of my life in UNCG.

A special and deepest gratitude to my parents, brother, my parents in law and dear friends for all their endless support, understanding and encouragement during theses years. Especially, thanks to my friend Zhifa Liu for helping me out of the difficult situation. Finally, I would like to express appreciation to my beloved husband,

Hang Wang who supported me in every possible way, and thanks to my adorable daughters, Jenny and Haley, their happy smile and every "Mom!" has driven me to this dissertation.

TABLE OF CONTENTS

Page

LIST OF TABLES viii

LIST OF FIGURES ix

CHAPTER

I. INTRODUCTION 1

I.1. Stochastic Process 1

I.2. Stationarity 1

I.3. Non-Stationarity 6

I.4. Covariance and Variogram Functions 12

II. SPECTRAL ANALYSIS AND LITERATURE REVIEW 17

II.1. Introduction to Spectral Analysis 17

II.2. Spectral Analysis under Stationarity 20

II.3. Spectral Analysis under Non-stationarity 29

II.4. Outline of This Dissertation 33

III. STRUCTURE FUNCTION AND ITS SPECTRAL DENSITY ESTIMATION 34

III.1. Introduction to Structure Function 34

III.2. Spectral Density Estimation Through Structure Function 44

III.3. Spectral Density Estimation Through Structure Function for Band-Limited Continuous Processes 61

III.4. Conclusions and Discussions 68

IV. SPECTRAL DENSITY FUNCTIONS AND ESTIMATION FOR POPULARLY USED VARIOGRAMS 70

IV.1. Spectral Densities for Commonly Used Variogram Functions 72

IV.2. Spectral Density Estimation for Power Variograms 80

V. DATA ANALYSIS 90

V.1. Introduction to the Graphical Procedure for Determining the Increment Order d 91

V.2. Spectral Estimation in Real Data Analysis 94

VI. FUTURE RESEARCH 100

BIBLIOGRAPHY 102

APPENDIX A. DERIVATION OF SPECTRAL DENSITIES THROUGH STRUCTURE FUNCTION $D_\tau(h)$ 106

LIST OF TABLES

Page

Table 1. Algorithm for Generating the Simulation Dataset. 27

Table 2. U.S. Monthly Single-Family Housing Starts, January 1964 - August 1978 (in Thousands) 95

Table 3. The Estimated Spectral Densities $\hat{f}(\omega)$ for the Points with High Powers and Their Corresponding Frequencies ω 98

LIST OF FIGURES

Page

Figure 1. White Noise Process with $\sigma^2 = 1$ 3

Figure 2. A Standard Brownian Motion Process. 8

Figure 3. Speech Recording of the Syllable $aaa \cdots hhh$ Sampled at $10,000$ Points Per Second with $n = 1020$ Points. 18

Figure 4. Plot for a Process of A Linear Combination of Two Cosine Curves. 20

Figure 5. Spectral Analysis for Detecting the Periodicities of the Above Process. 20

Figure 6. Plot for Seires of Semi-annual Sunspot Activities for $n = 459$ Time Periods. 23

Figure 7. Periodogram Analysis Showing Periodicities for the Above Example. 24

Figure 8. Estimated and Theoretical Covariance and Variogram Values under Stationarity. 28

Figure 9. Estimated and Theoretical Covariance and Variogram Values under Stationarity with Added Linear Trend. 30

Figure 10. Estimated and Theoretical Covariance and Variogram Values under Stationarity with Added Quadratic Trend. 31

Figure 11. Comparison of the Estimated and Theoretical Values for $D_\tau(h)$ under Stationarity Together with Estimations of Covariance and Variogram Functions. 43

Figure 12. Comparison of the Estimated and Theoretical Values for $D_\tau(h)$ under Stationarity with An Added Linear Trend, Together with Estimations of Covariance and Variogram Functions. 43

Figure 13. Comparison of the Estimated and Theoretical Values for $D_\tau(h)$ under Stationarity with An Added Quadratic Trend, Together with Estimations of Covariance and Variogram Functions. 44

Figure 14. Illustration of Aliasing Effect. 46

Figure 15. Comparison of the Estimated and Theoretical Spectral Density Values under Stationarity. 57

Figure 16. Comparison of the Estimated and Theoretical Spectral Density Values under Stationarity, After Removing the Aliasing Effect. 58

Figure 17. Comparison of the Estimated and Theoretical Spectral Density under Stationarity with an Added Linear Trend. 58

Figure 18. Comparison of the Estimated and Theoretical Spectral Density Values under Stationarity with an Added Linear Trend, After Removing the Aliasing Effect. 59

Figure 19. Comparison of the Estimated and Theoretical Spectral Density Values under Stationarity with an Added Quadratic Trend.. 59

Figure 20. Comparison of the Estimated and Theoretical Spectral Density Values under Stationarity with an Added Quadratic Trend, After Removing the Aliasing Effect. 60

Figure 21. The Estimated and Theoretical Values of a Band-limited Spectral Density for Stationary Process with an Added Linear Trend, with $\delta = 1$. 66

Figure 22. The Estimated and Theoretical Values of a Band-limited Spectral Density for Stationary Process with an Added Linear Trend, with $\delta = 1/2$. 67

Figure 23. The Estimated and Theoretical Values of a Band-limited Spectral Density for Stationary Process with an Added Linear Trend, with $\delta = 2$. 67

Figure 24. The Estimated and Theoretical Values of a Band-limited Spectral Density for Stationary Process with an Added Linear Trend, with $\delta = 2$, After Removing the Aliasing Effect. 68

Figure 25. Estimated and Theoretical Spectral Density for Power Variogram with $\alpha = 1/2$ and $\tau = 2$. 84

Figure 26. Estimated and Theoretical Spectral Density for Power Variogram After Removing Aliasing Effect with $\alpha = 1/2$ and $\tau = 2$. 85

Figure 27. Estimated and Theoretical Spectral Density for Power Variogram with $\alpha = 3/2$ and $\tau = 2$. 86

Figure 28. Estimated and Theoretical Spectral Density for Power Variogram with $\alpha = 3/2$ and $\tau = 2$. 86

Figure 29. Estimated and Theoretical Spectral Density for Brownian Motion Process with $\tau = 2$. 88

Figure 30. Estimated and Theoretical Spectral Density for Brownian Motion Process After Removing the Aliasing Effect with $\tau = 2$. 89

Figure 31. Scaled Semivariogram Estimation versus h for Determining $d = 0$ with the Expected Semivariogram and Confidence Band. 96

Figure 32. Scaled Linvariogram Estimation versus h for Determining $d = 1$ with the Expected Linvariogram and Confidence Band. 97

Figure 33. Scaled Quadvariogram Estimation versus h for Determining $d = 2$ with the Expected Semivariogram and Confidence Band. 97

Figure 34. Estimated Spectral Density $\hat{f}(\omega)$ for U.S. Monthly Housing Starts, January 1964-August 1978. 98

CHAPTER I

INTRODUCTION

In this chapter, we will give a brief introduction to some basic concepts in spatial statistics. Specifically, we will first introduce the concepts of stationarity (including strong and weak stationarity) as well as their relationships and non-stationarity (including intrinsic stationarity and stationary increments of dth order) with their relationships as well. In addition, the covariance and variogram functions will be introduced under stationarity and non-stationarity.

I.1. Stochastic Process

Let $\mathbb{R} = (-\infty, \infty)$. A Stochastic (Random) process in $\mathbb{R}$ is a collection of random variables with indexing on $\mathbb{R}$ or a subset of $\mathbb{R}$. There are many examples of stochastic processes in statistical analysis. An observed time series $\{Z(t) : t \in \mathbb{R}\}$ refers to a (discrete) stochastic process. Another well-known example is the so-called Bernoulli Process. It is one of the simplest stochastic processes, consisting of a collection of independent and identically distributed ($i.i.d.$) random variables with probability of p for the value 1 and probability of $1 - p$ for the value 0.

As Cryer and Kellet (1991)[CK91] mentioned, "to make statistical inferences about the structure of a stochastic process on the basis of an observed record (sequence) of the process, we must usually make some simplified assumptions about that structure, and the simplest assumption is stationarity."

I.2. Stationarity

One of the important criteria to classify a stochastic process is its stationarity. The analysis of stationary processes having the assumptions which depend only

on moments, is much simpler than the ones for non-stationary processes, and provides more information for prediction of future behaviors. Therefore, in statistics, non-stationarity is often transformed to be stationarity for further spectral analysis. However, in many real-life situations, the assumptions for stationarity in strict sense are too strong and most processes do not satisfy them (Nason, 2006[Nas06]). The second-order stationarity with weaker assumptions is normally considered and throughtout this dissertation, weak stationarity is called just "stationarity" for short.

I.2.1. Strong (Strict) Stationarity

Let $X(t)$ be a stochastic process, and let the joint distribution of $X(t)$ at $(t_1, t_2, \cdots, t_n)$ be expressed as $F_X\left(X(t_1), X(t_2), \cdots, X(t_n)\right)$. Then $X(t)$ is a strong stationary process if, for any finite number n points $t_1, t_2, ...t_n$ and any $h > 0$,

$$F_X\left(X(t_1), X(t_2), \cdots, X(t_n)\right) = F_X\left(X(t_1 + h), X(t_2 + h), \cdots, X(s_n + h)\right).$$

In other words, a strong (strict) stationary process in statistics, is a stochastic process whose finite-dimensional joint probability distribution does not change when the time is shifted. Consequently, the parameters such as mean and variance, if they exist, also remain constant over time.

The assumptions of strict stationarity is normally too strong, and it is often too restrictive for spatial applications. In addition, it is difficult to verify, and there is an uncertainty with the existence of moments. Another commonly used (but weaker) assumption is weak stationarity.

I.2.2. Weak (Second Order) Stationarity

A random process $\{X(t); t \in \mathbb{R}\}$ is weakly stationary (or stationary), if

$$E(X(t)) = \mu, \ \ \forall t \in \mathbb{R},$$

$$E(X^2(t)) < \infty, \ \ \forall t \in \mathbb{R},$$

$$Cov(X(t), X(t+h)) = C(h), \ \ \forall t, \forall h \in \mathbb{R}.$$

In other words, a random process $X(t)$ is stationary if it has constant first moment (mean), finite second moment, and that the covariance function $C(\cdot)$ of the process at two locations depends only on the displacement h. Obviously,

$$Var(X(t)) = Cov(X(t), X(t)) = C(0).$$

A simple example of stationary process is a White Noise Process. A White Noise Process is a stochastic process with uncorrelated ($Cov(X(t), X(s)) = 0$ if $t \neq s$) random variables which have zero mean and a finite common variance σ^2. Obviously, it is a stationary process. Figure I.1 shows a white noise process with $\sigma^2 = 1$.

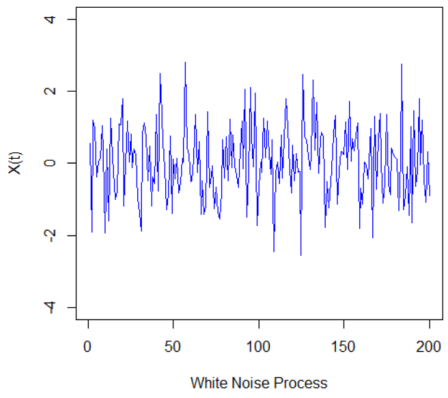

Figure 1. White Noise Process with $\sigma^2 = 1$

I.2.3. Relationship between Strong and Weak Stationarity

If the random process $\{X(t), t \in \mathbb{R}\}$ is strongly stationary with finite second moment, then $\{X(t), t \in \mathbb{R}\}$ is weakly stationary. In other words, if the second moment exists, then strong stationarity implies weak stationarity. The simple justification is given below.

Since the random process $\{X(t), t \in \mathbb{R}\}$ is a strongly stationary process, then for any n, the joint distribution of $(X(t_1), X(t_2), \cdots, X(t_n))$ is shift-invariant. In particular, the joint distribution of $(X(t_1), X(t_2))$ is the same as the joint distribution of $(X(t_1 + h), X(t_2 + h))$, for all t_1, t_2, and $h \in \mathbb{R}$. Since $\{X(t), t \in \mathbb{R}\}$ has finite second moment, and we have

$$E(X(t_1)) = E(X(t_2)) = E(X(t)) = \mu, \ \ \forall t,$$

$$Cov(X(t_1), X(t_2)) = Cov(X(t_1 + h), X(t_2 + h)) = C(h), \ \ \forall t_1, t_2, h.$$

So clearly, $Cov(X(t), X(t + h))$ doesn't depend on t. Therefore, the process $\{X(t), t \in \mathbb{R}\}$ is also a weakly stationary process.

Note that the existence of the second moment is critical for the above conclusion. As an example, if the finite-dimensional distribution of a stochastic process follows a multivariate Cauchy distribution and is assumed to be shift-invariant (so that the stochastic process is strongly stationary). However, it may not be weakly stationary since the Cauchy distribution has both undefined mean and variance.

On the other hand, weak stationarity doesn't imply strong stationarity, unless it is a Gaussian stochastic process. Here we have an example of a weak stationary process, but it is not a strongly stationary process. Let $\{X(t), t \in \mathbb{Z}\}$ is a sequence of random variables (a stochastic random process) defined as

$$X(t) = \begin{cases} Y(t), & \text{if } t \text{ is even,} \\ \frac{1}{\sqrt{2}}\left(Y^2(t) - 1\right), & \text{if } t \text{ is odd,} \end{cases}$$

where $Y(t) \overset{i.i.d.}{\sim} N(0, 1)$.

The above process gives:

$$E(X(t)) = \begin{cases} E(Y(t)) = 0, & \text{if } t \text{ is even,} \\ \frac{1}{\sqrt{2}} E\left(Y^2(t) - 1\right) = 0, & \text{if } t \text{ is odd,} \end{cases}$$

$$Var(X(t)) = \begin{cases} Var(Y(t)) = 1, & \text{if } t \text{ is even,} \\ \frac{1}{2} Var(Y^2(t) - 1) = 1, & \text{if } t \text{ is odd.} \end{cases}$$

Since $X(t)$ and $X(t+h)$ are independent random variables, we have

$$Cov(X(t), X(t+h)) = 0, \forall k.$$

Therefore, the stochastic process $\{X(t), t \in \mathbb{Z}\}$ is a weakly stationary process.

Now we note that

$$P(X(t) \leq 0) = \begin{cases} P(Y(t) \leq 0) = 0.5, & \text{when } t \text{ is even.} \\ P\left(\frac{1}{\sqrt{2}}(Y^2(t) - 1) \leq 0\right) = P(Y^2(t) \leq 1) = 0.6826, & \text{when } t \text{ is odd.} \end{cases}$$

Therefore, it is not identically distributed, and thus not strongly stationary.

But a Gaussian stationary process is an exception. The Gaussian process is one of the most widely used stochastic processes and one of the properties of such a process making it primarily popular is that a Gaussian process is completely determined by its mean and covariance functions.

A real-valued stochastic process $X(t), t \in \mathbb{R}$ is a Gaussian process if its finite-dimensional distributions have a multivariate normal distribution. For a stationary Gaussian process $X(t)$ with covariance function $C(h)$, we have $X(t) \sim N(\mu, C(0))$ for all t, and $(X(t+h), X(t))'$ has a bivariate normal distribution with covariance matrix given as follows, for all t and h,

$$\begin{bmatrix} C(0) & C(h) \\ C(h) & C(0) \end{bmatrix},$$

then the Gaussian stationary process is uniquely determined by its first and second moments, which means it is also a strongly stationary process.

I.3. Non-Stationarity

The assumption of stationarity is too strict most of the time in practice, and usually cannot be satisfied. It is necessary to seek for statistical methods to investigate non-stationary random processes. Here we discuss intrinsic stationarity and random processes with stationary increments.

I.3.1. Intrinsic Stationarity

A random process $\{X(t) : t \in \mathbb{R}\}$ is intrinsically stationary, if we have

$$E(X(t)) = \mu, \ \ \forall t \in \mathbb{R},$$

$$Var(X(t+h) - X(t)) = 2\gamma(h), \ \ \forall t, h \in \mathbb{R},$$

where $2\gamma(\cdot)$ is termed as the variogram function.

In other words, a random process $\{X(t) : t \in \mathbb{R}\}$ is intrinsically stationary if it has constant first moment (mean) and the variance of the difference between the values at any two time points or locations $t, t+h$ depends only on h, the displacement.

A one-dimensional (standard) Brownian Motion process $\{B(t), t \geq 0\}$ is a real-valued stochastic process with mean $\mu = 0$, and covariance function $Cov(B(t+h), B(t)) = \sigma^2 \min(t+h, t)$, which is not a function of only the displacement, indicating that this process is not a weakly stationary process. However,

$$
\begin{aligned}
&Var(B(t+h) - B(t)) \\
&= Cov(B(t+h), B(t+h)) + Cov(B(t), B(t)) - 2Cov(B(t+h), B(t)) \\
&= \sigma^2 \min(t+h, t+h) + \sigma^2 \min(t, t) - 2\sigma^2 \min(t+h, t) \\
&= \sigma^2(t+h) + \sigma^2 t - 2\sigma^2 \min(t+h, t).
\end{aligned}
$$

Therefore, the variance of the difference between two locations is given as,

$$
\begin{aligned}
Var(B(t+h) - B(t)) &= \begin{cases} \sigma^2(t+h+t-2t) = \sigma^2(h), & \forall h \geq 0, \\ \sigma^2(t+h+t-2t-2h) = \sigma^2(-h), & \forall h < 0, \end{cases} \\
&= \sigma^2 |h|, \quad \forall h \in \mathbb{R},
\end{aligned}
$$

It is a function of only the displacement h. Hence, the standard Brownian Motion process is intrinsically stationary. Figure I.2 shows a realization of this process.

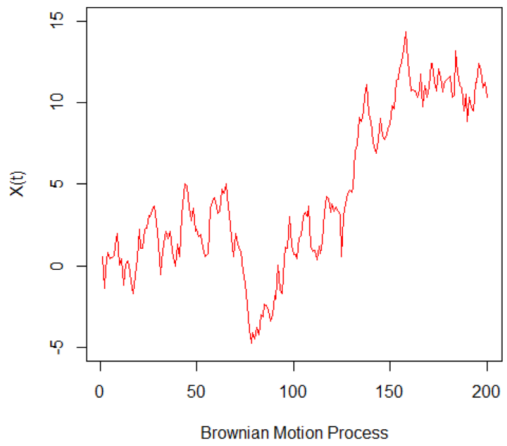

Figure 2. A Standard Brownian Motion Process.

A generalization of the variogram function from Brownian Motion is the Power Model, with the variogram function given by $2\gamma(h) = |h|^{\alpha}, (0 < \alpha < 2)$. Although the variogram $2\gamma(h)$ exists, there is no associated stationary covariance function, i.e. $C(h)$ does not depend only on the displacement h. Therefore, although the random process with power model variogram function is intrinsically stationary, it is not a weakly stationary process which implies that intrinsic stationarity does not imply weak stationarity. On the other hand, a weakly stationary process is an intrinsically stationary process. This can be easily justified. Let $\{X(t), t \in \mathbb{R}\}$ be a weakly stationary process with constant mean μ and covariance function $C(h)$, then the variogram function is given as follows.

$$\begin{aligned} 2\gamma(h) &= Var(X(t+h) - X(t)) \\ &= Var(X(t+h)) + Var(X(t)) - 2Cov(X(t+h), X(t)) \\ &= C(0) + C(0) - 2C(h) = 2C(0) - 2C(h), \text{ a function of } h, \end{aligned}$$

therefore, $X(t)$ is also a intrinsically stationary process.

I.3.2. Random Process with dth Order Stationary Increments

According to Yaglom(1958)[Yag58], for a random process $\{X(t), t \in \mathbb{R}\}$,

$$\Delta_\tau^{(d)} X(t) = \sum_{k=0}^{d} (-1)^k \binom{d}{k} X(t - k\tau),$$

is called the dth increments of $X(t)$ with the step size $\tau > 0$.

More specifically, a random dth increments $\Delta_\tau^{(d)} X(t)$ is called stationary (in the wide sense) if the expectations

$$E(\Delta_\tau^{(d)} X(t)) = c^{(n)}(\tau) = c\tau^n,$$

$$E(\Delta_\tau^{(d)} X(t+h))(\Delta_\tau^{(d)} X(t)) = D^{(d)}(t, \tau),$$

exist for all t, h, τ, and don't depend on t, where c is a constant.

In particular, when $d = 0$, we obtain the usual weakly stationary random processes, and when $d = 1$, and if the first order increment $\Delta_\tau^{(1)} X(t) = X(t) - X(t-\tau)$ is stationary, $X(t)$ is called a process with stationary increments of order 1. Similarly, when $d = 2$, and if the second order increments $\Delta_\tau^{(2)} X(t) = X(t) - 2X(t-\tau) + X(t-2\tau)$ is stationary, then $X(t)$ is called a process with stationary increments of order 2.

Note that the second order increment is just an additional increment based on the first increment, i.e., let $Y(t)$ represent $\Delta_\tau^{(1)} X(t)$, and $U(t)$ represent $\Delta_\tau^{(2)} X(t)$,

$$\begin{aligned} U(t) &= Y(t) - Y(t-\tau) \\ &= [X(t) - X(t-\tau)] - [X(t-\tau) - X(t-\tau-\tau)] \\ &= X(t) - 2X(t-\tau) + X(t-2\tau). \end{aligned}$$

In this dissertation, we will focus on two random processes with stationary increments of order 1 and 2 in our simulations. These processes were constructed

by adding the corresponding linear trend (order 1) and quadratic trend (order 2), respectively. The intrinsically stationary process, which is a more general process of stationary increments of order 1, is also considered in Chapter 4. Here we provide the propositions to justify these.

Proposition 1.1: A stationary process with an added linear trend is a stationary increment process with order 1. PROOF. Consider the process $X(t) = a + bt + S(t), a, b \in \mathbb{R}$, where $S(t)$ is a stationary process with constant mean μ. We need to show that the first increment $Y(t) = X(t) - X(t-\tau)$ is stationary.

$$\begin{aligned} Y(t) &= X(t) - X(t-\tau) \\ &= a + bt + S(t) - [a + b(t-\tau) + S(t-\tau)] \\ &= S(t) - S(t-\tau) + b\tau, \end{aligned}$$

$$\text{and} \quad E[Y(t)] = E[S(t) - S(t-\tau) + b\tau] = b\tau, \text{ constant with a fixed } \tau$$

$$\begin{aligned} Var[Y(t)] &= Var[S(t) - S(t-\tau) + b\tau] \\ &= Var[S(t)] + Var[S(t-\tau)] - Cov[[S(t), S(t-\tau)]. \end{aligned}$$

Since $S(t)$ is stationary, then $E(S^2(t)) < \infty$, and therefore, $Var[Y(t)] < \infty$, which means the second moment $E(Y^2(t)) < \infty$, then

$$\begin{aligned} &Cov[Y(t), Y(t+h)] \\ &= Cov[S(t) - S(t-\tau) + b\tau,\ S(t+h) - S(t+h-\tau) + b\tau] \\ &= Cov[S(t), S(t+h)] - Cov[S(t), S(t+h-\tau)] - Cov[S(t-\tau), S(t+h)] \\ &\quad + Cov[S(t-\tau), S(t+h-\tau)] + (b\tau)^2 \\ &= 2C(h) - C(h-\tau) + C(h+\tau) + (b\tau)^2. \end{aligned}$$

That is, $Cov[Y(t), Y(t+h)]$ is a function of the displacement h, with a fixed $\tau > 0$. Combined together, $Y(t)$ is a process satisfying all three conditions for a stationary process, and then our proposition follows.

Proposition 1.2: A stationary process with an added quadratic trend is a process with stationary increments of order 2. PROOF. Consider the process $X(t) = a+bt+ct^2+S(t), a, b, c \in \mathbb{R}$, where $S(t)$ is a stationary process with constant mean μ. Then we need to show that the second increment $U(t) = X(t)-2X(t-\tau)+X(t-2\tau)$ is stationary.

$$\begin{aligned} U(t) &= X(t) - 2X(t-\tau) + X(t-2\tau) \\ &= a + bt + ct^2 + S(t) - 2[a + b(t-\tau) + c(t-\tau)^2 + S(t-\tau)] \\ &\quad + [a + b(t-2\tau) + c(t-2\tau)^2 + S(t-2\tau)] \\ &= S(t) - 2S(t-\tau) + S(t-2\tau) + 2c\tau^2, \end{aligned}$$

$$\begin{aligned} \text{and} \quad E[U(t)] &= E[S(t) - 2S(t-\tau) + S(t-2\tau) + 2c\tau^2] \\ &= 2c\tau^2. \ (S(t) \text{ is stationary process with constant mean } \mu) \end{aligned}$$

Then $U(t)$ has a constant mean $2c\tau^2$, with a fixed τ. And since $S(t)$ is stationary, then $Var[U(t)] < \infty$, which means $E(U^2(t)) < \infty$.

$$\begin{aligned} &Cov[U(t), U(t+h)] \\ &= Cov[S(t) - 2S(t-\tau) + S(t-2\tau) + 2c\tau^2, \\ &\quad S(t+h) - 2S(t+h-\tau) + S(t+h-2\tau) + 2c\tau^2] \\ &= 6C(h) - 4C(h-\tau) - 4C(h+\tau) + C(h-2\tau) + C(h+2\tau) + 4c^2\tau^4. \end{aligned}$$

which is a function of the displacement h, with a fixed $\tau > 0$, concluding the proof.

I.4. Covariance and Variogram Functions

I.4.1. Covariance Function

In spatial statistics, the covariance function describes the spatial dependency of a random process. For a stochastic process $X(t)$ on a domain D, a covariance function is defined as the covariance of process at the two time points or locations.

Recall that if $\{X(t) : t \in \mathbb{R}\}$, is a stationary process with constant mean μ, then $Cov[X(t), X(t+h)] = C(h) = C(-h)$ is defined as the covariance function $C(\cdot)$ for all h, which can be expressed as follows

$$Cov[X(t), X(t+h)] = E[X(t) - \mu][X(t+h) - \mu].$$

A covariance function $C(\cdot)$ of the stationary process $X(t)$ must be positive definite, that is, for any n and any real numbers $a_i, i = 1, 2, \cdots, n$ and locations $t_i, i = 1, 2, \cdots, n$, one has to satisfy the following condition

$$\sum_{i=1}^{n} \sum_{j=1}^{n} a_i a_j C(t_i - t_j) \geq 0.$$

With this restriction, we note that for any linear combination of finite random variables $Y = \sum_{i=1}^{n} a_i X(t_i)$ at n locations $t_i, i = 1, 2, \cdots, n$,

$$Var\left(\sum_{i=1}^{n} a_i X(t_i)\right) = \sum_{i,j=1}^{n} a_i a_j C(t_i - t_j) \geq 0.$$

One of the most commonly used covariance function models in statistics is the Matérn covariance functions, given by Rasmussen and Williams (2006)[RW06]:

$$k_{\text{matern}}(r) = \frac{2^{1-\nu}}{\Gamma(\nu)} \left(\frac{\sqrt{2\nu} r}{\ell}\right)^{\nu} K_{\nu}\left(\frac{\sqrt{2\nu} r}{\ell}\right),$$

It has the smoothness parameter $\nu > 0$ and the distance parameter $\ell > 0$ (Minasny and McBratney, 2005)[MM05] and K_ν as a modified Bessel function developed by Abramowitz and Stegun (1965)[AS65].

The Matérn model is commonly used in spatial statistics due to its great flexibility with the smoothness parameter ν. When ν is small ($\nu \to 0$), it implies that the spatial process is rough, and when it is large ($\nu \to \infty$) that the process is smooth (Minasny and McBratney, 2005)[MM05].

Since the Matérn covariance functions only depend on the displacement between points, then if a random process has a constant mean and Matérn covariance function, then it is stationary.

The Matérn covariance functions become especially simple when ν is half-integer: $\nu = p + 1/2$, where p is a non-negative integer. In this case, the covariance function is a product of an exponential and a polynomial of order p, the general expression was derived and given by Abramowitz and Stegun(1965)[AS65]:

$$k_{\nu=p+1/2}(r) = exp\left(-\frac{\sqrt{2\nu}r}{\ell}\right)\frac{\Gamma(p+1)}{\Gamma(2p+1)}\sum_{i=0}^{p}\frac{(p+i)!}{i!(p-i)!}\left(\frac{\sqrt{8\nu}r}{\ell}\right)^{p-i}.$$

When $\nu = 1/2$, the process is actually an exponential model, but for $\nu > 7/2$, Rasmussen and Williams (2006)[RW06] stated that "in the absence of explicit prior knowledge about the existence of higher order derivatives, it is probably very hard from finite noisy training examples to distinguish between values of $\nu \geq 7/2$" .

With the above formula, we list the following three special cases with $\nu = 1/2$, $3/2$, and $5/2$, which are most of interest and commonly used in spatial statistics, geostatistics, machine learning and other fields.

$$k_{\nu=1/2}(r) = \exp\left(-\frac{r}{\ell}\right).$$
$$k_{\nu=3/2}(r) = \left(1 + \frac{\sqrt{3}r}{\ell}\right) exp\left(-\frac{\sqrt{3}r}{\ell}\right).$$
$$k_{\nu=5/2}(r) = \left(1 + \frac{\sqrt{5}r}{\ell} + \frac{5r^2}{3\ell^2}\right) exp\left(-\frac{\sqrt{5}r}{\ell}\right).$$

We will use Matérn covariance functions with $\nu = 3/2$ and $\ell = 1$ for further simulations, under which the covariance function is given by

$$C(h) = (1 + \sqrt{3}|h|)e^{-\sqrt{3}|h|}, \quad h \in \mathbb{R}.$$

I.4.2. Variogram Function

The variogram function was proposed by Matheron (1973)[Mat73] as an alternative measure to the covariance function. It is defined as the variance of the difference between two values at two time points or locations. When the process $X(t)$ is intrinsically stationary, $E[X(t)] = \mu$ constant.

$$2\gamma(h) = Var[X(t+h) - X(t)].$$

Here $\gamma(h)$ is called the semivariogram, a function of the displacement h. Moreover, if $\{X(t)\}$ is stationary and $C(h)$ is the corresponding covariance function, then we have $\gamma(h) = C(0) - C(h)$.

A valid continuous variogram function $2\gamma(\cdot)$ with $\gamma(0) = 0$ must be conditionally negative definite (CND), that is, for any finite number of time points or locations $\{s_i; i = 1, 2, \cdots, m\}$ and real constants $\{a_i;\ i = 1, 2, \cdots, m\}$ such that $\sum_{i=1}^{m} a_i = 0$, we have

$$\sum_{i=1}^{m}\sum_{j=1}^{m} a_i a_j \gamma(t_i - t_j)) \leq 0.$$

It implies that for any linear combination $Y = \sum_{i=1}^{n} a_i X(t_i)$ with $\sum_{i=1}^{m} a_i = 0$,

$$\begin{aligned}
&- Var\left(\sum_{i=1}^{m} a_i X(t_i)\right) \\
&= -E\left(\sum_{i=1}^{m} a_i X(t_i) - \sum_{i=1}^{m} a_i \mu\right)^2 = -E\left(\sum_{i=1}^{m} a_i X(t_i)\right)^2 \\
&= -E\left(\sum_{i=1}^{m}\sum_{j=1}^{m} a_i a_j X^2(t_i) + \sum_{i=1}^{m}\sum_{j=1}^{m} a_i a_j X^2(t_j) - \sum_{i=1}^{m}\sum_{j=1}^{m} a_i a_j X(t_i) Z(t_j)\right) \\
&= -E\left(\sum_{i=1}^{m}\sum_{j=1}^{m} a_i a_j \left[X^2(t_i) - 2X(t_i)X(t_j) + X^2(t_j)\right]\right) \\
&= -E\left(\sum_{i=1}^{m}\sum_{j=1}^{m} a_i a_j \left[X(t_i) - X(t_j)\right]^2\right) \\
&= \sum_{i=1}^{m}\sum_{j=1}^{m} a_i a_j \gamma(X(t_i) - X(t_j)) \\
&\leq 0,
\end{aligned}$$

and therefore, $Var\left(\sum_{i=1}^{m} a_i X(t_i)\right) \geq 0$ will be satisfied since the variogram function is conditionally non-negative definite.

Variogram and covariance functions both measure the strength of correlation as a function of displacement h. If a process is stationary, we usually use a covariance function to model the dependency, and if a process is intrinsically stationary, but not stationary, then the covariance function should be replaced by the variogram

function. Intuitively, things are (positively) spatially dependent if the quantities that are located close together are more similar (less variability) than the quantities that are located farther apart (more variability).

CHAPTER II

SPECTRAL ANALYSIS AND LITERATURE REVIEW

In this Chapter, we first provide a simple introduction to spectral analysis. Then the spectral analysis through periodogram under stationary time series is discussed. As one of the most commonly used methods for estimating the spectral density function under stationarity, periodogram is obtained from the inverse of Fourier transformation on the covariance function. Next, the covariance and variogram estimation are discussed with the corresponding simulation results. In Section 3, simulations are computed under non-stationarity for estimating the covariance and variogram functions. Literature review for the spectral analysis of random processes under non-stationarity is then provided at the end of this chapter.

II.1. Introduction to Spectral Analysis

Spectral analysis originated about a century ago when Schuster(1986)[Sch98] first detected periodicity in time series, and as one of the most important characteristics of time series, the studies and tests on detecting periodicity have been developed by Walker(1914)[Wal14], Fisher(1929)[Fis29], Jenkins and Priestley(1957)[JP57], Hannan(1961)[Han61], and many others. Spectral analysis is a topic that contributes in many diverse fields. For example, a signal can be measured and provides information on wear and other characteristics of mechanical parts by spectral contents in vibration monitoring; in speech analysis, spectral models can be used for both speech synthesis and speech recognition; we can also provide useful material for diagnosis by the spectral analysis of various signals measured from a patient (Stoica, et al. 2005)[SM$^+$05]; spectral analysis of a received signal can provide information for lo-

cating the signal source; even more, in economics, and many other fields, the spectral analysis provides information about "hidden periodocities", and further study on the cyclic behavior of the process. A summary of these early developments were given by Marple (1987)[MM87] and Brockwell and Davis (1991)[BD16].

In physical sciences, a simple application of spectral analysis is speech recognition. Speech recognition was a major goal during the last four decades, with the aim to extract the useful information from the speech signal and use the useful information to convert the acoustic signal into a sequence of words. Stationary sounds (e.g., vowel) can be recognized from a single spectrum. Shumway and Stoffer (2011)[SS11a] provided a simple example that a small 0.1 second (1000 points) sample of recorded speech for the phrase $aaa\cdots hhh$ was collected as a signal, and the problem of great interest is to produce a signature of this phrase by spectral analysis, so that it can be recognized when compared with the signatures in library syllables, and thus find a match.

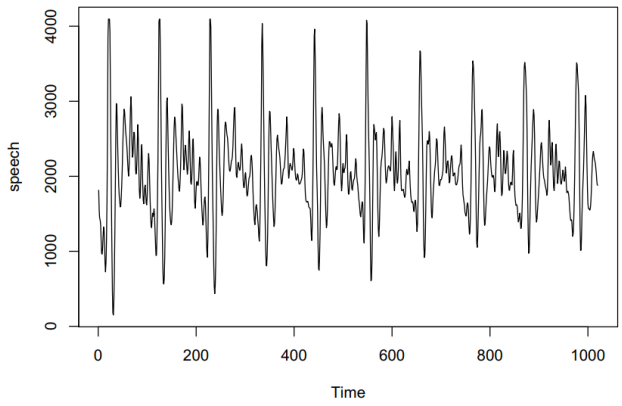

Figure 3. Speech Recording of the Syllable $aaa\cdots hhh$ Sampled at $10,000$ Points Per Second with $n = 1020$ Points.

Different approaches of computing the spectrum of speech have been developed recently by Ernawan, et al. (2011)[EAS11], Saini and Mehra (2015)[SM15]. In recent medical research, the spectral analysis of human voice has been recommended in the laboratories as a potentially useful tool in speech and language rehabilitation (Albertini, et al. 2009[AGM09] and Sigmund, 2007[Sig07]).

Estimation of the spectral density function is one of the most important parts of spectral analysis. It essentially measures the variance (or power) in a particular kind of periodic oscillation in the function by changing the time domain to the frequency domain. In other words, it provides information on the frequencies with strong or weak variations. We denote $f(\omega)$ as the spectral density of the variance function, where the variance is measured as a function of the frequency of oscillation ω. When the process is assumed to be stationary, its corresponding spectral density is widely used to detect the hidden periodicities and its cyclic activities.

For example (Cryer and Kellet, 1991[CK91]), Figure II.2 shows a linear combination of two cosine curves with a multiplier of 2 on the low-frequency curve and a multiplier of 3 on the higher-frequency curve,

$$Y(t) = 2cos\Big(2\pi t\frac{4}{96}\Big) + 3cos\Big[2\pi(t\frac{14}{96} + 0.3)\Big].$$

The "hidden" periodicities in Figure II.2 can be discovered easily by spectral analysis. Figure II.3 shows the estimation of the spectral density for the above process, and it clearly shows that the hidden periodicities contained in the series are two cosine-sine components at the frequencies $4/96(\approx 0.04167)$ and $14/96(\approx 0.14583)$ marked on the frequency axis, and that the higher-frequency component is much stronger.

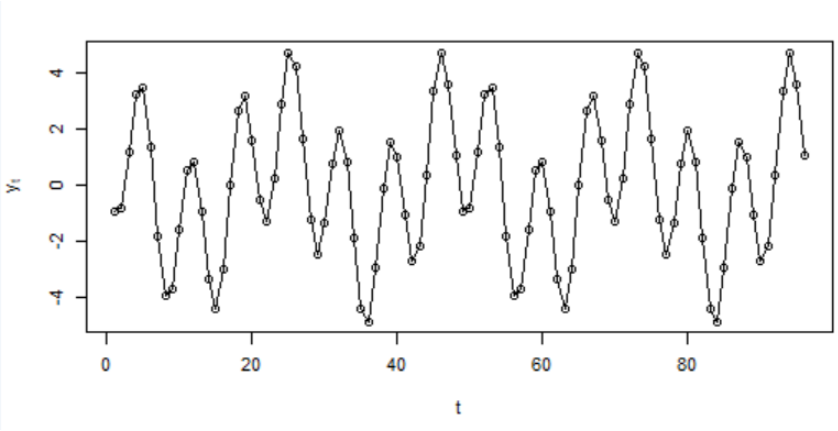

Figure 4. Plot for a Process of A Linear Combination of Two Cosine Curves.

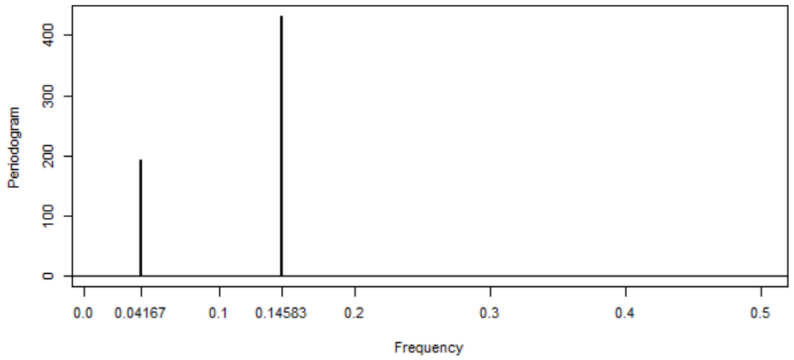

Figure 5. Spectral Analysis for Detecting the Periodicities of the Above Process.

II.2. Spectral Analysis under Stationarity

In this section, we will discuss the spectral analysis under stationarity. We will first provide a general idea for spectral representation of the covariance function, and then the periodogram for estimating the spectral density under stationarity is stated. The estimations of the covariance and variogram functions are also discussed, and the simulation results are presented.

II.2.1. Covariance Function and Its Spectral Representation

A given covariance function $C(h)$ of a continuous stationary process $\{X(t), t \in \mathbb{R}\}$ has the following spectral representation (Bochner, 1938[Boc38]):

$$C(h) = \int_{-\infty}^{\infty} e^{i\omega h} dF(\omega),$$

where $F(\omega)$ is a bounded monotone non-decreasing function of ω.

If $F(\omega)$ is further assumed to have the derivative $f(\omega)$ ($f(\omega) \geq 0, f(-\omega) = f(\omega)$), then according to Bochner (1938)[Boc38], we have

$$C(h) = \int_{-\infty}^{\infty} \cos(\omega h) f(\omega) d\omega,$$
$$\text{and} \quad f(\omega) = \int_{-\infty}^{\infty} \cos(\omega h) C(h) dh.$$

For a stationary time series $\{X(t), t \in \mathbb{Z}\}$, the spectral representation of the covariance function can be written as (Brockwell and Davis, 1991[BD91])

$$C(h) = \int_{-\pi}^{\pi} e^{i\omega h} f(\omega) d\omega.$$

If $\sum_{h=-\infty}^{\infty} |C(h)| < \infty$ is further assumed, as is the case in most applications for theoretical simplicity, the values $C(h)/2\pi$ are simply the Fourier coefficients in the Fourier series expansion of the periodic function $f(\omega)$,

$$f(\omega) = \frac{1}{2\pi} \sum_{h=-\infty}^{\infty} e^{-i\omega h} C(h).$$

Then $f(\omega)$ is called the spectral density for the stationary time series $X(t)$.

II.2.2. Periodogram for Estimating Spectral Density

The estimation of spectral analysis under stationarity has been well developed. Stoica and Moses (2005)[SM+05] mentioned that the main goal of spectral analysis is to convert a finite record from time domain to frequency domain, so that we can obtain the information for its distribution of power over frequency. It would, of course, be desirable that the estimated spectral density obtained from a finite record is as close to its true spectral density function as possible.

Depending on the information provided by the signal, the techniques for estimating the spectral density of a stationary process can generally be divided into parametric and non-parametric approaches. The parametric or model-based methods of spectral estimation assume that the signal satisfies a known functional model, and then proceeds by estimating the parameters in the assumed model, and then the signal's spectral analysis could be conducted from the estimated model. But as Jenkins and Watts (1968)[JW68] stated, that the non-parametric methods for estimating spectral density have no need for proposing modeling ahead of time, and only rely on the definitions of spectral density. Although the spectral density estimation provided by the parametric method may be more accurate than the non-parametric method, it depends strongly on whether a proper model is assumed for the given process. However, in many situations, the observed data do not satisfy the assumed models, so nonparametric methods may be prefered which do not require fitting any assumed models. This observation has motivated renewed interest in the nonparametric approach to spectral estimation (Stoica and Moses, 2005)[SM+05].

As one of the most commonly used non-parametric methods for estimating the spectral density, periodogram (the Fourier Transform of the covariance function) has been applied broadly for stationary random processes. It was named by Schus-

ter (1900)[Sch] as a motivation for this method determining the possible "hidden periodicities", where one of the purposes of the analysis is to identify the dominant frequencies (or periods) in the observed series. When the cycles are not the commonly used ones such as monthly or seasonally, the periodogram is a starting tool for identifying the hidden cyclical behavior in a series. It measures the relative strength of possible frequencies that might explain the oscillation pattern of the observed data and is the simplest technique to estimate the spectrum.

Figure II.4 shows an example of a periodogram for detecting the "hidden" periodicities in the field of astronomy (Shumway and Stoffer, 2011[SS11b]). The observed series ($n = 459$) is collected for the number of sunspots for each half year.

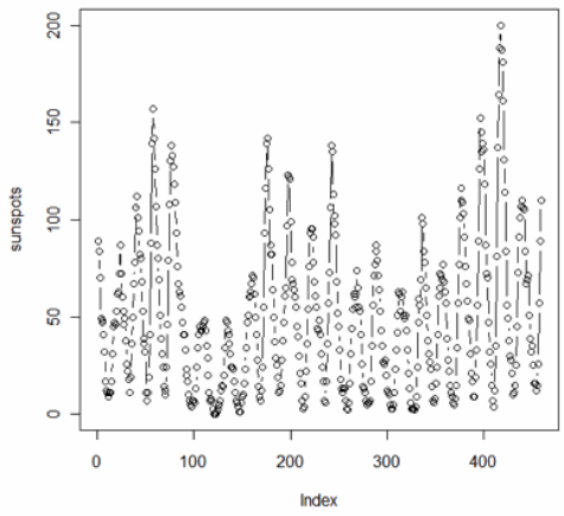

Figure 6. Plot for Seires of Semi-annual Sunspot Activities for $n = 459$ Time Periods.

Figure II.5 presents the periodogram of the given data. It shows a dominant peak at the frequency around 0.05, corresponding to a period of about $1/.05 = 20$ time periods. Since this is semi-annual data, there appears to be a dominant periodicity of about 10 years in sunspot activity.

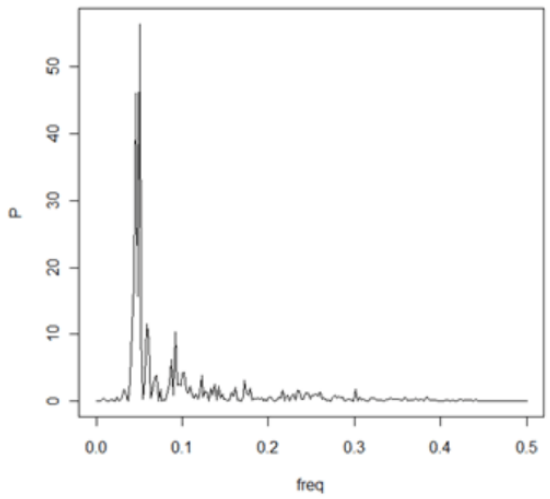

Figure 7. Periodogram Analysis Showing Periodicities for the Above Example.

When the process is stationary (that is, the covariance function $C(h)$ is well-defined, and it is non-negative definite), the spectral density can be estimated through the periodogram by the inverse Fourier transform. The use of the fast Fourier transform in the periodogram for estimating the spectral analysis was summarized in Bingham et al.(1967)[BGT67]. Brockwell and Davis (1991)[BD91] provided a detailed derivation of the periodogram.

More explicity, the periodogram $I(\omega_j)$ at the Fourier frequencies $\omega_j = 2\pi j/n$, where $\omega_j \in (\pi, \pi]$, $j \in \mathbb{F}_n = \{-(n/2)+1, \cdots, (n/2)\}$ for a stationary time series $\{X_1, X_2, \cdots, X_n\}$ in terms of the sample autocovariance function is given by

$$I_n(\omega_j) = n^{-1} \Big| \sum_{t=1}^{n} X_t \, e^{-it\omega_j} \Big|^2,$$

which is equivalent to

$$I_n(\omega_j) = \begin{cases} n|\bar{X}|^2, & \omega_j = 0 \\ \sum_{|k|<n} \hat{C}(k) e^{-ik\omega_j}, & \omega_j \neq 0, \end{cases}$$

where $\hat{C}(k) = n^{-1} \sum_{t=1}^{n-|k|} (X_t - \bar{X})(X_{t+|k|} - \bar{X})$ and $\bar{X} = n^{-1} \sum_{t=1}^{n} X_t$. A natural estimate of the spectral density $f(\omega_j)$ for $\omega_j \neq 0$ is given as $I(\omega_j)/(2\pi)$.

Despite the simplicity of the periodogram, and although it is unbiased, the method suffers from deficiencies. It is an inconsistent estimator, because of sampling variation, and therefore it doesn't converge to the true spectral density as $n \to \infty$, but this can be fixed by smoothing techniques. Warner (1998)[War98] provided a general idea of the smoothing method as well as a detailed introduction and summary of the smoothing methods. Simonoff (2012) [Sim12] and Einicke (2012)[Ein12] summarized more developed smoothing methods.

As mentioned above, the periodogram is obtained from the Fourier transform of the covariance function, the condition of stationarity is assumed to satisfy that the covariance function of the process is a function of only the dispacement h. Therefore, one of the important limitations of the periodogram for estimating the spectral density is that the periodogram can be only used to estimate the spectral density when the random process X_t is stationary.

II.2.3. Covariance and Variogram Estimation under Stationarity

Covariance and Variogram estimation is a fundamental problem for stationary stochastic processes, having wide-ranging applications (Solo, 1992)[Sol92] and playing a crucial role in spectral analysis (Koopmans, 1995[Koo95]). In practice, for a given realization of a process, the covariance or variogram function is unknown. Therefore, we need to obtain a valid and accurate estimator (compared with its theoretical values) in order to perform the spectral analysis. A natural estimator for covariance and variogram (known as *classical or empirical*) was proposed by Matheron (1962)[Mat62], based on the method-of-moments (MOM).

Let $\{X(t) : t = 0, 1, 2, \cdots, n-1\}$ be the observed time series (n data points in total) and assume that $X(t)$ is stationary with unknown constant mean μ_x. Then the covariance function is given by

$$C(h) = Cov[X(t), X(t+h)] = E[X(t) - \mu_x][X(t+h) - \mu_x].$$

The MOM estimator of the covariance function $C(\cdot)$ is then given by:

$$\hat{C}(h) = \frac{1}{n-h} \sum_{t=0}^{n-1-h} (X(t) - \bar{X})(X(t+h) - \bar{X}). \quad h = 0, 1, 2, \cdots, n-1.$$

Let $\{Y(t) : t = 0, 1, 2, \cdots, n-1\}$ be the observed time series and further assumed to be intrinsically stationary with unknown constant mean μ_y. Then the variogram function is given by

$$2\gamma(h) = Var[Y(t+h) - Y(t)] = E[(Y(t+h) - Y(t)]^2.$$

The MOM estimator for variogram function is then given by:

$$2\hat{\gamma}(h) = \frac{1}{n-h} \sum_{t=0}^{n-1-h} [Y(t+h) - Y(t)]^2, \quad h = 0, 1, 2, \cdots, n-1.$$

II.2.4. MOM Estimators of Covariance and Variogram Functions

Cressie (1993)[Cre93] stated that under stationarity, the covariance MOM estimator is actually a biased estimator of $C(h)$, and the variogram MOM estimator is also a biased estimator of $2\gamma(h)$, but its bias is with a smaller order than that for the covariance estimator. In addition, Cressie (1993)[Cre93] also stated that the variance and covariance of $\hat{C}(h)$ and $\hat{\gamma}(h)$ are both of $O(1/n)$. In this section, we conduct simulations to illustrate the performance of MOM covariance and variogram estimators assuming a stationary time series. Matérn covariance model with $\nu = 3/2$ and $\ell = 1$ is applied to generate the process. More explicity,

$$C(h) = (1 + \sqrt{3}h)\, e^{-\sqrt{3}h}, \quad h = k\tau,\ k = 0, 1, 2 \cdots, (n-1).$$

Throughout this dissertation, simulations follow the below algorithm to generate the time series $\{X_i = X(t_i), t_i = i\delta, i = 0, 1, 2, \cdots, (n-1)\}$ with step size $\delta > 0$.

Table 1. Algorithm for Generating the Simulation Dataset.

Step 1:	Generate an identical and independent distributed (*i.i.d.*) standard normal random vector which is given by $\boldsymbol{Z} = (Z_0, Z_1, \cdots, Z_k, \cdots, Z_{n-1})$.
Step 2:	Use the underlying covariance model to construct a variance-covariance matrix $\boldsymbol{\Sigma} = \Sigma_{ij}$, that is $\Sigma_{ij} = Cov[X(t_i), X(t_j)]$.
Step 3:	Then $\boldsymbol{X} = \boldsymbol{\Sigma}^{\frac{1}{2}}\boldsymbol{Z}$ is the observed time series on the pre-specified locations.

In this simulation, without loss of generality, we set $\delta = 1$ and $\mu = 0$. Simulations are conducted with sample size $n = 100$, and repeated for 1000 iterations. Both estimated covariance and variogram values (red points) are plotted along with their theoretical values (blue points) for comparison.

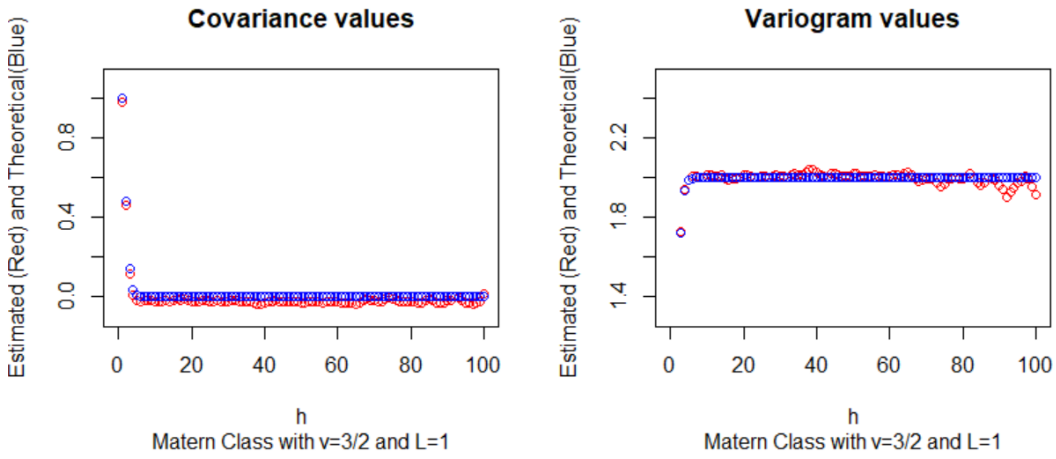

Figure 8. Estimated and Theoretical Covariance and Variogram Values under Stationarity.

The above simulations show that, under stationarity, the covariance function has a shift between the estimated and theoretical values. Variogram function provides a better estimation which confirms what Cressie (1993)[Cre93] had already stated.

Normally, if a process is stationary, we use a covariance function to model the dependency of random variables from two locations or time points, and when the random process is intrinsically stationary, the variogram function often replaces the covariance function.

II.3. Spectral Analysis under Non-stationarity

In this section, we first investigate the performance of the MOM covariance and variogram estimators under processes with stationary increments of order 1 and order 2, respectively. In particular, we present the simulation results for their performance when the underlying process is stationary with an added linear trend and quadratic trend, respectively. In Section 2.3.2, we provide a literature review on spectral analysis under non-stationarity, in particular, the random processes with stationary increments of order d.

II.3.1. Covariance and Variogram Estimation under Non-stationarity

We have checked the performance of MOM estimators of covariance and variogram functions under stationarity in Section 2.2.4, and both estimators have good performances when the underlying process is stationary. But for non-stationary processes, for example, processes with an added linear (or quadratic) trend which has been showed to be with stationary increments of order 1 (or 2), the performance of the MOM estimators for covariance and variogram functions also need to be checked for further estimation of spectral density functions.

We first conduct simulations to investigate the performance of MOM covariance and variogram estimators when the underlying process is a stationary process with an added linear trend. More explicitly, let $X(t)$ be a stationary process with Matérn covariance model when $\nu = 3/2$ and $\ell = 1$ as given above. Let $Y_t = X_t + (a + bt)$, where $a + bt$ is the added linear trend. Note that, from Proposition 1.1, Y_t is also a random process with stationary increments of order 1. In our simulation, data is generated according to the algorithm specified in Section 2.2.4, with $a = b = 1$.

Note that in order to compute the MOM covariance and variogram estimators, we need to remove the estimated trend first, so the resulting data $\{Z_t\}$ are generated. The same steps and formulas are applied to $Z(t)$ for estimating the covariance and variogram functions and their estimated values (red points) are plotted with their theoretical values (blue points). Simulations are conducted $n = 100$, and repeated for 1000 iterations. Figure II.7 shows the simulation results under stationarity with an added linear trend.

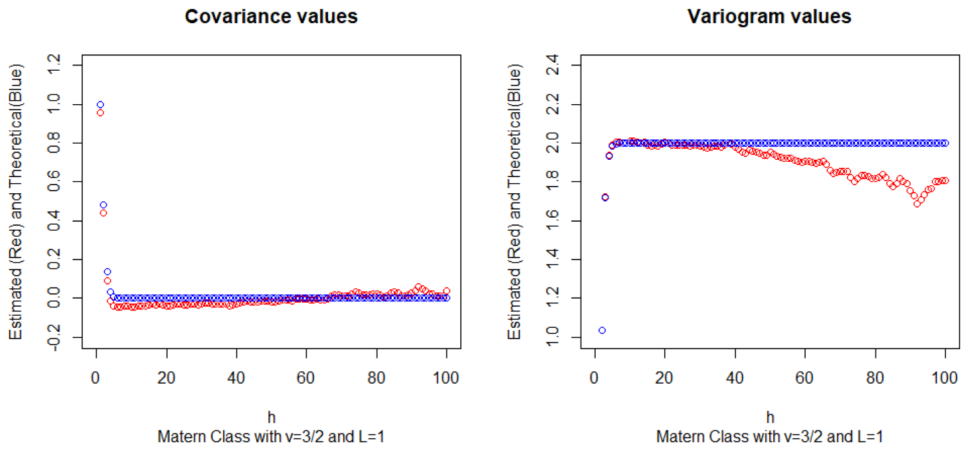

Figure 9. Estimated and Theoretical Covariance and Variogram Values under Stationarity with Added Linear Trend.

The above results show that under stationarity with an added linear trend, the covariance function estimation is away from the theoretical values and the variogram function estimator performs worse. Parallel steps are applied to a stationary process with an added quadratic trend, a process with stationary increment of order 2: $Q(t) = a + bt + ct^2 + X(t)$. In our simulation, we set $a = b = c = 1$, and $X(t)$ is stationary with Matérn covariance function of $\nu = 3/2$ and $\ell = 1$. Here are the simulation results.

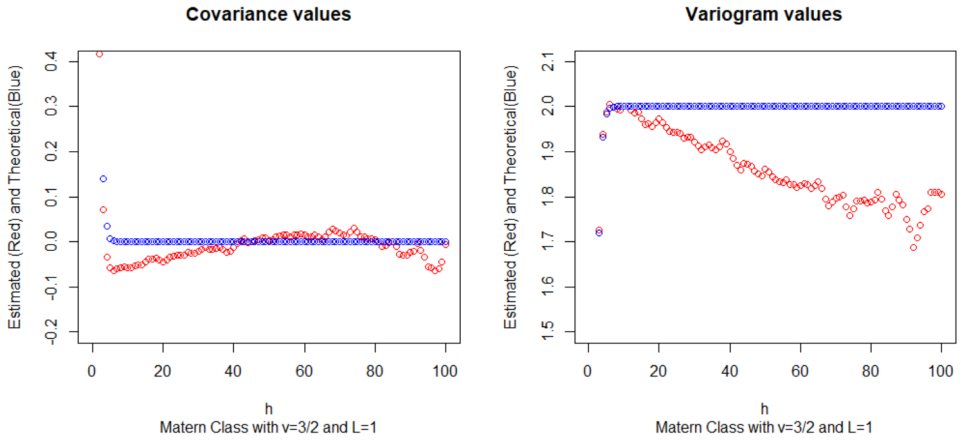

Figure 10. Estimated and Theoretical Covariance and Variogram Values under Stationarity with Added Quadratic Trend.

Figure II.8 shows the simulation results that under stationary increments of order 2, the MOM estimators of covariance and variogram functions performs even worse. It seems that both MOM covariance and variogram estimators perform unsatisfactorily as the order of stationary increments increases. Therefore, it is necessary to seek estimation methods when underlying processes are not stationary.

II.3.2. Literature Review on Spectral Analysis under Non-stationarity

For intrinsically stationary processes, the statistical dependence of the data is often modeled through variogram function, instead of the covariance function. Therefore, the variogram function has been well studied due to its role in spectral density estimations for intrinsically stationary processes.

Valid variogram functions must satisfy conditional negative definiteness. However, Cressie (1993)[Cre93] mentioned that the usual MOM estimations of variogram functions based on a sample is not guaranteed to be conditionally negative-definite. To ensure this property, strategies have been developed to estimate variogram functions by fitting conditionally negative definite models to data in the form of a sample

variogram (Cressie, 1985)[Cre85]. But a non-parametric method for estimating variogram functions that is guaranteed to be conditionally negative definite is also desired (Cressie, 2015)[Cre15].

Huang et al. (2011)[HHC11] proposed a new non-parametric variogram estimator for its spectral representation, the methodology is based on estimation of the variogram's spectrum by solving a regularized inverse problem through quadratic programming, and the estimated variogram is guaranteed to be conditionally negative-definite.

Yang and Zhu (2016)[YZ15] extended Huang et al. (2011)[HHC11]'s work, and provided a semiparametric estimation to estimate the spectral density function on the real line. Both methods seem to focus on the estimation when the underlying process is intrinsically stationary. Therefore, it is necessary to develop a unified method that could be applied for a larger class of non-stationary processes.

For random processes with stationary increments of order d, the notion of the structure equation was developed by Yaglom(1955)[Yag55]. He also provided its properties, as well as its spectral representation. Some other related work includes Matheron's (1973)[Mat73] Intrinsic Random Functions (IRFs) and generalized covariance function.

Zhang and Huang (2014)[ZH14] provided a detailed derivation of the inversion formula where the spectrum can be represented by structure function, and their theorems offer a way to estimate the spectral function from an easily estimated structure function.

In addition, by directly applying the formulas, one can derive the spectral density function of commonly used power variogram. However, Zhang and Huang (2014)[ZH14] focused on theoretical derivations and further research on spectrum estimation and practical procedures are yet to be developed.

II.4. Outline of This Dissertation

In Chapter 3, we first introduce the structure function $D_\tau(h)$ and its properties provided by Yaglom(1955)[Yag55]. Simulations are also conducted to check the performance of its MOM estimator under both stationarity and non-stationarity. Estimation of the spectral density of a continuous random process through the structure function $D_\tau(h)$ under both stationarity and non-stationarity are then discussed in details. In Chapter 4, the spectral analyses for intrinsically stationary processes are discussed for some commonly used variogram functions. The estimations of their spectral densities are derived through the structure function. In particular, the estimation of spectral density for power models are discussed in details with simulations. In Chapter 5, we provide a spectral density estimation for a real dataset for U.S. monthly single-family housing starts from January 1964 to August 1978 (Dickey et al. 1986)[DBM86]. An interpretation of the result is provided at the end of this chapter. Finally, some future research directions will be discussed in Chapter 6.

CHAPTER III

STRUCTURE FUNCTION AND ITS SPECTRAL DENSITY ESTIMATION

In this chapter, we first provide an introduction to the structure function $D_\tau(h)$ and its properties. We then consider its MOM estimator under both stationarity and non-stationarity. The respective simulations are conducted to demonstrate the advantages of our proposed structure function estimator. In Section 3.2, we propose the spectral density estimation of a random process through the structure function $D_\tau(h)$ under both stationarity and non-stationarity. We discuss the asymptotic unbiasedness of our estimation method and the potential aliasing effect when the discretized data are sampled on $\mathbb{R}$. Simulations are conducted to demonstrate the performance of our proposed estimation method. Finally in Section 3.3, we apply our estimation method when the spectral density is band-limited. Some conclusions and discussions are given in Section 3.4.

III.1. Introduction to Structure Function

Consider a random process $\{X(t), t \in \mathbb{R}\}$ with stationary increments of dth order. Let $\tau > 0$ be the step size. The notion of a structure function is given below (Yaglom, 1955, 1987)[Yag58][Yag55].

$$D_\tau(h) = E\Big[[\Delta_\tau{}^{(d)} X(t)][\Delta_\tau{}^{(d)} X(t+h)]\Big],\ h \in \mathbb{R},$$

where

$$\Delta_\tau^{(d)} X(t) = \sum_{k=0}^{d} (-1)^k \binom{d}{k} X(t - k\tau).$$

First we consider three special cases when $d = 0, 1$, and 2. When $d = 0$, $\Delta_\tau^{(0)} X(t) = X(t)$, that is, the random process itself is a stationary process with a constant mean μ_x and covariance function $C_x(h)$.

Then the structure function is given by

$$D_\tau(h) = E\left[(X(t)(X(t+h)\right], \quad \text{for } \tau > 0.$$

More explicitly,

$$\begin{aligned} D_\tau(h) &= E[X(t)X(t+h)] \\ &= E[(X(t)-\mu_x)+\mu_x][(X(t+h)-\mu_x)+\mu_x] \\ &= E[(X(t)-\mu_x)(X(t+h)-\mu_x)] + \mu_x E[X(t)-\mu_x] \\ &\quad +\mu_x E[X(t+h)-\mu_x] + \mu_x^2 \\ &= Cov(X(t), X(t+h)) + \mu_x^2 \\ &= C_x(h) + \mu_x^2. \end{aligned}$$

That is, when $X(t)$ is stationary, the structure function is the stationary covariance shifted by a constant. When $d = 1$,

$$\Delta_\tau^{(1)} X(t) = \sum_{k=0}^{1} (-1)^k \binom{1}{k} X(t - k\tau) = X(t) - X(t-\tau),$$

is a stationary process. Its structure function is given by

$$D_\tau(h) = E\left[(X(t) - X(t-\tau))(X(t+h) - X(t+h-\tau))\right], \text{ for } \tau > 0.$$

In particular, when $h = 0$, we have $D_\tau(0) = E[Y(t) - Y(t-\tau)]^2$, which is actually the variogram function of $X(t)$.

Now let $X(t)$ be a stationary process with a constant mean μ_x and covariance function $C_x(h)$. Letting $Y(t) = X(t) + a + bt$, $a, b \in \mathbb{R}$, it is a random process with stationary increments of order 1 (Proposition 2.1). Then

$$\begin{aligned}
C_y(h) &= Cov[Y(t) - Y(t-\tau), Y(t+h) - Y(t+h-\tau)] \\
&= Cov[X(t) - X(t-\tau) + b\tau,\ X(t+h) - X(t+h-\tau) + b\tau] \\
&= Cov[X(t) - X(t-\tau),\ X(t+h) - X(t+h-\tau)] \\
&= E[X(t) - X(t-\tau)][X(t+h) - X(t+h-\tau)] \\
&= Cov[X(t), X(t+h)] - Cov[X(t), X(t+h-\tau)] \\
&\quad -Cov[X(t-\tau), X(t+h)] + Cov[X(t-\tau), X(+h-\tau)] \\
&= 2C_x(h) - C_x(h-\tau) - C_x(h+\tau),
\end{aligned}$$

$$\begin{aligned}
\mu_y &= E[Y(t) - Y(t-\tau)] = E[X(t) + a + bt - (a + b(t+h) + X(t+h))] \\
&= b\tau.
\end{aligned}$$

Then for a stationary process with an added linear trend, the structure function is given by

$$D_\tau(h) = C_y(h) + \mu_y^2 = 2C_x(h) - C_x(h-\tau) - C_x(h+\tau) + (b\tau)^2.$$

When $d = 2$,

$$\Delta_\tau^{(2)} X(t) = \sum_{k=0}^{2} (-1)^k \binom{1}{k} X(t - k\tau) = X(t) - 2X(t-\tau) + X(t-2\tau),$$

is a stationary process and its structure function for $\tau > 0$ is given by

$$D_\tau(h) = E[X(t) - 2X(t-\tau) + X(t-2\tau)][X(t+h) - 2X(t+h-\tau) + X(t+h-2\tau)].$$

In particular, let $X(t)$ be a stationary process with a constant mean μ_x and covariance function $C_x(h)$, and let $Y(t) = X(t) + a + bt + ct^2$, $a, b, c \in \mathbb{R}$, a random process with stationary increments of order 2 (Proposition 2.2). Then

$$\begin{aligned}
& C_y(h) \\
= \; & Cov[Y(t) - 2Y(t-\tau) + Y(t-2\tau),\ Y(t+h) - 2Y(t+h-\tau) + Y(t+h-2\tau)] \\
= \; & Cov[X(t) - 2X(t-\tau) + X(t-2\tau) + 2c\tau^2, \\
& \quad X(t+h) - 2X(t+h-\tau) + X(t-2\tau) + 2c\tau^2] \\
= \; & Cov[X(t) - 2X(t-\tau) + X(t-2\tau),\ X(t+h) - 2X(t+h-\tau) + X(t-2\tau)] \\
= \; & E[X(t) - 2X(t-\tau) + X(t-2\tau)][X(t+h) - 2X(t+h-\tau) + X(t-2\tau)] \\
= \; & 6C_x(h) - 4C_x(h-\tau) - 4C_x(h+\tau) + C_x(h-2\tau) + C_x(h+2\tau),
\end{aligned}$$

$$\begin{aligned}
\mu_y &= E[Y(t) - 2Y(t-\tau) + Y(t-2\tau)] \\
&= E[X(t) - 2X(t-\tau) + X(t-2\tau) + 2c\tau^2] \\
&= 2c\tau^2.
\end{aligned}$$

Now the structure function for $Y(t)$ is given by

$$\begin{aligned}
& D_\tau(h) \\
= \; & C_y(h) + \mu_y^2 \\
= \; & 6C_x(h) - 4C_x(h-\tau) - 4C_x(h+\tau) + C_x(h-2\tau) + C_x(h+2\tau) + (2c\tau^2)^2.
\end{aligned}$$

The above results will be extensively used in our simulations in this chapter.

III.1.1. Properties of the Structure Function $D_\tau(h)$

1. By definition, $D_\tau(0) = E\Big[{\Delta_\tau}^{(d)} X(t)\Big]^2$, which is non-negative.

2. $|D_\tau(h)| \leq D_\tau(0)$ for all $h \in \mathbb{R}$. This is due to the Cauchy-Schwartz inequality.

3. $D_\tau(-h) = D_\tau(h)$, that is, $D_\tau(h)$ is symmetric about 0.

   PROOF:

$$\begin{aligned} D_\tau(-h) &= E\Big[[{\Delta_\tau}^{(d)} X(t)][{\Delta_\tau}^{(d)} X(t-h)]\Big] \\ &= E\Big[[{\Delta_\tau}^{(d)} X(t+h)][{\Delta_\tau}^{(d)} X((t+h)-h)]\Big] \\ &= E\Big[[{\Delta_\tau}^{(d)} X(t+h)][{\Delta_\tau}^{(d)} X((t)]\Big] \\ &= D_\tau(h) \quad \text{(By the definition of } D_\tau(h)). \end{aligned}$$

4. $D_\tau(h)$ is positive definite for each fixed τ.

   PROOF: $\forall n \in \mathbb{Z}$, $\forall a_1, a_2, \cdots, a_n \in \mathbb{R}$ and $t_1, t_2, \cdots, t_n \in \mathbb{R}$, we have

$$\begin{aligned} & \sum_{i=1}^{n}\sum_{j=1}^{n} a_i a_j D_\tau(t_i - t_j) \\ = & \sum_{i=1}^{n}\sum_{j=1}^{n} a_i a_j E[\Delta_\tau^d X(t_i)][\Delta_\tau^d X(t_j)] \\ = & E[\sum_{i=1}^{n} a_i \Delta_\tau^d X(t_i)]^2 \\ \geq & 0. \end{aligned}$$

   Therefore, $D_\tau(\cdot)$ is positive definite for each fixed $\tau > 0$.

III.1.2. Estimation of Structure Function $D_\tau(h)$

In this section, we investigated the MOM estimator for the structure function $D_\tau(h)$. We assume $X(t), t \in \mathbb{R}$ is a random process with stationary increments of order d. Let $\boldsymbol{X} = (X(0), X(\delta), X(2\delta), \cdots, X((n-1)\delta))$ be the observed data vector of size n with a fixed step size $\delta > 0$. Throughout this dissertation, for notational simplicity, we simply rewrite the above random vector $\boldsymbol{X}$ as $\{X_0, X_1, \cdots, X_{n-1}\}$ and set $\tau = \delta$.

Based on the above observed data, the MOM estimator for $D_\tau(h)$ is given by

$$\hat{D}_\tau(h) = \sum_{R(h)} [\Delta^{(d)} X_i][\Delta^{(d)} X_{i+k}] / \sum_{R(h)} 1, \qquad \text{where } R(h) = \{i : 0 \le i \le i + |k| \le n-1\}$$

which can be represented as follows:

$$\hat{D}_\tau(h) = \frac{1}{n - |k| - d} \sum_{i=d}^{n-1-|k|} [\Delta^{(d)} X_i][\Delta^{(d)} X_{i+|k|}],$$

where $h = k\tau$, $k = 0, \pm 1, \pm 2, \cdots, \pm(n-1-d)$, and

$$\Delta^{(d)} X_i = \sum_{m=0}^{d} (-1)^m \binom{d}{m} X_{i-m}.$$

III.1.3. Properties of $\hat{D}_\tau(h)$

Proposition 3.1: $\forall h \in \mathbb{R}$, $\hat{D}_\tau(-h) = \hat{D}_\tau(h)$.

PROOF:

$$\begin{aligned}
\hat{D}_\tau(-h) &= \frac{1}{n - |-k| - d} \sum_{i=d}^{n-1-|-k|} [\Delta^{(d)} X_i][\Delta^{(d)} X_{i+|-k|}] \\
&= \frac{1}{n - |k| - d} \sum_{i=d}^{n-1-|k|} [\Delta^{(d)} X_i][\Delta^{(d)} X_{i+|k|}] \\
&= \hat{D}_\tau(h).
\end{aligned}$$

Proposition 3.2: The MOM estimator of the structure function, $\hat{D}_\tau(h)$ is an unbiased estimator of $D_\tau(h)$.

PROOF:

$$\begin{aligned}
E[\hat{D}_\tau(h)] &= E\left[\sum_{R(h)}[\Delta^{(d)}X_i][\Delta^{(d)}X_{i+|k|}]/\sum_{R(h)1}\right] \\
&= E\left[\frac{1}{n-|k|-d}\sum_{i=d}^{n-1-|k|}[\Delta^{(d)}X_i][\Delta^{(d)}X_{i+|k|}]\right] \\
&= \frac{1}{n-|k|-d}\sum_{i=d}^{n-1-|k|}E[\Delta^{(d)}X_i][\Delta^{(d)}X_{i+|k|}] \\
&= \frac{1}{n-|k|-d}\,(n-|k|-d)D_\tau(h) \\
&= D_\tau(h), \quad h=k\tau,\, k=0,\pm1,\pm2,\cdots,\pm(n-1-d).
\end{aligned}$$

where $R(h)=\{i: 0\le i\le i+|k|\le n-1\}$.

In order to further estimate the spectral density, the same as considered for covariance estimator justification under statioary time series, we consider the following estimator instead for $D_\tau(h)$ throughout the rest of this dissertation,

$$\hat{D}_\tau(h)=\frac{1}{n-d}\sum_{i=d}^{n-1-|k|}[\Delta^{(d)}X_i][\Delta^{(d)}X_{i+|k|}].$$

Proposition 3.3: $\hat{D}_\tau(h)$ is positive definite.

PROOF: Consider the following $(n-d)\times 2(n-d)$ matrix Γ, with the non-zero entries shifted to the left for each row going down.

$$\Gamma = \begin{pmatrix} 0 & \cdots & \cdots & 0 & \Delta^{(d)}X_1 & \Delta^{(d)}X_2 & \cdots & \Delta^{(d)}X_{n-d} \\ 0 & \cdots & 0 & \Delta^{(d)}X_1 & \Delta^{(d)}X_2 & \cdots & \Delta^{(d)}X_{n-d} & 0 \\ \vdots & \cdots & \cdots & \cdots & \cdots & \cdots & \iddots & \vdots \\ 0 & \Delta^{(d)}X_1 & \Delta^{(d)}X_2 & \cdots & \Delta^{(d)}X_{n-d} & 0 & \cdots & 0 \end{pmatrix}$$

$$\Gamma\Gamma' = \begin{pmatrix} \hat{D}(0) & \hat{D}(1\tau) & \cdots & \hat{D}((n-1-d)\tau) \\ \hat{D}(-1\tau) & \hat{D}(0) & \cdots & \hat{D}((n-2-d)\tau) \\ \vdots & \vdots & \ddots & \vdots \\ \hat{D}((n-1-d)\tau & \hat{D}((n-2-d)\tau) & \cdots & \hat{D}(0) \end{pmatrix}_{(n-d)\times(n-d)}$$

By Proposition 3.1, $\hat{D}_\tau(-h) = \hat{D}_\tau(h)$, the above matrix $\Gamma\Gamma'$ is symmetric. Therefore $\forall n \in \mathbb{Z}$, $\forall a_1, a_2, \cdots, a_{n-d} \in \mathbb{R}$ and $h_{ij} = t_i - t_j = k_{ij}\tau$ with $k_{ij} \in R(h) = \{i : 0 \le i \le i + |k| \le n-d\}$, we have

$$\begin{aligned} & \sum_{i=1}^{n-d}\sum_{j=1}^{n-d} a_i a_j \hat{D}(h_{ij}) \\ = & \begin{pmatrix} a_1 & \cdots & a_{n-d} \end{pmatrix} \begin{pmatrix} \hat{D}(0) & \hat{D}(1\tau) & \cdots & \hat{D}((n-1-d)\tau) \\ \hat{D}(-1\tau) & \hat{D}(0) & \cdots & \hat{D}((n-2-d)\tau) \\ \vdots & \vdots & \ddots & \vdots \\ \hat{D}((n-1-d)\tau & \hat{D}((n-2-d)\tau) & \cdots & \hat{D}(0) \end{pmatrix} \begin{pmatrix} a_1 \\ a_2 \\ \vdots \\ a_{n-d} \end{pmatrix} \\ = & \boldsymbol{a}'\Gamma\Gamma'\boldsymbol{a} = (\Gamma'\boldsymbol{a})'(\Gamma'\boldsymbol{a}) \ge 0. \end{aligned}$$

III.1.4. Simulation Results for Estimations of Structure Function $D_\tau(h)$

In this section, we explore the performance of the proposed MOM structure function estimator via simulations. We assume the underlying process is with stationary increments of orders $d = 0, 1$ and 2, respectively. More explicitly, we consider three different underlying processes: the stationary process, the stationary process with an added linear trend, and the stationary process with an added quadratic trend. We follow the same setup as given in Sections 2.2 and 2.3, assuming the step size $\tau = 1$, and the Matérn covariance function with parameters $\nu = 3/2$ and $\ell = 1$ is given by by the following equation,

$$C(h) = (1 + \sqrt{3}|h|)e^{-\sqrt{3}|h|}.$$

Under the above scenarios, we compute the corresponding theoretical $D_\tau(h)$'s. When $d = 0$, since $\mu = 0$, we have the theoretical $D_\tau(h)$ given by

$$D_\tau(h) = C(h).$$

When $d = 1$, with a linear trend with $a = b = 1$, we have

$$D_\tau(h) = 2C(h) - C(h-1) - C(h+1) + 1.$$

When $d = 2$, with a quadratic trend with $a = b = c = 1$, we have

$$D_\tau(h) = 2C(h) - C(h-1) - C(h+1) + 1.$$

Simulations are conducted with $n = 100$ and repeated for 1000 iterations, respectively. The estimated $\hat{D}_\tau(h)$ values are calculated and are plotted (red points) along with the theoretical values (blue points) for each value of d. For comparison, the estimates of covariance and variogram functions along with the corresponding

theoretical values are also plotted on the same scale. Figures III.1-III.3 show the simulation results for each of the above scenarios.

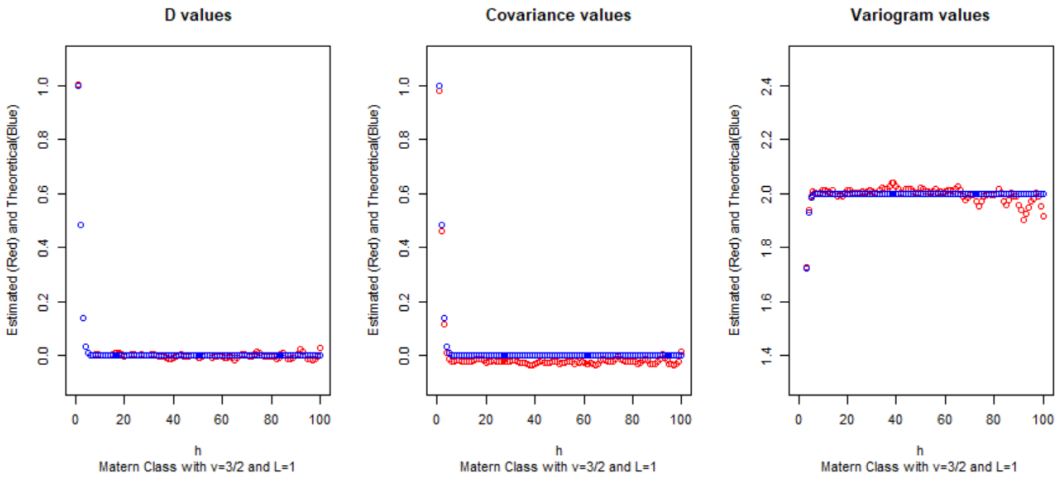

Figure 11. Comparison of the Estimated and Theoretical Values for $D_\tau(h)$ under Stationarity Together with Estimations of Covariance and Variogram Functions.

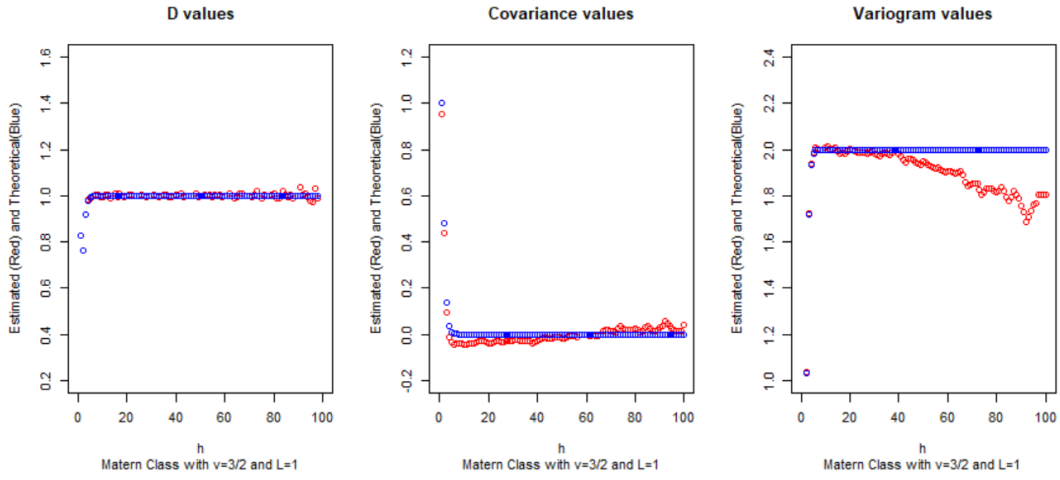

Figure 12. Comparison of the Estimated and Theoretical Values for $D_\tau(h)$ under Stationarity with An Added Linear Trend, Together with Estimations of Covariance and Variogram Functions.

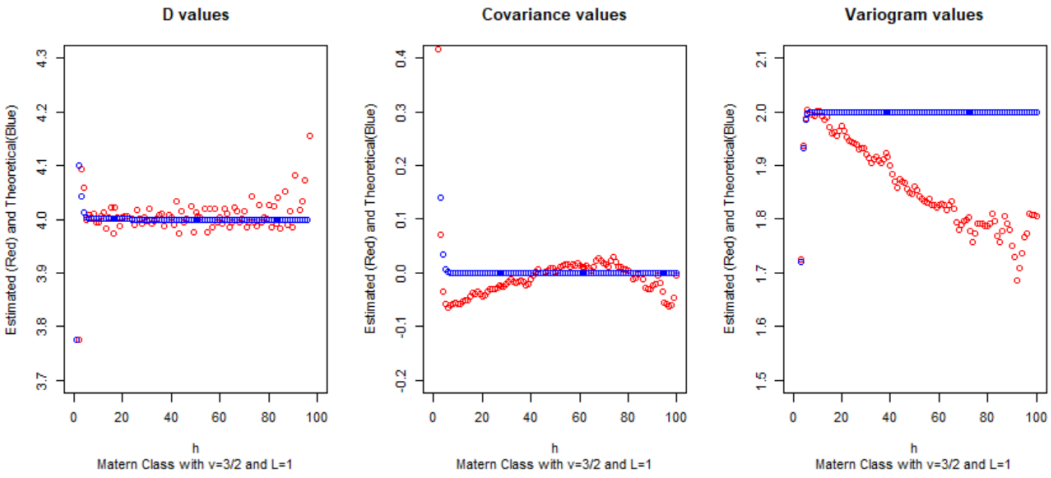

Figure 13. Comparison of the Estimated and Theoretical Values for $D_\tau(h)$ under Stationarity with An Added Quadratic Trend, Together with Estimations of Covariance and Variogram Functions.

From the above plots, the MOM estimator of the structure function $D_\tau(h)$ maintains its stability as the order of stationary increments increases, performing comparably or better than the MOM covariance and variogram estimators under both stationarity and stationarity with an added (linear or quadratic) trend.

III.2. Spectral Density Estimation Through Structure Function

When a random process is with stationary increments of order d, Zhang and Huang (2014)[ZH14] proved an inversion formula that obtains the spectral density function through the structure function $D_\tau(h)$. This offers a way to estimate the spectral density from an easily estimated structure function.

In Section 3.2.1, we first outline the theoretical setup and apply it on three processes that we have considered previously. We then discuss the aliasing effect due to the discretized data observations. In Section 3.2.3, we propose our spectral density estimator through the MOM structure function estimator and then discuss its properties. Lastly, simulations are conducted to demonstrate the performance of

our proposed estimator in recovering the true underlying spectral density function. Some conclusions and discussions are given in Section 3.4.

III.2.1. Spectral Density Through the Structure Function $D_\tau(h)$

Yaglom(1955)[Yag55] has shown that the structure function $D_\tau(h)$ has the following spectral representation

$$D_\tau(h) = \int_{-\pi}^{\pi} e^{i\omega h}(1-e^{i\tau\omega})^d(1-e^{-i\tau\omega})^d \frac{(1+\omega^2)^d}{\omega^{2d}} f(\omega)d\omega,$$

assuming that the spectral density $f(\omega)$ exists.

Zhang and Huang (2014)[ZH14] provided its inversion formula for the spectral density function $f(\omega)$, for $\omega \in [\omega_1, \omega_2]$, under which $(1-\cos(\omega\tau))/\omega^2$ has no zeros for ω, the spectral density $f(\omega)$ is given as follows,

$$f(\omega) = f_\tau(\omega) q(\tau, \omega),$$

$$\text{where} \quad f_\tau(\omega) = \int_{-\infty}^{\infty} e^{-i\omega h} D_\tau(h) dh,$$

$$\text{and} \quad q(\tau,\omega) = \frac{1}{2^d(1-\cos\tau\omega)^d}\left(\frac{\omega^2}{1+\omega^2}\right)^d. \tag{III.1}$$

Note that by Zhang and Huang (2014)[ZH14], the spectral density $f(\omega)$ is actually free of τ. This result offers a way to estimate a spectral density function through an easily estimated structure function $D_\tau(h)$.

In particular, when $d=0$, $q(\tau,\omega)=1$; when $d=1$, $q(\tau,\omega)=\frac{\omega^2}{2(1-\cos\tau\omega)(1+\omega^2)}$; and when $d=2$, $q(\tau,\omega)=\frac{\omega^4}{4(1-\cos\tau\omega)^2(1+\omega^2)^2}$. Note that when $\omega=0$, we will assign $q(\tau,0)=1/\tau^{2d}$ since $\lim_{\omega\to 0} q(\tau,\omega) = 1/\tau^{2d}$.

In practice, to estimate the true spectral density of a continuous process based on a discretized time series, as we mentioned in Chapter 2, there will exist the alising effect due to the difference of considerations. In the next section, the aliasing effect will be considered and discussed in detail.

III.2.2. Aliasing Effect

Aliasing refers to the effect which is produced when a signal is sampled at a frequency that is not high enough to be distinguished from another signal, and therefore it is not possible to create an accurate spectral representation of it. With the aliasing effect, the signal cannot be reconstructed from the original signal, and then become indistinguishable (or aliases of one another). When a signal is banded at a fixed frequency range, the power from other signals that is above the fixed band range will be added to the original signal, and therefore be aliases with the other signals. This frequency limit is called *Nyquist frequency*(Olshausen, 2000)[Ols00].

Cryer and Chan (2008)[CC08] provided a simple example to illustrate the aliasing effect. Consider two cosine curves, one with frequency $f = \pi/2$ (solid, red) and the one shown with blue dashed lines at frequency $f = 3\pi/2$.

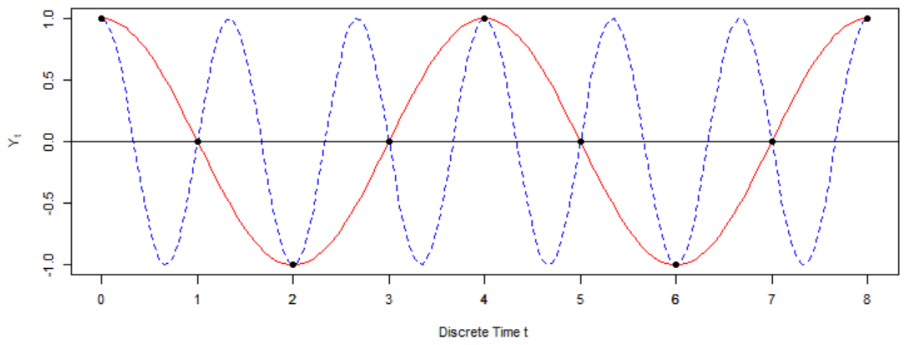

Figure 14. Illustration of Aliasing Effect.

If we only observe the series at the discrete-time points $0, 1, 2, 3, \cdots$, then two series are identical. With discrete-time observations, we can never distinguish between these two curves. Then the power from the blue curve will be added to the power of the red curve. We say that the two frequencies $\pi/2$ and $3\pi/2$ are aliased with one another.

To illustrate the statistical properties concerning aliasing effects, we follow closely the development of Yaglom(1987)[Yag87].

We assume $\{X(t), t \in \mathbb{R}\}$ is a stationary random process with covariance function $C(h)$ and its corresponding spectral density function $f(\omega)$, both of which are related via Fourier transformation (Yaglom, 1987)[Yag87]:

$$\begin{aligned} C(h) &= \int_{-\infty}^{\infty} e^{i\omega h} f(\omega) d\omega, \quad h \in R, \\ f(\omega) &= \frac{1}{2\pi} \int_{-\infty}^{\infty} e^{-i\omega h} C(h) dh, \quad \omega \in R. \end{aligned} \tag{III.2}$$

Let $\{X(t_k), t_k = k\delta, k = 0, \pm 1, \pm 2, \cdots\}$, or for short, $\{X_k, k = 0, \pm 1, \pm 2, \cdots\}$, be the discretized sample (time series) of $X(t)$ at the sampling locations $t_k = k\delta, k = 0, \pm 1, \pm 2, \cdots$ with equal-spacing $\delta > 0$. Let $C_\delta(k) = C(k\delta)$ be the covariance function of the stationary time series $\{X_k, k = 0, \pm 1, \pm 2, \cdots\}$, and $f_\delta(\omega)$, $\omega \in (-\pi/\delta, \pi/\delta]$ be the corresponding spectral density.

Then $C_\delta(h)$ and $f_\delta(\omega)$ are related via Fourier transformation,

$$C_\delta(h) = \int_{-\pi/\delta}^{\pi/\delta} e^{ih\delta\omega} f_\delta(\omega) d\omega, \quad h = k = 0, \pm 1, \pm 2, \cdots, \tag{III.3}$$

$$f_\delta(\omega) = \frac{1}{2\pi} \sum_{k=-\infty}^{\infty} C_\delta(k) e^{-ik\delta\omega}, \quad \omega \in (-\pi/\delta, \pi/\delta]. \tag{III.4}$$

In addition, $f_\delta(\omega)$ is related to the spectral density function $f(\omega)$ according to the following formula from Yaglom(1987)[Yag87]:

$$f_\delta(\omega) = \sum_{k=-\infty}^{\infty} f\left(\omega + \frac{2k\pi}{\delta}\right), \quad \omega \in (-\pi/\delta, \pi/\delta]. \tag{III.5}$$

Note that with the discrete sample observations from a stationary random process, our goal is to estimate the spectral density function $f(\omega)$ over the frequency interval $\omega \in (-\pi/\delta, \pi/\delta]$. For a stationary time series, $f_\delta(\omega)$ can be estimated through (smoothed) periodograms. However, as one can see from equation (III.5), the estimated periodograms contain not only the true spectral density of the continuous process, corresponding to the term $k = 0$ in equation (III.5), but also contains the power coming from the frequencies that are differing by $2k\pi/\delta, k = \pm 1, \pm 2, \cdots$. In other words, when applied to stationary random processes, the components, which can not be distinguished from the original signal with frequencies as an integer multiple of $2\pi/\delta$ is the aliasing effect and the frequencies $\omega + 2\pi k/\delta$, $k = \pm 1, \pm 2, \cdots$, are the *aliases* of the frequency ω (Yaglom, 1987)[Yag87].

III.2.3. Spectral Density Estimation through $\hat{D}_\tau(h)$

Now we consider the spectral density estimation through a seires of finite observations. Let $\{X(t_k), t_k = k\delta, k = 0, 1, 2, \cdots, (n-1)\}$ be the observed data values of the underlying process $X(t)$ on equally spaced locations with step size $\delta > 0$. We propose the following spectral density estimator

$$\hat{f}(\omega) = \hat{f}_\tau(\omega) q(\tau, \omega), \quad -\pi/\delta < \omega \leq \pi/\delta. \tag{III.6}$$

Here $\hat{f}_\tau(\omega)$ is estimated through the structure function estimator $\hat{D}_\tau(h)$ and $q(\tau, \omega)$ is given by (III.1). Note that $\hat{D}_\tau(h)$ is symmetric and positive definite (Section 3.2.1), therefore, we can obtain the spectral density estimator $\hat{f}_\tau(\omega)$ through the

inverse Fourier transformation of the structure function estimator $\hat{D}_\tau(h)$ (Brockwell and Davis, 1991)[BD91], that is,

$$\hat{f}_\tau(\omega) = \frac{1}{2\pi} \sum_{|k|<n-d} \hat{D}_\tau(k) e^{-ik\tau\omega}, \quad -\pi/\tau < \omega \leq \pi/\tau. \tag{III.7}$$

Remark 1: As we can see from the above approach, the derivation of $\hat{f}_\tau(\omega)$ mimics the derivation of a periodogram in estimating the spectrum for stationary processes. Therefore, all the asymptotic properties regarding the periodogram can be carried over to $\hat{f}_\tau(\omega)$, and to $\hat{f}(\omega)$. For example, parallel to a result for the periodogram, we have the following proposition.

Proposition 3.4. If $X(t)$ is a random process with stationary increments of order d, and assume that $D_\tau(\cdot)$ is absolutely integrable, then

$$E\hat{f}(\omega) \to f(\omega), \quad \text{if } \omega \neq 0.$$

Moreover, for any $\omega_0 > 0$ and with $\omega_0 < \omega < \pi/\delta$, $E\hat{f}(\omega)$ converges uniformly to $f(\omega)$.

Remark 2: For a stationary process, the periodogram is not a consistent estimator of the spectral density function due to its bias at $\omega = 0$. The same phenomenon occurs for $\hat{f}_\tau(\omega)$ and hence for $\hat{f}(\omega)$. Therefore, smoothing methods used for periodogram could be potentially applied to our proposed spectral density estimator. This will be an area for future research.

III.2.4. Aliasing Effect for the Process with Stationary Increments

In this section, the aliasing effects for both a stationary process and a process with stationary increments of order d are discussed in details.

Consider a random process $\{X(t)\}$ with stationary increments of order d with corresponding spectral density $f(\omega)$. According to Zhang and Huang (2014)[ZH14], we have the following inversion fomula:

$$f(\omega) = f_\tau(\omega) q(\tau, \omega),$$

with

$$f_\tau(\omega) = \int_{-\infty}^{\infty} D_\tau(h) e^{-i\omega h} dh, \qquad q(\tau, \omega) = \frac{1}{2^d (1 - \cos(\tau\omega))^d} \left(\frac{\omega^2}{1 + \omega^2} \right)^d.$$

Note that $D_\tau(h)$ is symmetric and positive definite, hence, we can treat it as a covariance function. Therefore, to estimate $f_\tau(\omega)$ from an equally spaced time series, we need to consider the aliasing effect.

Now we consider a general formula for the aliasing effect when the continuous process $X(t)$ is with stationary increments of order d in $\mathbb{R}$. Denote $U(t) = \Delta_\tau^{(d)} X(t)$, and so it is stationary in $\mathbb{R}$. Let $\{X(t_k), t_k = k\delta, k = 0, \pm 1, \pm 2, \cdots\} = \{X_k, k = 0, \pm 1, \pm 2, \cdots\}$ be the observed discretized sample (time series) of $X(t)$. We choose the step size $\tau = l\delta$ for some integer $l > 0$, and let $\{U_k, k = 0, \pm 1, \pm 2, \cdots\}$ be the corresponding discretized sample (time series) of $U(t)$ and $D_\tau(h), h = k\delta, k = 0, \pm 1, \pm 2, \cdots$ be the structure function based on $\{U_k\}$. Therefore, the spectral density function based on time series $\{U_k\}$ through the inverse Fourier transformation on $D_\tau(\cdot)$ is given by

$$f_\delta^\tau(\omega) = \frac{1}{2\pi} \sum_{k=-\infty}^{\infty} D_\tau(k\delta) e^{-ik\delta\omega}, \qquad \omega \in (-\pi/\delta, \pi/\delta].$$

On the other hand, parallel to the approach for stationary process as seen by (III.5), we have the $f_\delta^\tau(\omega)$ also given as follows.

$$\begin{aligned} f_\delta^\tau(\omega) &= \sum_{k=-\infty}^{\infty} f_\tau\left(\omega + \frac{2k\pi}{\delta}\right), \qquad -\pi/\delta < \omega \le \omega/\delta \\ &= f_\tau(\omega) + \sum_{k=1}^{\infty}\left[f_\tau\left(\omega + \frac{2k\pi}{\delta}\right) + f_\tau\left(\omega - \frac{2k\pi}{\delta}\right)\right]. \end{aligned}$$

Hence, the spectral density function of the discretized time series $\{X_k\}$ is given by

$$\begin{aligned} f_\delta(\omega) &= f_\delta^\tau(\omega) q(\tau,\omega) \\ &= f_\tau(\omega) q(\tau,\omega) + \sum_{k=1}^{\infty}\left[f_\tau\left(\omega + \frac{2k\pi}{\delta}\right) + f_\tau\left(\omega - \frac{2k\pi}{\delta}\right)\right] q(\tau,\omega) \\ &= f(\omega) + \sum_{k=1}^{\infty}\left[f_\tau\left(\omega + \frac{2k\pi}{\delta}\right) + f_\tau\left(\omega - \frac{2k\pi}{\delta}\right)\right] q(\tau,\omega) \\ &= f(\omega) + f_a(\omega), \end{aligned} \tag{III.8}$$

where

$$\begin{aligned} f_a(\omega) &= \sum_{k=1}^{\infty}\left[f_\tau\left(\omega + \frac{2k\pi}{\delta}\right) q(\tau, \omega + 2k\pi/\delta) \cdot \frac{q(\tau,\omega)}{q(\tau,\omega+2k\pi/\delta)}\right. \\ &\qquad \left. + f_\tau\left(\omega - \frac{2k\pi}{\delta}\right) q(\tau, \omega - 2k\pi/\delta) \cdot \frac{q(\tau,\omega)}{q(\tau,\omega+2k\pi/\delta)}\right] \\ &= \sum_{k=1}^{\infty}\left[f\left(\omega + \frac{2k\pi}{\delta}\right)\frac{q(\tau,\omega)}{q(\tau,\omega+2k\pi/\delta)} + f\left(\omega - \frac{2k\pi}{\delta}\right)\frac{q(\tau,\omega)}{q(\tau,\omega-2k\pi/\delta)}\right] \end{aligned}$$

Now we consider

$$\frac{q(\tau,\omega)}{q(\tau,\omega \pm 2k\pi/\delta)} = \frac{2^d(1-\cos(\tau(\omega \pm 2k\pi/\delta)))^d \omega^{2d}(1+(\omega \pm 2k\pi/\delta)^2)^d}{2^d(1-\cos(\tau\omega))^d(1+\omega^2)^d(\omega \pm 2k\pi/\delta)^{2d}}.$$

Since we normally choose τ as a multiplier of the δ, that is, $\tau = l\delta$ for an integer $l > 0$,

$$1 - \cos(\tau(\omega \pm 2k\pi/\delta)) = 1 - \cos(\tau\omega \pm 2k\pi l) = 1 - \cos(\tau\omega).$$

Hence

$$\frac{q(\tau,\omega)}{q(\tau,\omega \pm 2k\pi/\delta)} = \frac{\omega^{2d}(1+(\omega \pm 2k\pi/\delta)^2)^d}{(1+\omega^2)^d(\omega \pm 2k\pi/\delta)^{2d}} = \left(\frac{\omega^2}{1+\omega^2}\right)^d \cdot \frac{(1+(\omega \pm 2k\pi/\delta)^2)^d}{(\omega \pm 2k\pi/\delta)^{2d}},$$

implying

$$\begin{aligned} f_a(\omega) = \sum_{k=1}^{\infty} \Bigg[& f\left(\omega + \frac{2k\pi}{\delta}\right) \frac{(1+(\omega+2k\pi/\delta)^2)^d}{(\omega+2k\pi/\delta)^{2d}} \\ & + f\left(\omega - \frac{2k\pi}{\delta}\right) \frac{(1+(\omega-2k\pi/\delta)^2)^d}{(\omega-2k\pi/\delta)^{2d}} \Bigg] \frac{\omega^{2d}}{(1+\omega^2)^d}. \end{aligned}$$

III.2.5. Simulations for Spectral Density Estimation with Structure Function

In this section, we conduct simulations to investigate the performance of our proposed spectral density estimator given in Section 3.2.3. We will assume the underlying process to be one of the following three cases: a stationary process $\{X(t)\}$ $(d = 0)$, a stationary process with an added linear trend $\{Y(t) : Y(t) = X(t) + a + bt, a, b \in \mathbb{R}\}$ $(d = 1)$, and a stationary process with an added quadratic trend $\{Z(t) : Z(t) = X(t) + a + bt + ct^2, a, b, c \in \mathbb{R}\}$ $(d = 2)$, respectively.

First, we indicate that the above three processes $X(t), Y(t)$, and $Z(t)$ have the same covariance structure. In fact, generally, we have the following proposition. The proof of the result is straightforward, and so is skipped.

Proposition 3.5: Let $U(t) = X(t) + p(t), t \in R$ where $p(t)$ is a deterministic polynomial of t up to a certain degree. Then $Cov[U(t), U(t+h)] = Cov[X(t), X(t+h)]$, that is, $U(t)$ and $X(t)$ have the same covariance structure.

Throughout simulations, we use the Matérn covariance model for the stationary process $X(t)$ due to its flexibility and generality. Moreover, without loss of generality, we assume $E(X(t)) = 0$. According to Rasmussen and Williams (2006)[RW06], for the given Matérn class of covariance function of the form

$$C_{\text{matern}}(r) = \frac{2^{1-\nu}}{\Gamma(\nu)}\Big(\frac{\sqrt{2\nu}r}{\ell}\Big)^{\nu} K_{\nu}\Big(\frac{\sqrt{2\nu}r}{\ell}\Big), r, \nu, \ell > 0,$$

the corresponding spectral density in D-dimension of a continuous process is given by

$$f(\omega) = \frac{2^D\, \pi^{D/2}\, \Gamma(\nu + \frac{D}{2})\, (2\nu)^{\nu}}{\Gamma(\nu)\ \ell^{2\nu}} \Big(\frac{2\nu}{\ell^2} + 4\pi^2\omega^2\Big)^{-(\nu+\frac{D}{2})}.$$

For simulation, we set $\nu = 3/2$ and $\ell = 1$, so that the stationary covariance function is given by

$$C(h) = (1 + \sqrt{3}|h|)\, e^{-\sqrt{3}|h|}, h \in \mathbb{R},$$

and its corresponding theoretical spectral density function is given by

$$f_X(\omega) = \frac{2}{\pi} \cdot \frac{3^{\frac{3}{2}}}{(3 + \omega^2)^2}, \quad \omega \in \mathbb{R}.$$

Then we have the following two propositions for deriving the spectral density for the processes $\{Y(t)\}$ and $\{Z(t)\}$.

Proposition 3.6. Let $Y(t) = X(t) + a + bt$, where $X(t)$ is a stationary process with covariance function $C_X(h)$ and the corresponding spectral density function $f_X(\omega)$. Obviously, $Y(t)$ is a random process with stationary increments of order 1 with spectral density $f_Y(\omega)$. Then

$$f_Y(\omega) = f_X(\omega) \cdot \left(\frac{\omega^2}{1+\omega^2} \right).$$

PROOF: We want to derive the spectral density function for $Y(t)$, which is a random process with stationary increments of order 1. Therefore, its spectral density is given by (Zhang and Huang, 2014[ZH14]):

$$f_Y(\omega) = f_\tau(\omega) \cdot q(\tau, \omega),$$

where

$$f_\tau(\omega) = \int_{-\infty}^{\infty} D_\tau(h) e^{-ih\omega} dh, \quad q(\tau,\omega) = \frac{1}{2(1-\cos\tau\omega)} \left(\frac{\omega^2}{1+\omega^2} \right).$$

Now we notice that $D_\tau(h) = 2C_X(h) - C_X(h-\tau) - C_X(h+\tau) + (b\tau)^2$. Then we have

$$\begin{aligned}
& f_\tau(\omega) \\
= & \int_{-\infty}^{\infty} D_\tau(h) e^{-ih\omega} dh = \int_{-\infty}^{\infty} (2C_X(h) - C_X(h-\tau) - C_X(h+\tau) + (b\tau)^2) e^{-ih\omega} dh \\
= & 2\int_{-\infty}^{\infty} C_X(h) e^{-ih\omega} dh - \int_{-\infty}^{\infty} C_X(h-\tau) e^{-ih\omega} dh - \int_{-\infty}^{\infty} C_X(h+\tau) e^{-ih\omega} dh \\
= & 2f_X(\omega) - \int_{-\infty}^{\infty} C_X(u) e^{-i(u+\tau)\omega} du - \int_{-\infty}^{\infty} C_X(u) e^{-i(u-\tau)\omega} du \\
= & 2f_X(\omega) - e^{-i\tau\omega} f_X(\omega) - e^{i\tau\omega} f_X(\omega) = (2 - e^{-i\tau\omega} - e^{i\tau\omega}) f_X(\omega) \\
= & 2(1-\cos(\tau\omega)) f_X(\omega).
\end{aligned}$$

$$f_Y(\omega) = 2(1-\cos(\tau\omega)) f_X(\omega) \cdot \frac{1}{2(1-\cos\tau\omega)} \left(\frac{\omega^2}{1+\omega^2} \right) = f_X(\omega) \cdot \left(\frac{\omega^2}{1+\omega^2} \right).$$

Proposition 3.7. Let $Z(t) = X(t) + a + bt + ct^2$, where $X(t)$ is a stationary process with covariance function $C_X(h)$ and the corresponding spectral density function $f_X(\omega)$. Obviously, $Z(t)$ is a random process with stationary increments of order 2 with spectral density $f_Z(\omega)$. Then

$$f_Z(\omega) = f_X(\omega) \cdot \left(\frac{\omega^2}{1+\omega^2} \right)^2.$$

The proof of this proposition is straightforward, similar to the one for Proposition 3.6, which is skipped here.

Now we consider the analysis on aliasing effect from Section 3.2.4 under three scenarios. Recall that the spectral density function based on the discretized time series is given by

$$f_\delta(\omega) = f(\omega) + f_a(\omega), \quad \omega \in (-\pi/\delta, \pi/\delta]. \tag{III.9}$$

Here the theoretical spectral densities $f(\omega)$ are $f_X(\omega)$ (for $d = 0$), $f_Y(\omega)$ (for $d = 1$), and $f_Z(\omega)$ (for $d = 2$), respectively. Next we provide the aliasing effect in detail on the above scenarios.

First, if $d = 0$, that is, $X(t)$ itself is stationary. (III.8) reduces to (III.5) and the spectral density function of $X(t)$ is given by

$$\begin{aligned} f_\delta(\omega) &= \sum_{k=-\infty}^{\infty} f_X\left(\omega + \frac{2k\pi}{\delta}\right), \quad \omega \in (-\pi/\delta, \pi/\delta] \\ &= f_X(\omega) + \sum_{k=1}^{\infty} \left[f_X\left(\omega + \frac{2k\pi}{\delta}\right) + f_X\left(\omega - \frac{2k\pi}{\delta}\right) \right], \end{aligned}$$

where

$$f_a(\omega) = \sum_{k=1}^{\infty} \left[f_X\left(\omega + \frac{2k\pi}{\delta}\right) + f_X\left(\omega - \frac{2k\pi}{\delta}\right) \right].$$

Next if $Y(t) = X(t) + a + bt$, where $X(t)$ is stationary with spectral density function $f_X(\omega)$, and so the spectral density function of $Y(t)$ is given by

$$f_Y(\omega) = f_X(\omega)\left(\frac{\omega^2}{1+\omega^2}\right).$$

Therefore,

$$f(\omega \pm 2k\pi/\delta) = f_Y(\omega \pm 2k\pi/\delta) = f_X(\omega \pm 2k\pi/\delta)\left(\frac{(\omega \pm 2k\pi/\delta)^2}{1+(\omega \pm 2k\pi/\delta)^2}\right).$$

Hence, we have,

$$f_a(\omega) = \sum_{k=1}^{\infty}\left(f_X(\omega + 2k\pi/\delta) + f_X(\omega - 2k\pi/\delta)\right)\left(\frac{\omega^2}{1+\omega^2}\right),$$

and

$$\begin{aligned} f_\delta(\omega) &= f_Y(\omega) + \sum_{k=1}^{\infty}\left(f_X(\omega + 2k\pi/\delta) + f_X(\omega - 2k\pi/\delta)\right)\left(\frac{\omega^2}{1+\omega^2}\right) \\ &= \sum_{k=-\infty}^{\infty} f_X(\omega + 2k\pi/\delta)\left(\frac{\omega^2}{1+\omega^2}\right). \end{aligned} \tag{III.10}$$

Finally, if $Z(t) = X(t) + a + bt + ct^2$ is considered, which is a the stationary process with an added quadratic trend (therefore, it is the process with stationary increments of order 2), we have

$$f_\delta(\omega) = f_Z(\omega) + f_a(\omega), \quad -\pi/\delta < \omega \leq \pi/\delta,$$

with the aliasing effect component given by

$$f_a(\omega) = \sum_{k=1}^{\infty}\left(f_X(\omega + 2k\pi/\delta) + f_X(\omega - 2k\pi/\delta)\right)\left(\frac{\omega^2}{1+\omega^2}\right)^2.$$

Simulations are conducted with sample size $n = 100$ and repeated for 1000 iterations. The estimated spectral density $\hat{f}_\delta(\cdot)$ (red points) through the estimated structure function $\hat{D}_\tau(h)$ are plotted together with the theoretical spectral density $f(\omega)$ (green curve) for the corresponding continuous processes. Throughout this dissertation, due to the symmetry of the spectral density at $\omega = 0$, we only compare the spectral density functions for $\omega > 0$. Figures III.5-III.10 are the simmulation results for the processes $\{X(t)\}$, $\{Y(t)\}$ and $\{Z(t)\}$, respectively.

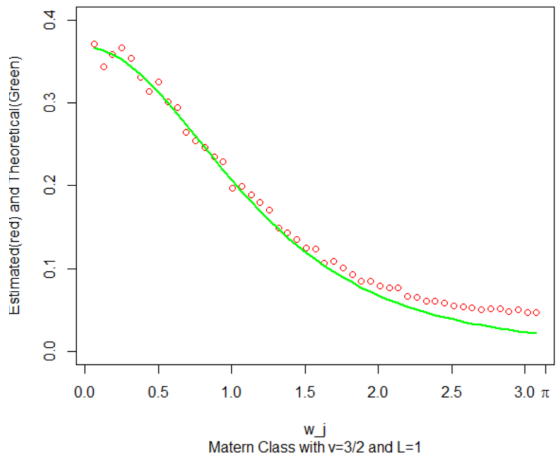

Figure 15. Comparison of the Estimated and Theoretical Spectral Density Values under Stationarity

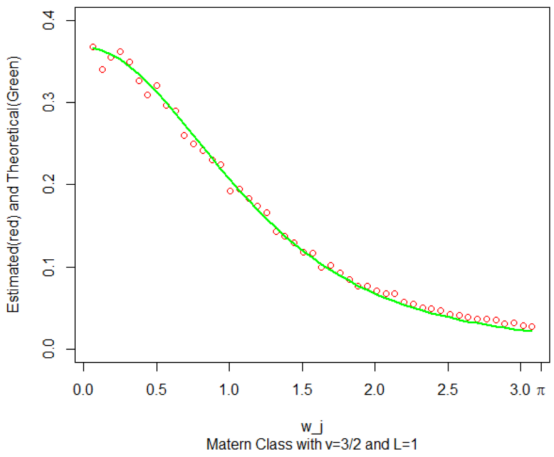

Figure 16. Comparison of the Estimated and Theoretical Spectral Density Values under Stationarity, After Removing the Aliasing Effect.

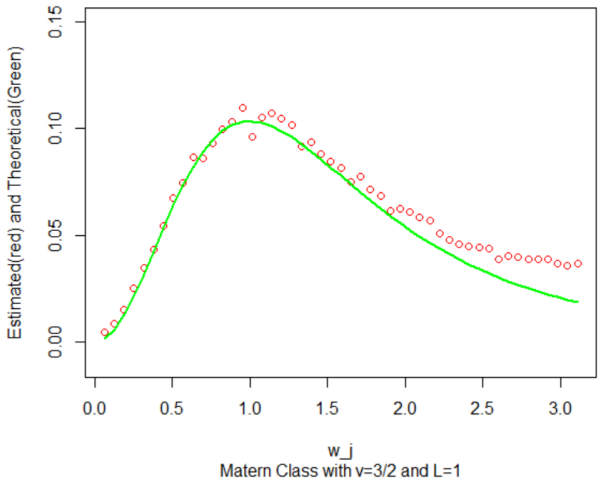

Figure 17. Comparison of the Estimated and Theoretical Spectral Density under Stationarity with an Added Linear Trend.

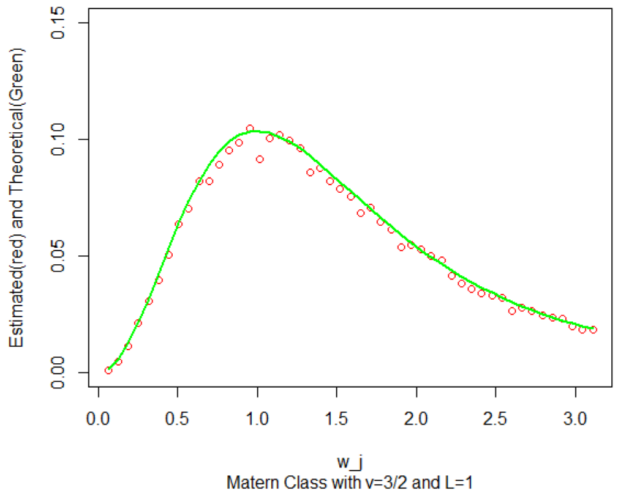

Figure 18. Comparison of the Estimated and Theoretical Spectral Density Values under Stationarity with an Added Linear Trend, After Removing the Aliasing Effect.

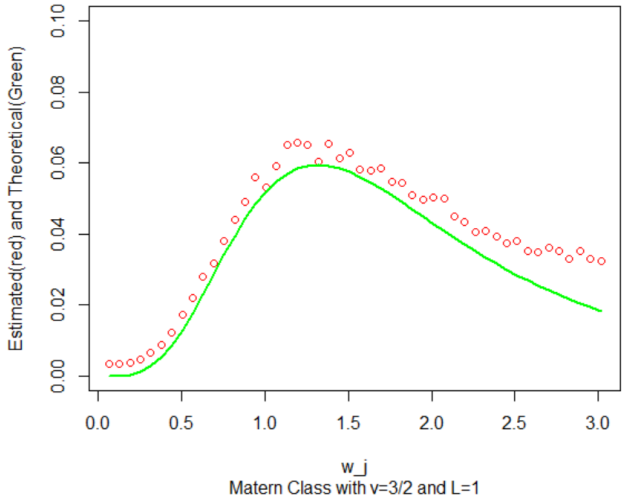

Figure 19. Comparison of the Estimated and Theoretical Spectral Density Values under Stationarity with an Added Quadratic Trend.

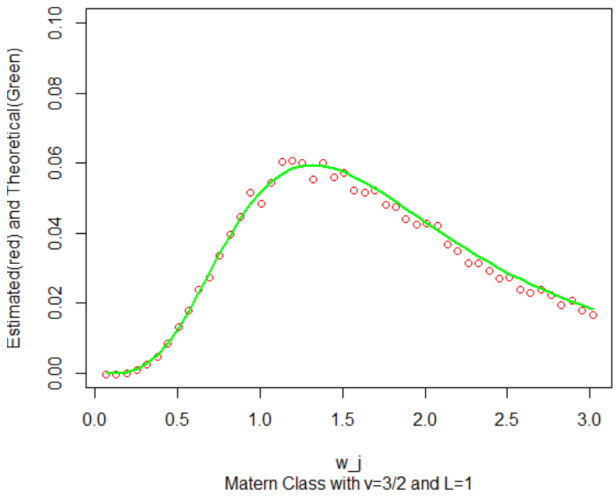

Figure 20. Comparison of the Estimated and Theoretical Spectral Density Values under Stationarity with an Added Quadratic Trend, After Removing the Aliasing Effect.

The above graphs show that under all these three cases, there is a shift (especially the tail of the curve) between the estimated $\hat{f}_\delta(\omega)$ and theoretical spectral densities $f(\omega)$ for $\omega \in (-\pi, \pi]$, especially on the high frequencies, which is due to the aliasing effect. After removing the aliasing effect, the estimated spectral densities $f_\delta(\omega)$ match very well with the theoretical spectral densities for the continuous processes $\{X(t)\}$, $\{Y(t)\}$ and $\{Z(t)\}$, respectively. Therefore, the proposed estimator for the spectral density through the estimation of structure function performs well for all these three processes.

Remark: The results in this dissertation are based on the simulations with sample size $n = 100$. We also conducted simulations with exponential model when the sample size $n = 20$, the results are similar. However, when $n = 20$ with Matérn model $\nu = 3/2$ and $\ell = 1$, the simulation results are not as good as what we expected. The minimum requirement of the sample size needs further investigation.

III.3. Spectral Density Estimation Through Structure Function for Band-Limited Continuous Processes

It would be ideal, of course, if all the frequencies outside the band $-\pi/\delta < \omega \leq \pi/\delta$ made no contribution at all to the process $X(t)$, so that the aliasing effect would be eliminated and the spectral density can be estimated as accurately as possible. One of the best known methods for anti-aliasing is to apply the Nyquist Theorem which is also related to the Nyquist interval or Nyquist frequency, and correspondingly a more practical alternative is to limit the bandwidth of the signal processes (Olshausen, 2000)[Ols00].

A band-limited process is a random process whose power-spectral density occupies a finite bandwidth. In other words, a band-limited process is a process with the spectral density within the band range, and zero otherwise. In real life situations, almost all of the processes in nature are band-limited because for most of the physical systems, there always exists a bandwidth limit.

Therefore, the case of the so-called band-limited random process $X(t)$ is of special interest from the point of view of using the discrete sample. In this section, we first assume the underlying process $Y(t)$ to be the random process with stationary increments of order 1, in particular, we assume $Y(t) = X(t) + a + bt$, where a and b are constants, $X(t)$ is stationary, and it (and so $Y(t)$) has the band-limited spectral density function $f(\omega)$ with support $\omega \in (-\pi, \pi]$. We then discuss how the sampling frequencies affect the estimates of the true spectral density. Finally we conduct simulations to demonstrate how our proposed spectral density estimator performs under various of sampling frequencies.

III.3.1. Sampling Frequencies and Aliasing Effect

In this section, the aliasing effect for the stationary process with an added linear trend is discussed with different step sizes at $\delta = 1$, $\delta = 1/2$, and $\delta = 2$. Here we consider that the spectral density function for the continuous stationary process $\{X(t)\}$, noted as $f_X(\omega)$ is band-limited with support $-\pi < \omega \leq \pi$. Then by Proposition 3.6, the spectral density function for the stationary process with an added linear trend $\{Y(t) = X(t) + a + bt, a, b \in \mathbb{R}\}$, noted as $f_Y(\omega)$, is given by

$$f_Y(\omega) = f_X(\omega)\left(\frac{\omega^2}{1+\omega^2}\right), -\pi < \omega \leq \pi.$$

Let $C(h)$ be the covariance function for $X(t)$ (and so for $Y(t)$), then through the inverse Fourier transform, we have

$$C(h) = \int_{-\infty}^{\infty} f_X(\omega)e^{i\omega h}d\omega = \int_{-\pi}^{\pi} f_X(\omega)e^{i\omega h}dh.$$

Now observations of a continuous process of stationary increments of order 1 ($\{Y(t)\}$) is carried out only at uniformly spaced time points δ units apart, denoted as $\{Y(t_k) = Y_k : t_k = k\delta, k = 0, \pm 1, \pm 2, \cdots .\}$.

Then refer to (III.10), with any $\delta > 0$, the spectral density function for the discretized sample of the process $\{Y(t)\}$ is given as

$$\begin{aligned} f_\delta(\omega) &= f_Y(\omega) + \sum_{k=1}^{\infty}(f_X(\omega + 2k\pi/\delta) + f_X(\omega - 2k\pi/\delta))\left(\frac{\omega^2}{1+\omega^2}\right) \\ &= \sum_{k=-\infty}^{\infty} f_X(\omega + 2k\pi/\delta)\left(\frac{\omega^2}{1+\omega^2}\right), \end{aligned}$$

where the corresponding aliasing effect is given by

$$f_a(\omega) = \sum_{k=1}^{\infty}(f_X(\omega + 2k\pi/\delta) + f_X(\omega - 2k\pi/\delta))\left(\frac{\omega^2}{1+\omega^2}\right).$$

In particular, if the step size is $\delta = 1$, the spectrum of observations $\{Y_k : k = 0, \pm 1, \pm 2, \cdots\}$ is concentrated within $-\pi/\delta < \omega \leq \pi/\delta \Rightarrow \omega \in (-\pi, \pi]$, which is exactly the same with the bandwidth. Therefore, there will not be any aliasing effect existed for this case. Then the estimated spectral density $f_\delta(\omega)$ should be able to recover the true spectral density of the continuous process $\{Y(t)\}$, that is

$$f_\delta(\omega) = \begin{cases} f_Y(\omega), & -\pi < \omega \leq \pi \\ 0, & \text{otherwise.} \end{cases}$$

If the step size $\delta = 1/2$, the spectrum of observations $\{Y_k : k = 0, \pm 1, \pm 2, \cdots\}$ is concentrated within $-\pi/\delta < \omega \leq \pi/\delta \Rightarrow \omega \in (-2\pi, 2\pi]$, which is larger than the bandwidth $(-\pi, \pi]$. Then there will still not be any aliasing effect existed for this case.

Therefore, the estimated spectral density $f_\delta(\omega)$ can recover the true spectral density of the continuous process $\{Y(t)\}$, that is

$$\begin{aligned} f_\delta(\omega) &= \begin{cases} f_Y(\omega) & -2\pi < \omega \leq 2\pi \\ 0 & \text{otherwise.} \end{cases} \\ &= \begin{cases} f_Y(\omega) & -\pi < \omega \leq \pi, \quad \text{since the support of } f_Y(\omega) \text{ is on } (-\pi, \pi) \\ 0 & \text{otherwise.} \end{cases} \end{aligned}$$

If the step size $\delta = 2$, the spectrum of observations $\{Y_k : k = 0, \pm 1, \pm 2, \cdots\}$ is concentrated within $-\pi/\delta < \omega \leq \pi/\delta \Rightarrow \omega \in (-\pi/2, \pi/2]$, which is smaller than the bandwidth $(-\pi, \pi]$.

Then refer to (III.10), when $\omega \in [0, \pi/2]$, $f_X(\omega - \pi)\left(\frac{\omega^2}{1+\omega^2}\right)$ will be added to the true spectral density of $\{Y(t)\}$, and when $\omega \in (-\pi/2, 0)$, $f_X(\omega + \pi)\left(\frac{\omega^2}{1+\omega^2}\right)$ will be added to the true spectral density of $\{Y(t)\}$, both leading to the aliasing effect. More explicity,

$$f_\delta(\omega) = \begin{cases} f_Y(\omega) + f_X(\omega - \pi)\left(\frac{\omega^2}{1+\omega^2}\right), & \omega \in [0, \pi/2] \\ f_Y(\omega) + f_X(\omega + \pi)\left(\frac{\omega^2}{1+\omega^2}\right), & \omega \in (-\pi/2, 0) \\ 0 & \text{otherwise.} \end{cases}$$

Therefore, we can only estimate $f_Y(\omega)$ in the frequency range $(-\pi/2, \pi/2]$, and the estimated $\hat{f}_Y(\omega)$ is "contaminated" with either $f_X(\omega - \pi)\left(\frac{\omega^2}{1+\omega^2}\right)$ when $\omega \in [0, \pi/2]$ or $f_X(\omega + \pi)\left(\frac{\omega^2}{1+\omega^2}\right)$ when $\omega \in (-\pi/2, 0)$.

In summary, from the above three cases, we need to choose $\delta \leq 1$ to avoid the aliasing effect when a band-limited spectral function of a continuous process has the support of $(-\pi, \pi]$. In general, given a band-limited spectral function supported on $(-\omega_c, \omega_c]$, we need to choose a proper sample rate in order to avoid the aliasing effect. This is related to the well-known Nyquist theorem, which indicates that a band-limited continuous-time signal can be sampled and perfectly reconstructed from its samples if the sampling frequency is at least twice of the highest frequency of the band, and this theorem provided us a detailed instruction for the proper sampling frequency.

III.3.2. Simulation Results

Here we investigate our proposed spectral estimator under various sampling frequencies through simulations. We assume that the underlying process $X(t)$ is stationary with band-limited Matérn covariance function with $\nu = 3/2$ and $\ell = 1$, supported on $(-\pi, \pi]$. More specifically, we assume

$$f_X(\omega) = \begin{cases} \frac{2}{\pi} \cdot \frac{3^{\frac{3}{2}}}{(3+\omega^2)^2}, & -\pi < \omega \leq \pi \\ \\ 0, & \text{otherwise.} \end{cases}$$

By the inverse Fourier transform, the covariance function of $X(t)$ is given by

$$\begin{aligned} C_X(h) &= \int_{-\infty}^{\infty} f_X(\omega) e^{i\omega h} d\omega = \int_{-\pi}^{\pi} f_X(\omega) e^{i\omega h}\, d\omega \\ &= \frac{2}{\pi} \cdot 3^{\frac{3}{2}} \int_{-\pi}^{\pi} \frac{1}{(3+\omega^2)^2} (\cos h\omega + i \sin h\omega)\, d\omega \\ &= \frac{4}{\pi} \cdot 3^{\frac{3}{2}} \int_{0}^{\pi} \frac{\cos(h\omega)}{(3+\omega^2)^2}\, d\omega \end{aligned}$$

No closed form is available to integrate the above integral. We pursue a numerical approximation on $C_X(h)$ to be used in our simulations.

We now consider $Y(t) = X(t) + 1 + t$, which is now the process with stationary increments of order 1. The data generation for simulations follows exactly the same as what was proposed in Section 3.3, except that the covariance values to generate the data are given through numerical approximation given above.

For $\delta = 1$ and $\delta = 1/2$, as shown previously in Section 3.3.1, we have the proposition that the estimated spectral densities $f_\delta(\omega)$ under both cases can recover the true spectral density $f_Y(\omega)$, for $\omega \in (-\pi, \pi]$.

$$f_\delta(\omega) = \begin{cases} f_Y(\omega), & -\pi < \omega \leq \pi \\ 0, & \text{otherwise.} \end{cases} = \begin{cases} \frac{2}{\pi} \frac{3^{\frac{3}{2}}}{(3+\omega^2)^2} \left(\frac{\omega^2}{1+\omega^2} \right), & -\pi < \omega \leq \pi \\ 0, & \text{otherwise.} \end{cases}$$

Simulations are conducted with sample size $n = 100$ and repeated for 1000 iterations. Figure III.11 and Figure III.12 are the simulation results for $\delta = 1$ and $\delta = 1/2$, respectively.

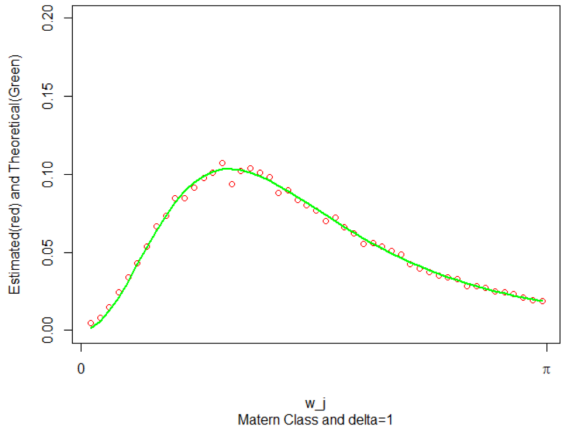

Figure 21. The Estimated and Theoretical Values of a Band-limited Spectral Density for Stationary Process with an Added Linear Trend, with $\delta = 1$.

Figure III.11 and Figure III.12 demonstrated the conclusions as what we expected from our propositions. That is, when $\delta = 1$ and $\delta = 1/2$, the aliasing effect will be eliminated when estimating the spectral density through the structure function $D_\tau(h)$.

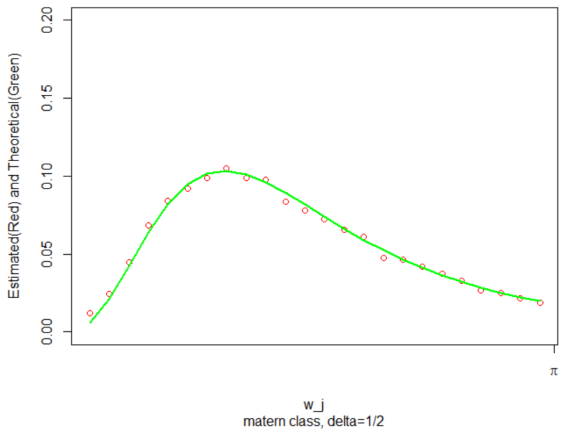

Figure 22. The Estimated and Theoretical Values of a Band-limited Spectral Density for Stationary Process with an Added Linear Trend, with $\delta = 1/2$.

The following graphs are the simulation results for $\delta = 2$.

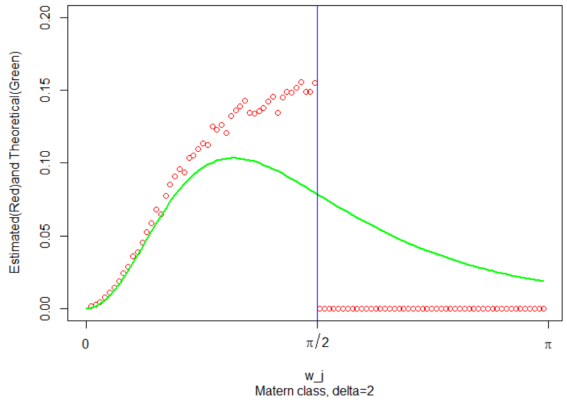

Figure 23. The Estimated and Theoretical Values of a Band-limited Spectral Density for Stationary Process with an Added Linear Trend, with $\delta = 2$.

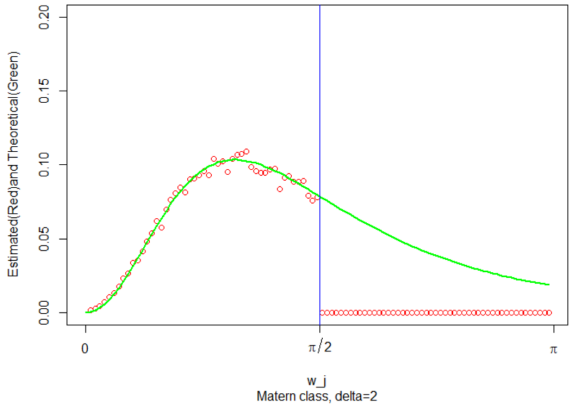

Figure 24. The Estimated and Theoretical Values of a Band-limited Spectral Density for Stationary Process with an Added Linear Trend, with $\delta = 2$, After Removing the Aliasing Effect.

The above graphs indicate that when $\delta = 2$, the aliasing effect exists. After removing the aliasing effect, as we expected, the estimated spectral density matches well with the true theoretical spectral density.

Similar simulations are also conducted for a stationary process with added quadratic trend. The same conclusion can also be made regarding the performance of our proposed spectral density estimator.

III.4. Conclusions and Discussions

In this chapter, we propose a non-parametric spectral density estimation method for estimating the underlying spectral density when the random process is with stationary increments. The method is based on the inversion formula such that the spectral density can be represented by a non-negative definite structure function. We perform simulation studies to estimate the spectral density function when the underlying process is the stationary process with added either a linear trend or quadratic trend. It is noted that when observations are sampled over a continuous process on $\mathbb{R}$, the aliasing effect needs to be considered. Our results show the estimated spectral

density matches well with the theoretical counterpart, after removing any potential aliasing effect. Our proposed method will be further discussed in Chapter 4 when the underlying process is an intrinsically stationary process as well as applied for data analysis in Chapter 5.

CHAPTER IV

SPECTRAL DENSITY FUNCTIONS AND ESTIMATION FOR POPULARLY USED VARIOGRAMS

In Chapter 2, when a process is stationary, estimation of the spectral density could be obtained by periodograms from the covariance function through the inverse of Fourier transformation. In parallel, when a process is intrinsically stationary, one can also obtain the spectral density through the variogram function. However, there are limited results for estimating the spectral density through a variogram estimator in the literature, which is possibly due to the difficulty in verifying/guaranteeing the conditionally nonnegative positiveness of a variogram estimator. In this chapter, we first show that intrinsic stationarity implies the stationarity increments of order 1. In Section 4.2, we derive the spectral densities for some commonly used variogram models through the structure function $D_\tau(h)$. Lastly in Section 4.3, we apply the spectral density estimation method in Chapter 3 to the intrinsically stationary process with power variogram models.

Before we compute the spectral densities through the structure function, we will first prove the following proposition. The proposition provides the basis for our estimation method through the rest of this chapter.

Proposition 4.1: Intrinsically Stationary Process $\Rightarrow$ Process with stationary increments of order 1.

PROOF: Assume that $\{X(t)\}$ is an intrinsically stationary process, then by definition, $Var[X(t+\tau) - X(t)] = 2\gamma(\tau)$, a function depending only on the displacement τ. In addition, we have that $E(X(t)) = \mu$, a constant, implying $E(\Delta_\tau X(t)) = 0$.

Now with the following identity,

$$(a-b)(c-d) = \frac{1}{2}((a-d)^2 + (c-b)^2 - (a-c)^2 - (b-d)^2),$$

we have,

$$\begin{aligned}
& Cov(\Delta_\tau X(t+h), \Delta_\tau X(t)) \\
= \; & E[(X(t+h+\tau) - X(t+h)][(X(t+\tau) - X(t)] \\
= \; & \frac{1}{2}\Big[E(X(t+h+\tau) - X(t))^2 + E(X(t+h) - X(t+\tau))^2 \\
& -E(X(t+h+\tau) - X(t+\tau))^2 - E(X(t+h) - X(t))^2\Big] \\
= \; & \frac{1}{2}\Big[2\gamma(h+\tau) + 2\gamma(h-\tau) - 2\gamma(h) - 2\gamma(h)\Big] \\
= \; & \gamma(h+\tau) + \gamma(h-\tau) - 2\gamma(h),
\end{aligned}$$

which is a function of τ and h, denoted as $D_\tau(h)$. Hence $\Delta_\tau X(t)$ is a process with stationary increment of order 1, concluding the proof of this proposition.

Remark: From the above proof, we note the following relationship between $D_\tau(h)$ and $\gamma(\tau)$, which will be extensively used later:

$$D_\tau(0) = 2\gamma(\tau), \text{ and } D_\tau(h) = \gamma(h+\tau) + \gamma(h-\tau) - 2\gamma(h).$$

IV.1. Spectral Densities for Commonly Used Variogram Functions

In this section, we first introduce the procedure based on the inversion formula given in Zhang and Huang (2014)[ZH14] to calculate the spectral density for a given variogram function. Then we apply the procedure to derive the spectral density functions for commonly used variogram models, including exponential, power, spherical, hole-effect etc. Finally we give some discussion to generate the results.

According to Zhang and Huang (2014)[ZH14], the spectral density for a given variogram function $\gamma(u)$ is given by

$$\begin{aligned} f(\omega) &= \frac{1}{2\pi}\left(\lim_{T\to\infty}\int_{-T}^{T}(\gamma(u+\tau)+\gamma(u-\tau) \right. \\ &\qquad \left. -2\gamma(u))\cos(u\omega)du\right)\frac{1}{2(1-\cos(\tau(\omega))}\left(\frac{\omega^2}{1+\omega^2}\right) \\ &= \frac{1}{2\pi}\left(\int_{0}^{\infty}(\gamma(u+\tau)+\gamma(u-\tau)-2\gamma(u))\cos(u\omega)du\right)\frac{1}{1-\cos(\tau\omega)}\left(\frac{\omega^2}{1+\omega^2}\right), \end{aligned}$$

since $\gamma(u)=\gamma(-u)$ is symmetric at $u=0$.

Note that the above calculation involves the following two steps.

1. Show that

$$\lim_{T\to\infty}\int_{-T}^{T}(\gamma(u+\tau)+\gamma(u-\tau)-2\gamma(u))\cos(u\omega)du,$$

   or in particular

$$\int_{0}^{\infty}(\gamma(u+\tau)+\gamma(u-\tau)-2\gamma(u))\cos(u\omega)du$$

   exists for each given variogram function.

2. Note that the spectral density function $f(\omega)$ does not depend on τ. Hence, we will take $\tau\to 0$ to derive the spectral density function.

Now we derive the spectral density function for each of commonly used variogram functions.

IV.1.1. Spherical Variogram

The spherical variogram is given by, for $h \geq 0$, $c_s, a_s > 0$.

$$\gamma(h) = \begin{cases} c_s \left(\frac{3}{2} \left(\frac{h}{a_s} \right) - \frac{1}{2} \left(\frac{h}{a_s} \right)^3 \right), & 0 < h < a_s \\ c_s, & h \geq a_s, \end{cases}$$

Proposition 4.2. The spectral density function for the above spherical variogram is given by

$$f(\omega) = \frac{3c_s}{2\pi\omega^2 a_s^3} \left((\omega a_s - \sin(\omega a_s))^2 + (1 - \cos(\omega a_s))^2 \right) \cdot \left(\frac{1}{1+\omega^2} \right).$$

PROOF: We go through the above two steps. Note that

$$\begin{aligned} & \gamma(u+\tau) + \gamma(u-\tau) - 2\gamma(u) \\ = & \begin{cases} c_s \left(\frac{3}{a_s} (\tau - u) - \frac{1}{a_s^3} (\tau^3 - u^3 + 3u^2\tau) \right), & 0 < u < \tau, \\ c_s \left(-\frac{1}{a_s^3} (3u\tau^2) \right), & u \geq \tau, \\ 0, & u \geq a_s. \end{cases} \end{aligned}$$

Obviously, $\int_0^\infty (\gamma(u+\tau) + \gamma(u-\tau) - 2\gamma(u)) \cos(u\omega) du$ exists, and it is given by

$$\begin{aligned} & \int_0^\infty (\gamma(u+\tau) + \gamma(u-\tau) - 2\gamma(u)) \cos(u\omega) du \\ = & c_s \int_0^\tau \left(\frac{3}{a_s} (\tau - u) - \frac{1}{a_s^3} \left(\tau^3 - u^3 + 3u^2\tau \right) \right) \cos(u\omega) du \\ & -c_s \int_\tau^{a_s} \frac{1}{a_s^3} \left(3u\tau^2 \right) \cos(u\omega) du \\ = & c_s \left(\frac{3}{a_s} \frac{1 - \cos(\omega\tau)}{\omega^2} - \frac{1}{a_s^3} \left(\frac{3\left(\omega^2\tau^2 + 2\right)\left(\omega\tau \sin(\omega\tau) - 1\right) + 6\cos(\omega\tau)}{\omega^4} \right) \right) \\ & -c_s \left(\frac{1}{a_s^3} \frac{3\tau^2 \left(\omega a_s \sin\left(\omega a_s\right) + \cos\left(\omega a_s\right) - \omega\tau \sin(\omega\tau) - \cos(\omega\tau) \right)}{\omega^2} \right) \end{aligned}$$

Since $f(\omega)$ does not depend on τ, after the above term is divided by $(1-\cos(\omega\tau))$, we let $\tau \to 0$ to have

$$f(\omega) = \frac{c_s}{2\pi}\left(\frac{3}{a_s}\frac{1}{\omega^2} - \frac{II}{a_s^3} - \frac{III}{a_s^3}\right)\left(\frac{\omega^2}{1+\omega^2}\right),$$

$$\begin{aligned}
II &= \lim_{\tau\to 0}\left(\frac{3\left(\omega^2\tau^2+2\right)\left(\omega\tau\sin(\omega\tau)-1\right)+6\cos(\omega\tau)}{\omega^4}\right)\frac{1}{1-\cos(\omega\tau)} \\
&= \lim_{\tau\to 0}\left(\frac{3\omega^2\tau^2(\omega\tau\sin(\omega\tau)-1)}{\omega^4(1-\cos(\omega\tau))} + \frac{6\omega\tau\sin(\omega\tau)}{\omega^4(1-\cos(\omega\tau))} - \frac{6(1-\cos(\omega\tau))}{\omega^4(1-\cos(\omega\tau))}\right) \\
&= -\frac{6}{\omega^4} + \frac{12}{\omega^4} - \frac{6}{\omega^4} = 0. \\
III &= \lim_{\tau\to 0}\frac{3\tau^2\left(\omega a_s\sin\left(\omega a_s\right)+\cos\left(\omega a_s\right)-\omega\tau\sin(\omega\tau)-\cos(\omega\tau)\right)}{\omega^2}\frac{1}{1-\cos(\omega\tau)} \\
&= \frac{6\left(\omega a_s\sin\left(\omega a_s\right)+\cos\left(\omega a_s\right)-1\right)}{\omega^4}.
\end{aligned}$$

Hence, the spectral density function for spherical variogram is given by

$$\begin{aligned}
f(\omega) &= \frac{3c_s}{2\pi\omega^4 a_s^3}\left(\omega^2a_s^2 - 2\omega a_s\sin(\omega a_s) - 2\cos(\omega a_s) + 2\right)\left(\frac{\omega^2}{1+\omega^2}\right) \\
&= \frac{3c_s}{2\pi\omega^4 a_s^3}\left(\omega^2a_s^2 - 2\omega a_s\sin(\omega a_s) - 2\cos(\omega a_s)\right. \\
&\qquad\qquad \left.+1+\cos^2(\omega a_s)+\sin^2(\omega a_s)\right)\left(\frac{\omega^2}{1+\omega^2}\right) \\
&= \frac{3c_s}{2\pi\omega^2 a_s^3}\left((\omega a_s-\sin(\omega a_s))^2+(1-\cos(\omega a_s))^2\right)\left(\frac{1}{1+\omega^2}\right).
\end{aligned}$$

IV.1.2. Rational Quadratic Variogram:

The rational quadratic variogram is given by

$$\gamma(h) = c_r \frac{h^2}{1 + h^2/a_r}, h \neq 0, c_r, a_r > 0$$

Proposition 4.3. The spectral density function for the above rational quadratic variogram is given by

$$f(\omega) = \frac{c_r a_r^{3/2}}{2} e^{-\sqrt{a_r}\omega} \left(\frac{\omega^2}{1+\omega^2} \right).$$

The proof is straightforward but tedious, which is given in the Appendix.

IV.1.3. Exponential Variogram

The Exponential variogram is given by

$$\gamma(h) = \begin{cases} 0, & h = 0 \\ c_e \left(1 - \exp(-h/a_e)\right), & h \neq 0, \end{cases}$$

with $c_e, a_e > 0$. Then we have

Proposition 4.4. The spectral density function for the above exponential variogram function is given by

$$f(\omega) = \frac{a_e c_e}{\pi} \frac{1}{1 + a_e^2 \omega^2} \left(\frac{\omega^2}{1+\omega^2} \right).$$

Again, the proof of the above proposition is straightforward but tedious. We leave it in the Appendix.

IV.1.4. Discussions

The above calculations (as well as the calculation of the spectral density for the power variogram $2\gamma(h) = |h|^\alpha, 0 < \alpha < 2$ in Zhang and Huang (2014)[ZH14]) lead us to consider a more general result regarding the derivation of the spectral density function.

First, it has been noted, for example Yaglom (1987)[Yag87], that if $2\gamma(h)$ is the variogram of an intrinsically stationary process,

$$\lim_{h\to\infty} \frac{2\gamma(h)}{|h|^2} = 0.$$

That is, the variogram function $\gamma(h) = o(|h|^2)$.

Now we consider the following two cases, where $\gamma(h) = O(|h|^\alpha)$, for $0 \le \alpha < 1$ and $1 < \alpha < 2$. Here is the result we propose for future research.

Remark. Under further assumptions on $\gamma(h)$, we have

Let $\gamma(h) = O(|h|^\alpha)$, for $1 < \alpha < 2$. If we assume that $\gamma(\tau)$ has continuous second derivative for $\tau > 0$, and

$$0 \le \int_0^\infty \cos(u\omega)\gamma''(u)du < \infty.$$

Then the spectral density $f(\omega)$ is given by the following equation,

$$f(\omega) = \frac{1}{\pi(1+\omega^2)} \int_0^\infty \cos(u\omega)\gamma''(u)du, \quad \omega > 0.$$

Let $\gamma(h) = O(|h|^\alpha)$, for $0 < \alpha < 1$. If we assume that $\gamma(\tau)$ has continuous first derivative for $\tau > 0$, and

$$0 \leq \int_0^\infty \sin(u\omega)\gamma'(u)du < \infty.$$

Then the spectral density $f(\omega)$ is given by the following equation,

$$f(\omega) = \frac{\omega}{\pi(1+\omega)} \int_0^\infty \sin(u\omega)\gamma'(u)du, \quad \omega > 0.$$

Now we derive Propositions 4.2 - 4.4 by applying the above conjectures.

Power variogram. The power variogram is given by $2\gamma(h) = h^\alpha$, $h > 0$ and $0 < \alpha < 2$. First, for $1 < \alpha < 2$, since

$$\gamma"(h) = \frac{\alpha(\alpha-1)}{2} h^{\alpha-2}$$

and

$$\begin{aligned}
\int_0^\infty \gamma"(u)\cos(u\omega)du &= \frac{\alpha(\alpha-1)}{2} \int_0^\infty \frac{\cos(u\omega)}{u^{2-\alpha}}du \\
&= \frac{\alpha(\alpha-1)}{2} \frac{\Gamma(\alpha-1)}{\omega^{\alpha-1}} \cos((\alpha-1)\pi/2) \\
&= \frac{\Gamma(\alpha+1)}{2} \frac{\sin(\alpha\pi/2)}{\omega^{\alpha-1}} > 0,
\end{aligned}$$

and due to the following formula provided by Gradshteyn and Ryzhik (2007)[GR14],

$$\int_0^\infty \frac{\cos(ax)}{x^{1-\mu}}dx = \frac{\Gamma(\mu)}{a^\mu}\cos(\mu\pi/2), \quad 0 < \mu < 1.$$

Hence, for the power model with $1 < \alpha < 2$, (we choose $\mu = \alpha - 1$ in the above identity)

$$f(\omega) = \frac{1}{\pi(1+\omega^2)} \frac{\Gamma(\alpha+1)}{2} \frac{\sin(\alpha\pi/2)}{\omega^{\alpha-1}} = \frac{\Gamma(\alpha+1)}{2\pi(1+\omega^2)} \frac{\sin(\alpha\pi/2)}{\omega^{\alpha-1}}.$$

When $0 < \alpha < 1$, we have $\gamma'(h) = \frac{\alpha}{2} h^{\alpha-1}$, and

$$\begin{aligned} \int_0^\infty \gamma'(u) \sin(u\omega) du &= \frac{\alpha}{2} \int_0^\infty \frac{\sin(u\omega)}{u^{1-\alpha}} du \\ &= \frac{\alpha}{2} \frac{\Gamma(\alpha)}{\omega^\alpha} \sin(\alpha\pi/2) = \frac{\Gamma(\alpha+1)}{2} \frac{\sin(\alpha\pi/2)}{\omega^\alpha} > 0, \end{aligned}$$

Therefore, based on the following ((3.761.4) formula provided by Gradshteyn and Ryzhik (2007)[GR07]), we have

$$\int_0^\infty \frac{\sin(ax)}{x^{1-\mu}} dx = \frac{\Gamma(\mu)}{a^\mu} \sin(\mu\pi/2), \quad 0 < \mu < 1.$$

Hence, when $0 < \alpha < 1$, (we choose $\mu = \alpha$)

$$f(\omega) = \frac{\omega}{\pi(1+\omega^2)} \frac{\Gamma(\alpha+1)}{2} \frac{\sin(\alpha\pi/2)}{\omega^\alpha} = \frac{\Gamma(\alpha+1)}{2\pi(1+\omega^2)} \frac{\sin(\alpha\pi/2)}{\omega^{\alpha-1}}.$$

In summary, when $0 < \alpha < 2, \alpha \neq 1$,

$$f(\omega) = \frac{\Gamma(\alpha+1)}{2\pi(1+\omega^2)} \frac{\sin(\alpha\pi/2)}{\omega^{\alpha-1}}.$$

This matches with what has been given in Zhang and Huang (2014).

Remark: When $\alpha = 1$, the conjecture seems not working. We need to calculate it directly through the structure function $D_\tau(h) = (\tau - |u|) I_{|u|<\tau}$ as given in Zhang and Huang (2014).

Spherical variogram. We note that $\gamma(h) = o(|h|^\alpha)$ with $0 < \alpha < 1$. We apply the second part of the proposition. We have $\gamma'(h) = c_s\left(\frac{3}{2}\left(\frac{1}{a_s}\right) - \frac{3}{2}\left(\frac{h^2}{a_s^3}\right)\right)$. Moreover,

$$\begin{aligned}\int_0^\infty \sin(u\omega)\gamma'(u)du &= \frac{3c_s}{2a_s^3}\int_0^{a_s}\sin(u\omega)\left(a_s^2-u^2\right)du \\ &= \frac{3c_s}{2a_s^3}\left(\frac{2+a_s^2\omega^2-2\cos(a_s\omega)+2a_s\omega\sin(a_s\omega)}{\omega^3}\right) \\ &= \frac{3c_s}{2a_s^3}\left(\frac{(1-\cos(a_s\omega))^2+(a_s\omega-\sin(a_s\omega))^2}{\omega^3}\right).\end{aligned}$$

The spectral density is then given by

$$f(\omega) = \frac{3c_s}{2\pi a_s^3}\left(\frac{(1-\cos(a_s\omega))^2+(a_s\omega-\sin(a_s\omega))^2}{\omega^2}\right)\left(\frac{1}{1+\omega^2}\right).$$

Rational quadratic variogram. Note that $\gamma(h) = o(|h|^\alpha)$ with $0 < \alpha < 1$. We apply the second part of the proposition. For this variogram function,

$$\gamma'(h) = \frac{2ha_r^2c_r}{(a_r+h^2)^2}, h > 0,$$

$$\int_0^\infty \sin(u\omega)\gamma'(u)du = 2a_r^2c_r\int_0^\infty \sin(u\omega)\frac{udu}{(a_r+u^2)^2} = 2a_r^2c_r\frac{\omega\pi e^{-\sqrt{a_r}\omega}}{4\sqrt{a_r}}.$$

Hence, the spectral density is given by

$$\begin{aligned}f(\omega) &= \frac{\omega}{\pi(1+\omega^2)}\int_0^\infty \sin(u\omega)\gamma'(u)du \\ &= \frac{\omega}{\pi(1+\omega^2)}2a_r^2c_r\frac{\omega\pi e^{-\sqrt{a_r}\omega}}{4\sqrt{a_r}} \\ &= \frac{a_r^{3/2}c_r}{2}e^{-\sqrt{a_r}\omega}\left(\frac{\omega^2}{1+\omega^2}\right).\end{aligned}$$

Exponential variogram. Again, we also note that $\gamma(h) = o(|h|^\alpha)$ with $0 < \alpha < 1$. We apply the second part of the proposition. Note that

$$\gamma'(h) = \frac{c_e}{a_e} \exp(-h/a_e), \quad h > 0,$$

and

$$\int_0^\infty \sin(u\omega)\gamma'(u)du \;=\; \frac{c_e}{a_e}\int_0^\infty \sin(u\omega)\exp(-u/a_e)du = \frac{c_e}{a_e}\frac{\omega}{(1/a_e)^2+\omega^2},$$

Therefore, the spectral density is given by

$$f(\omega) = \frac{\omega}{\pi(1+\omega^2)}\int_0^\infty \sin(u\omega)\gamma'(u)du = \frac{c_e a_e}{\pi(1+a_e^2\omega^2)}\left(\frac{\omega^2}{1+\omega^2}\right).$$

Note that all the results above match well what we have actually calculated.

IV.2. Spectral Density Estimation for Power Variograms

We now bring our attention to the special density estimation for the intrinsically stationary process, which is the random process with stationary increments of order 1. Among those commonly used variograms introduced in Section 4.2, the power variogram, which is given by $2\gamma(h) = |h|^\alpha$, $0 < \alpha < 2$, is an unbounded function of the displacement. In addition, there does not exist a corresponding stationary covariance function $C(h)$. In fact, its covariance function is given by $Cov(X(s), X(t)) = (|s|^\alpha + |t|^\alpha - |s-t|^\alpha)/2$, where $X(t)$ is the underlying intrinsically stationary process. Power variograms have been widely studied and commonly used in practice, for example, see Yaglom (1987)[Yag87], Cressie (1993)[Cre93], Huang et al. (2011b)[HHC11]) etc. among others. In this section, we will investigate the proposed spectral density estimation in Chapter 3 under the intrinsically stationary process with power variogram models.

Let $X(t)$ be an intrinsically random process with constant mean μ and modeled by the power variogram function. It is well known that the power variogram has the following spectral function (Yaglom (1987)[Yag87] and Schoenberg (1938)[Sch38]).

$$f(\omega) = \frac{\Gamma(\alpha+1)}{2\pi\omega^2}\Big(\frac{\sin(\alpha\pi/2)}{|\omega|^{\alpha-1}}\Big),\ \omega \in \mathbb{R}.$$

The above result was also derived by Zhang and Huang (2014)[ZH14] through the structure functions, giving the following spectral density function.

$$f(\omega) = \frac{\Gamma(\alpha+1)}{2\pi(1+\omega^2)}\Big(\frac{\sin(\alpha\pi/2)}{|\omega|^{\alpha-1}}\Big),\ \omega \in \mathbb{R}.$$

In this section, we will perform our simulations based on the theoretical spectral density given by Zhang and Huang (2014)[ZH14]. The performance of our proposed spectral density estimator are investigated under the power variogram models with $\alpha = 1/2, 1$, and $3/2$, respectively.

IV.2.1. Power Variogram Model with $\alpha = 1/2$

When $\alpha = 1/2$, the theoretical spectral density $f(\omega)$ is given by

$$f(\omega) = \frac{\sqrt{2\pi}}{8\pi}\frac{|\omega|^{1/2}}{1+\omega^2}, \quad \omega \in \mathbb{R}. \tag{IV.1}$$

We now assume $X(t)$ is intrinsically stationary with mean 0 and power variogram function with $\alpha = 1/2$. By Proposition 4.1, we have the following inversion formula:

$$f(\omega) = f_\tau(\omega) \cdot q(\tau, \omega),$$

with

$$f_\tau(\omega) = \int_{-\infty}^{\infty} D_\tau(h) e^{-i\omega h} dh, \quad \text{and} \quad q(\tau,\omega) = \frac{1}{2(1-\cos(\tau\omega))}\left(\frac{\omega^2}{1+\omega^2}\right).$$

Now let $\{X_k = X(t_k), t_k = k\delta, k = 0, \pm 1, \pm 2, \cdots\}$ be the observed gridded realizations of the continuous process $X(t)$ above. Therefore, we need to consider the aliasing effect. For simplicity, we set $\delta = 1$ and $\tau = 2$ as the step size for process differencing. Note that with $\delta = 1$ so that the estimated spectral density $f_\delta(\omega)$ will have the support of $(-\pi, \pi]$.

From the remark of Proposition 4.1, we have the following relationship between the structure function $D_\tau(h)$ and the variogram function $\gamma(h)$,

$$D_\tau(h) = \gamma(h + \tau) + \gamma(h - \tau) - 2\gamma(h).$$

In particular, for the power variogram $2\gamma(h) = |h|^\alpha$, we have

$$D_\tau(h) = \frac{1}{2}(|h + \tau|^\alpha + |h - \tau|^\alpha - 2|h|^\alpha).$$

Hence, under the discrete time series $\{X_k, k = 0, \pm 1, \pm 2, \cdots\}$, the theoretical spectral density is given by, for $\omega \in (-\pi, \pi]$,

$$\begin{aligned} f_\delta(\omega) &= \frac{1}{2\pi} \sum_{k=-\infty}^{\infty} D_\tau(k) e^{-ik\omega} \cdot q(\tau, \omega) \\ &= \frac{1}{2\pi} \Big[2 \sum_{k=1}^{\infty} D_\tau(k) \cos(k\omega) + D_\tau(0) \Big] \cdot q(\tau, \omega) \\ &= \frac{1}{2\pi} \Big[\sum_{k=1}^{\infty} (|k + \tau|^\alpha + |k - \tau|^\alpha - 2|k|^\alpha) \cos(k\omega) + |\tau|^\alpha \Big] \cdot q(\tau, \omega). \end{aligned}$$

When $\alpha = 1/2$ and $\tau = 2$, we introduce the following lemma.

Lemma 4.2. For $\omega \in R$, the infinite series

$$S = \sum_{k=3}^{\infty} (\sqrt{k+2} + \sqrt{k-2} - 2\sqrt{k}) \cos(k\omega) \text{ converges.}$$

The proof of the above series is straightforward and deferred in the Appendix.

Then based on the convergency of S, we can show that the following $f_\delta(\omega)$ is finite, and be able to derive the aliasing effect for power model with $\alpha = 1/2$.

$$\begin{aligned}
& f_\delta(\omega) \\
= & \frac{1}{2\pi} \left[\sum_{k=1}^{\infty} (|k+\tau|^\alpha + |k-\tau|^\alpha - 2|k|^\alpha) \cos(k\omega) + |\tau|^\alpha \right] \cdot \frac{1}{2(1-\cos(2\omega))} \left(\frac{\omega^2}{1+\omega^2} \right) \\
= & \frac{\omega^2}{4\pi(1-\cos(2\omega))(1+\omega^2} \left(\sum_{k=1}^{\infty} (|k+2|^{1/2} + |k-2|^{1/2} - 2|k|^{1/2}) \cos(k\omega) + \sqrt{2} \right) \\
= & \frac{1}{4\pi(1-\cos(2\omega))} \left(\frac{\omega^2}{1+\omega^2} \right) \Big(\sqrt{2} + (\sqrt{3}-1)\cos(\omega) + (2-2\sqrt{2})\cos(2\omega) \\
& \qquad + \sum_{k=3}^{\infty} (\sqrt{k+2} + \sqrt{k-2} - 2\sqrt{k}) \cos(k\omega) \Big),
\end{aligned}$$

On the other hand, we also have

$$\begin{aligned}
f_\delta(\omega) &= \sum_{k=-\infty}^{\infty} f_X(\omega + 2k\pi/\delta) \left(\frac{\omega^2}{1+\omega^2} \right) \\
&= \sum_{k=-\infty}^{\infty} f_X(\omega + 2k\pi) \left(\frac{\omega^2}{1+\omega^2} \right) \qquad (\delta = 1) \\
&= f(\omega) + \sum_{k=1}^{\infty} \Big[f_X(\omega + 2k\pi) + f_X(\omega - 2k\pi) \Big] \left(\frac{\omega^2}{1+\omega^2} \right) \\
&= f(\omega) + f_a(\omega),
\end{aligned}$$

Here f is the theoretical spectral density given by (IV.1) and $f_a(\omega)$ is the aliasing component given by

$$\begin{aligned} f_a(\omega) &= \sum_{k=1}^{\infty} \Big[f(\omega + 2k\pi) + f(\omega - 2k\pi) \Big] \left(\frac{\omega^2}{1+\omega^2} \right) \\ &= \frac{\sqrt{2\pi}}{8\pi} \cdot \sum_{k=1}^{\infty} \Big[\frac{1}{|\omega + 2k\pi|^{3/2}} + \frac{1}{|\omega - 2k\pi|^{3/2}} \Big] \left(\frac{\omega^2}{1+\omega^2} \right). \end{aligned}$$

Now the observed finite gridded sample of size n $\{X_0, X_1, X_2, \cdots, X_{n-1}\}$ is generated via the algorithm given in Chapter 2 with the covariance function given by

$$Cov(X(s), X(t)) = \frac{1}{2}(|s|^{1/2} + |t|^{1/2} - |s-t|^{1/2}).$$

Simulations are then conducted with the sample size $n = 100$, repeated for 1000 iterations. We plot $f(\omega)$ as the theoretical values and then compare them with estimates $\hat{f}_\delta(\omega) \cdot q(\tau, \omega)$ obtained through the inverse of Fourier transformation of the structure function $\hat{D}_\tau(h)$.

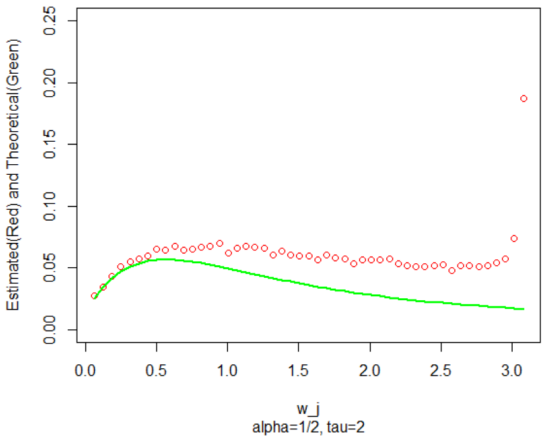

Figure 25. Estimated and Theoretical Spectral Density for Power Variogram with $\alpha = 1/2$ and $\tau = 2$.

The above graph shows a shift between the estimated and theoretical spectral densities. Now we remove the aliasing component $f_a(\omega)$ leading to the following plot, which is a good match between the estimated values and the true values.

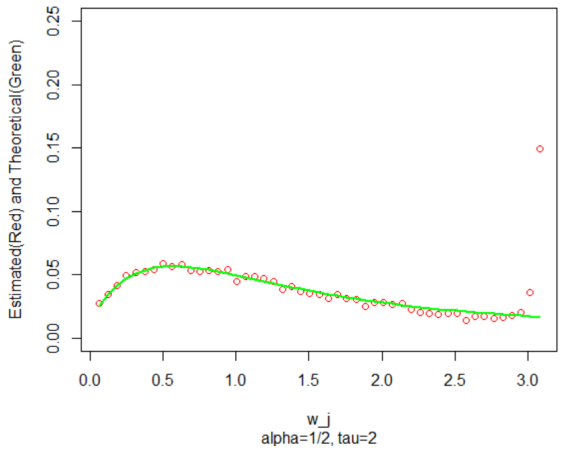

Figure 26. Estimated and Theoretical Spectral Density for Power Variogram After Removing Aliasing Effect with $\alpha = 1/2$ and $\tau = 2$.

IV.2.2. Power Variogram Model with $\alpha = 3/2$

A similar approach is given for $\alpha = 3/2$, and the spectral density is given by

$$f(\omega) = \frac{3\sqrt{2\pi}}{32\pi\,|\omega|^{1/2}(1+\omega^2)}, \qquad \omega \in \mathbb{R}.$$

Here we set $\delta = 1$ and $\tau = 2$, and we obtain the following two plots.

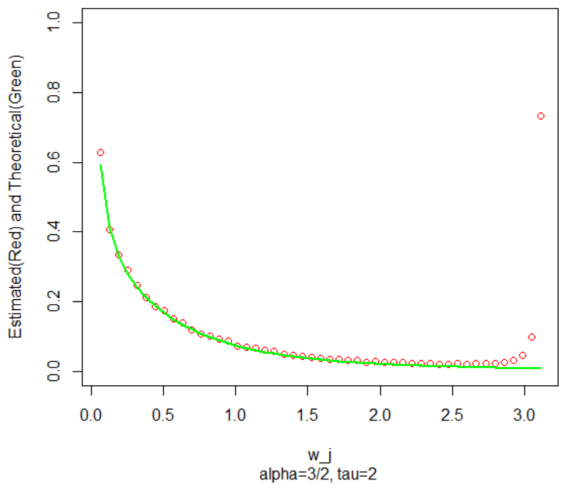

Figure 27. Estimated and Theoretical Spectral Density for Power Variogram with $\alpha = 3/2$ and $\tau = 2$.

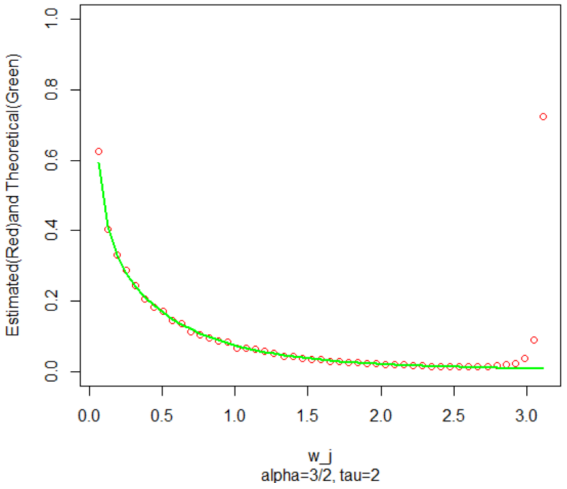

Figure 28. Estimated and Theoretical Spectral Density for Power Variogram with $\alpha = 3/2$ and $\tau = 2$.

Figure IV.3 shows the comparison of the estimated spectral density values with the true values when the aliasing effect exists, and Figure IV.4 shows that the estimated spectral density matches with the true spectral density after removing the aliasing effect. Therefore the same conclusion is also reached.

IV.2.3. Power Variogram Model with $\alpha = 1$

Lastly, we investigate the performance of our proposed estimator when the underlying intrinsically stationary process $X(t)$, sometimes referred as the Brownian Motion process, which is also the random process with power variogram of order $\alpha = 1$ and the spectral density function given by

$$f(\omega) = \frac{1}{2\pi(1+\omega^2)}, \quad \omega \in R.$$

The structure function of $X(t)$ is given by Zhang and Huang (2014)[ZH14].

$$D_\tau(h) = (\tau - |h|)I_{|h|<\tau}, \quad h \in R.$$

When a time series $\{X_k, k = 0, \pm 1, \pm 2, \cdots\}$ (here $\delta = 1$) of the process $X(t)$ is observed, we have, setting $\tau = 2$,

$$\begin{aligned}
D_2(h) &= \begin{cases} 2, & h = 0 \\ 1, & h = 1 \\ 0, & h \geq 2, \end{cases} \\
f_\delta(\omega) &= \frac{1}{2\pi} \sum_{k=-\infty}^{\infty} D_2(k) e^{-i\omega k} \cdot q(\tau, \omega) \\
&= \frac{1}{2\pi} \Big[2 \sum_{k=1}^{\infty} D_2(k) \cos(\omega k) + D(0) \Big] \cdot q(\tau, \omega) \\
&= \frac{1}{2\pi} \Big[2\cos\omega + 2 \Big] \cdot \frac{1}{2(1-\cos(2\omega))} \left(\frac{\omega^2}{1+\omega^2} \right) \\
&= \frac{1}{2\pi} \cdot \frac{1}{2(1-\cos\omega)} \left(\frac{\omega^2}{1+\omega^2} \right), \omega \in (-\pi, \pi].
\end{aligned}$$

On the other hand, we have the spectral desnty $f_\delta(\omega)$ based on the observed time seires given as

$$\begin{aligned} f_\delta(\omega) &= \frac{1}{2\pi\omega^2} + \frac{1}{2\pi}\sum_{k=1}^{\infty}\left[\frac{1}{(\omega+2k\pi)^2} + \frac{1}{(\omega-2k\pi)^2}\right]\left(\frac{\omega^2}{1+\omega^2}\right) \\ &= f(\omega) + f_a(\omega), \end{aligned}$$

with

$$f_a(\omega) = \frac{1}{2\pi}\sum_{k=1}^{\infty}\left[\frac{1}{(\omega+2k\pi)^2} + \frac{1}{(\omega-2k\pi)^2}\right]\left(\frac{\omega^2}{1+\omega^2}\right).$$

Simulations are conducted with the sample size $n = 100$, repeated for 1000 iterations. Similar conclusions can be draw based on the following two plots.

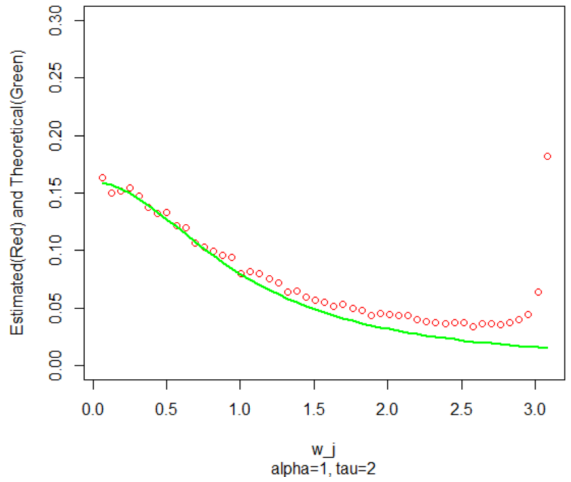

Figure 29. Estimated and Theoretical Spectral Density for Brownian Motion Process with $\tau = 2$.

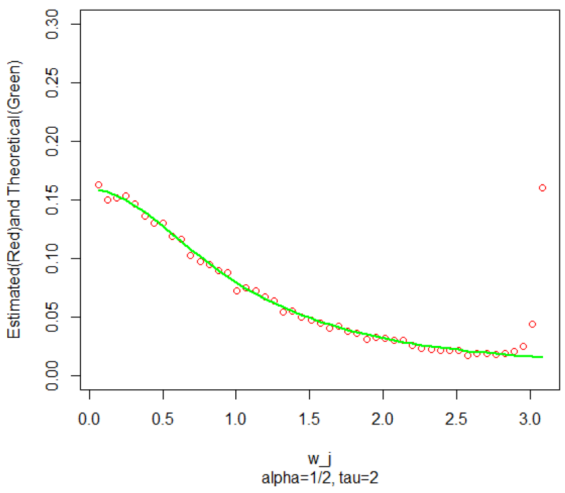

Figure 30. Estimated and Theoretical Spectral Density for Brownian Motion Process After Removing the Aliasing Effect with $\tau = 2$.

IV.2.4. Conclusions

In summary, our proposed spectral density estimation method performs well in estimating the spectrum when the underlying process is an intrinsically stationary process with power variogram models, consistent with what we have seen from Chapter 3. In addition, we can also consider an intrinsically stationary process with the band-limited spectral density, where the true spectral density could be fully recovered. As a final remark, in our simulations we have also experimented with a different τ value such as $\tau = 3$. The same conclusions as above have been obtained. In all, the proposed estimation method through the structure function seems to provide an effective way to estimate the underlying spectral function of a continuous process with stationary increments of order d.

CHAPTER V

DATA ANALYSIS

Given an unknown process, to apply the procedures for estimating the spectral density through the structure function $D_\tau(h)$, we need first determine the order (d) of the stationary increments (how much differencing the process is needed to achieve second-order stationarity). In this chapter, we will first briefly introduce the graphical procedure for determining nonstationarity for integrated processes provided by Cressie (1988)[Cre88], and then in Section 5.2, we will follow Cressie's method and provide the spectral analysis for a real data.

Yajima(1985)[Yaj85] worked on the problem of estimating increment order d based on residual mean squares by fitting an $AR(k)$ model to the dth differencing of the process. But this method is not pratical in real life situations, because it requires a large order k and the user needs to specify two "arbitrary" increasing functions of k. Then the residual mean square terms $(n-k-\delta)$ will become rather few. Dickey et al. (1986)[DBM86] provided a method for determining the increment order d based on the hypothesis tests for $H_0 : d = 1$ versus $H_1 : d = 0$, but no further testing for higher order. Box and Jenkins(1970)[BJRL70] provided plotting techniques, for example, a graphical inspection of autocorrelation functions of $X_t, \Delta X_t, \Delta^2 X_t, \cdots$. But this method was demonstrated to be dissatisfied by Anderson(1985)[And85] through a series of examples diagnosed by Box-Jenkins method that are actually nonstationary. Cressie (1988[Cre88], 1990[Cre90]) provided a upgraded graphical procedure for determining nonstationarity for integrated processes, by generating plots that were scaled version of semivariogram, linvariogram and quadvariogram. This procedure

has been proved to be practical and convenient. Here we will briefly introduce his procedure for determining the order d of the stationary increments, and apply it to our data analysis.

Brockwell and David[BD87] mentioned that in practice, the stationary increment order d which is the differencing times required to be stationary, is found to be very small, and normally stops at $d = 1$ or $d = 2$, and therefore, our approach focuses on the increment order that is no more than 2.

V.1. Introduction to the Graphical Procedure for Determining the Increment Order d

Given an observed data set $\{X_i, i = 0, 1, 2, \cdots, (n-1)\}$, to determine the order d, according to Cressie (1988)[Cre88], the scaled version of semivariogram, linvariogram and quadvariogram which are $\hat{\gamma}(h)/\hat{C}_X(0)$, $\hat{\gamma}_1(h)/\hat{C}_{\Delta X}(0)$, $\hat{\gamma}_2(h)/\hat{C}_{\Delta^2 X}(0)$ are calculated, respectively.

In particular, the scaled semivariogram is calculated as $\hat{\gamma}(h)/\hat{C}_X(0)$, where,

$$\begin{aligned} \hat{\gamma}(h) &= \frac{1}{2}\sum_{R(h)}(X_{t_i} - X_{t_j})^2 / \sum_{R(h)} 1; \\ R(h) &= \{(i,j) : (t_i, t_j) = (i, i+h) \text{ or } (i, i-h)\}, \end{aligned}$$

and

$$\hat{C}_X(h) = \sum_{t=1}^{n-h}(X_{t+h} - \bar{X})(X_t - \bar{X})/(n-h);$$

$$\hat{C}_X(0) = \frac{1}{n}\sum_{t=1}^{n}(X_t - \bar{X})^2.$$

The scaled linvariogram is calculated as $\hat{\gamma}_1(h)/\hat{C}_{\Delta X}(0)$ with

$$\hat{\gamma}_1(h) = \frac{1}{h}\Big\{\sum_{j=1}^{h-1}\frac{\hat{\alpha}(j)}{2j(j+1)}\Big\};$$

where

$$\begin{aligned}\hat{\alpha}(h) &= \sum_{R(h)}(hX_{t_i}-(h+1)X_{t_j}+X_{t_\ell})^2/\sum_{R(h)}1,\\ R(h) &= \{(i,j,\ell):(t_i,t_j,t_\ell)=(i,i+1,i+h+1)\text{ or }(i,i-1,i-h-1)\},\end{aligned}$$

and

$$\hat{C}_{\Delta X(0)} = \frac{1}{n-1}\sum_{t=1}^{n-1}(Y_t-\bar{Y})^2;$$

where

$$Y_t = \Delta^{(1)}X_t = X_t - X_{t-1}.$$

The scaled quadvariogram is calculated as $\hat{\gamma}_2(h)/\hat{C}_{\Delta^2 X}(0)$, with

$$\hat{\gamma}_2(h) = \frac{6\Big[\sum_{j=1}^{h-2}\{(h-1-j)\hat{\beta}(j)\}/4j(j+1)(j+2)\Big]}{h^3};$$

where

$$\begin{aligned}\hat{\beta}(h) &= \sum_{R(h)}\Big[-h(h+1)X_{t_i}+2h(h+2)X_{t_j}-(h+2)(h+1)X_{t_\ell}+2X_{t_m}\Big]^2/\sum_{R(h)}1,\\ R(h) &= \{(i,j,\ell,m):(t_i,t_j,t_\ell,t_m)=(i,i+1,i+2,i+h+2)\\ &\qquad\qquad\text{or }(i,i-1,i-2,i-h-2)\},\end{aligned}$$

and

$$\begin{aligned}\hat{C}_{\Delta^{(2)}X(0)} &= \frac{1}{n-2}\sum_{t=1}^{n-2}(Z_t-\bar{Z})^2;\\ \text{where}\qquad Z_t &= \Delta^{(2)}X_t = X_t-2X_{t-1}+X_{t-2}.\end{aligned}$$

To determine the smallest order d of the stationary increments, we need to plot the above scaled semivariogram, linvariogram and quadvariogram versus h one by one, until we have an observed leveling out with expected. For further verification, Cressie (1988)[Cre88] provided a judgment to make sure the decision is right, instead of only depending on the visual graphs, and the procedures are discribed as below, which follows closely on the procedures provided by Cressie (1988)[Cre88]. If the initial leveling out occurs for the scaled semivariogram, which means the process is stationary ($d = 0$), then the expected curve is

$$e(h) = 1.$$

Then the confidence band is given by

$$e(h) \pm 2\{var(\hat{\gamma}(h)/\hat{C}_X(0))\}^{1/2}, (n/3) \leq h \leq (n/2),$$

which was proved to be approximated to

$$e(h) \pm \frac{2 \cdot 1.35}{n^{1/2}}, \quad (n/3) \leq h \leq (n/2).$$

If it occurs for the scaled linvariogram, which means it is a process with stationary increments of order 1 ($d = 1$), then the expected curve is

$$e(h) = \frac{1}{2} - (\frac{1}{2h}).$$

Then the confidence band is given by

$$e(h) \pm 2\{var(\hat{\gamma}_1(h)/\hat{C}_{\Delta X}(0))\}^{1/2}, (n/3) \leq h \leq (n/2),$$

which was proved to be approximated to

$$e(h) \pm \frac{2 \cdot 0.15}{n^{1/2}}, \quad (n/3) \leq h \leq (n/2).$$

If it occurs for the scaled quadvariogram,which means it is a process with stationary increments of order 2 ($d = 2$), then the expected curve is

$$e(h) = \frac{1}{4} - (\frac{1}{2h}) - (\frac{1}{4h^2}) + (\frac{1}{2h^3}).$$

Then the confidence band is given by

$$e(h) \pm 2\{var(\hat{\gamma}_2(h)/\hat{C}_{\Delta^2 X}(0))\}^{1/2}, (n/3) \leq h \leq (n/2),$$

which was proved to be approximated to

$$e(h) \pm \frac{2 \cdot 0.09}{n^{1/2}}, \quad (n/3) \leq h \leq (n/2).$$

If the scaled variogram curve falls outside of the confidence band within the range of $h \in [n/3, n/2]$, we need to continue on the higher order until the scaled variogram falls totally inside the confidence band, then we may stop and make the decision on the corresponding order d.

V.2. Spectral Estimation in Real Data Analysis

The following example is a series $\{X_t\}$ of U.S. monthly single-family housing starts, January 1964-August 1978 (Dickey et al. 1986)[DBM86], totally 176 data points. The data are presented in the following table. Due to seasonal behavior of the series, the data are transformed to $Z_t = X_t - X_{t-12}$ (Dickey et al. 1986)[DBM86]. This leaves $n = 164$ Z-values for estimating the spectral density.

Table 2. U.S. Monthly Single-Family Housing Starts, January 1964 -August 1978 (in Thousands)

58.008	62.448	82.180	94.927	98.230	100.875	89.885	91.988
79.757	89.435	67.514	55.227	52.149	47.205	82.150	100.931
98.408	97.351	96.489	88.830	80.876	85.750	72.351	61.198
46.561	50.361	83.236	94.343	84.748	79.828	69.068	69.362
59.404	53.530	50.212	37.972	40.157	40.274	66.592	79.839
87.341	87.594	82.344	83.712	78.194	81.704	69.088	47.026
45.234	55.431	79.325	97.983	86.806	81.424	86.398	82.522
80.078	85.560	64.819	53.847	51.300	47.909	71.941	84.982
91.301	82.741	73.523	69.465	71.504	68.039	55.069	42.827
33.363	41.367	61.879	73.835	74.848	83.007	75.461	77.291
75.961	79.393	67.443	69.041	54.856	58.287	91.584	116.013
115.627	116.946	107.747	111.663	102.149	102.882	92.904	80.362
76.185	76.306	111.358	119.840	135.167	131.870	119.078	131.324
120.491	116.990	97.428	73.195	77.105	73.560	105.136	120.453
131.643	114.822	114.746	106.806	84.504	86.004	70.488	46.767
43.292	57.593	76.946	102.237	96.340	99.318	90.715	79.782
73.443	69.460	57.898	41.041	39.791	39.959	62.498	77.777
92.782	90.284	92.782	90.655	84.517	93.826	71.646	55.650
53.997	72.585	92.443	107.804	112.242	119.627	112.807	112.798
108.038	109.114	89.368	71.584	55.746	87.172	125.802	138.772
152.198	149.061	138.181	140.527	131.644	135.398	109.310	87.123
63.349	72.800	121.391	139.857	154.928	154.278	139.219	140.106

V.2.1. Determine the Order $\boldsymbol{d}$

The first step is to determine the stationary increments order d following the above steps provided by Cressie(1988)[Cre88]. The scaled version of semivariogram, linvariogram and quadvariogram were plotted as $\hat{\gamma}(h)/\hat{C}_X(0)$ versus h, $\hat{\gamma}_1(h)/\hat{C}_{\Delta X}(0)$ versus h, $\hat{\gamma}_2(h)/\hat{C}_{\Delta^2 X}(0)$ versus h, respectively. At the same time, the confidence band was also calculated and plotted in the same plot.

The following three figures show the sequence of the scaled variogram plots, and it is clear that initial leveling out occurs at $d = 1$, but also possibly at $d = 0$ or $d = 2$. Therefore, we need the confidence band to further confirm our conclusion.

If $d = 0$, $e(h) = 1$, then we have the confidence band as $\{e(h) \pm 0.211, 55 \leq h \leq 82\}$, the graph shows that the scaled semivariogram falls outside of the confidence band curve (red) within $55 \leq h \leq 82$, therefore, we need to keep moving on the higher order $d = 1$.

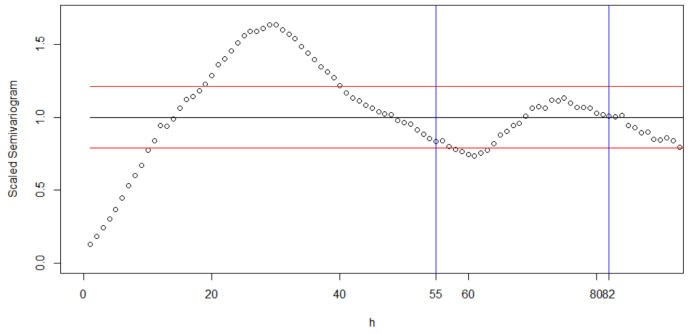

Figure 31. Scaled Semivariogram Estimation versus h for Determining $d = 0$ with the Expected Semivariogram and Confidence Band.

If $d = 1$, $e(h) = \frac{1}{2} - (\frac{1}{2h})$, then we have the confidence band as $\{e(h) \pm 0.023, 55 \leq h \leq 82\}$, the graph shows that the scaled linvariogram falls totally inside of the confidence band curve (red) within $55 \leq h \leq 82$, therefore, we may stop here to make the decision that $d = 1$.

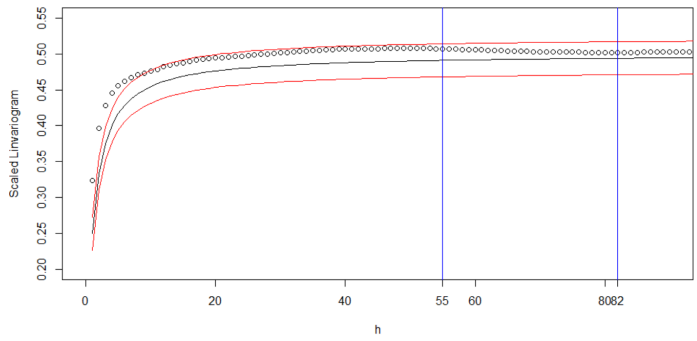

Figure 32. Scaled Linvariogram Estimation versus h for Determining $d = 1$ with the Expected Linvariogram and Confidence Band.

To be more positive about the decision, we continued on the higher order $d = 2$ with $e(h) = \frac{1}{4} - (\frac{1}{2h}) - (\frac{1}{4h^2}) + (\frac{1}{2h^3})$ and the confidence band $\{e(h) \pm 0.014, 55 \leq h \leq 82\}$. Figure V.3 shows that the scaled quadvariogram falls outside of the confidence band within $55 \leq h \leq 82$, therefore, we will keep our decision that $d = 1$.

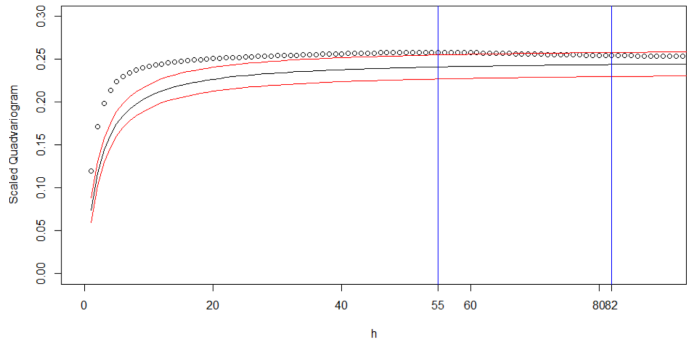

Figure 33. Scaled Quadvariogram Estimation versus h for Determining $d = 2$ with the Expected Semivariogram and Confidence Band.

V.2.2. Spectral Analysis with $d = 1$

After determining the order d of the stationary increments, we can apply our procedures in Chapter 3 for estimating the spectral density through the structure

function $D_\tau(h)$ with $d = 1$. The following is the graph of the estimated spectral density for the above example. The frequencies with high power of spectral densities were marked as red. Here we set 10 as a breakthrough point for the high power.

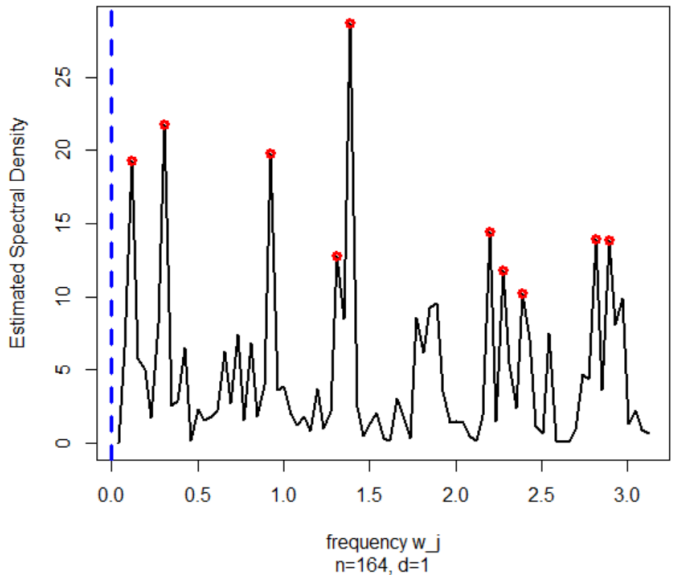

Figure 34. Estimated Spectral Density $\hat{f}(\omega)$ for U.S. Monthly Housing Starts, January 1964-August 1978.

The above graph shows that there are a total of 10 points having high power, and the corresponding frequencies are listed in the following table.

Table 3. The Estimated Spectral Densities $\hat{f}(\omega)$ for the Points with High Powers and Their Corresponding Frequencies ω

Frequency ω	0.12	0.31	0.93	1.31	1.39	2.20	2.27	2.39	2.81	2.89
Estimated $\hat{f}(\omega)$	19.30	21.78	19.74	12.77	28.67	14.44	11.75	10.21	13.96	13.85

With the above information, we can see that there are several dominant peak groups at around $0.25, 0.92, 1.35, 2.28$ and 2.85. If we consider the frequency with highest power at 28.67 with corresponding frequency $\omega = 1.388$, we have the hidden periodicity of $2\pi/1.39 \approx 4.52$ time periods. Since this is monthly data, there appears to be a dominant periodicity of about 5 months in the U.S. Housing Start during January 1964-August 1978.

In practice, the interrpretation of spectrum depends strongly on the knowledge of the related fields. Therefore, to better understand the above estimated spectrum, we need more background of the housing starts.

CHAPTER VI

FUTURE RESEARCH

There are a number of research areas that we will explore after this dissertation. First, we would like to explore the assumptions in the remark of Section 4.2. We believe that additional requirements on the variogram function $2\gamma(h)$ will be minimum, and so our result could be potentially applied to obtain the spectral density for a given variogram function. In addition, we will explore in more details on the asymptotic properties of the spectral density estimator proposed in Chapter 3.

Secondly, throughout this dissertation work, we have assumed that we observe a gridded sample with equal-spacing along the real line. However, in real applications, it is often that the observed data might not be equally spaced on $\mathbb{R}$. Therefore, it is very important that we extend our study to handle non-gridded observations in our future work. One approach in literature is the so-called gridization, which projects the irregularly observed points to their nearest grids. Various issues might come up due to gridization such as the selection of grid size as well as efficiency consideration.

Our dissertation work is closely related to the so-called Intrinsic Random Functions (IRFs) (Matheron 1973)[Mat73]) and is associated with the generalized covariance functions (Christakos, 1984[Chr84]). For example, the stationary process, or the random process with stationary increments of order 0 in our context, is actually the IRF-1, while the intrinsically stationary process, which is the random process with stationary increments of order 1 in our context, is the IRF0, and so on. The theory of IRFs is to study a broader classes of non-stationary phenomena at a minimum price of certain restrictions. As an example, for a stationary process, the positive

definiteness of the covariance function guarantees that any finite linear combination of observed random measurements has finite non-negative variance. But for an intrinsically stationary process, this finiteness of the variance holds for a certain finite linear combinations of observed random measurements, where the sum of coefficients equals to zero. However, the IRF0 can deal with a larger class of phenomena, such as Brownian Motion, where the variance might be unbounded. As one of our future research areas, we will explore such a connection and extend our approach to the IRF domain. As our long term research direction, we want to extend our approach from the random process in $\mathbb{R}$ to the random field on $\mathbb{R}^2$, or in general, $\mathbb{R}^n$. In addition, we would like to connect our approach with the IRFs on $\mathbb{R}^n$. As far as we know, this will totally be a new research area in spatial statistics.

BIBLIOGRAPHY

[AGM09] G Albertini, S Giaquinto, and M Mignano, *Spectral analysis of the human voice: a potentially useful tool in rehabilitation*, European journal of physical and rehabilitation medicine **45** (2009), no. 4, 537–545.

[And85] O.D. Anderson, *Time series analysis: theory and practice*, Elsevier, 1985.

[AS65] Milton Abramowitz and Irene A Stegun, *With formulas, graphs, and mathematical tables*, National Bureau of Standards Applied Mathematics Series e **55** (1965), 953.

[BD87] Peter J Brockwell and Richard A Davis, *Time series: theory and methods*, Springer Science & Business Media, 1987.

[BD91] ———, *Inference for the spectrum of a stationary process*, Time Series: Theory and Methods, Springer, 1991, pp. 330–400.

[BD16] ———, *Introduction to time series and forecasting*, springer, 2016.

[BGT67] Christopher Bingham, M Godfrey, and J Tukey, *Modern techniques of power spectrum estimation*, IEEE Transactions on audio and electroacoustics **15** (1967), no. 2, 56–66.

[BJRL70] George EP Box, Gwilym M Jenkins, Gregory C Reinsel, and Greta M Ljung, *Time series analysis: forecasting and control*, John Wiley & Sons, 1970.

[Boc38] S Bochner, *Fourier integrals*, Science **87** (1938), no. 2260, 370–370.

[CC08] Jonathan D. Cryer and Kung-Sik Chan, *Time series regression models*, Springer, 2008.

[Chr84] George Christakos, *On the problem of permissible covariance and variogram models*, Water Resources Research **20** (1984), no. 2, 251–265.

[CK91] Jonathan D Cryer and Natalie Kellet, *Time series analysis*, Springer, 1991.

[Cre85] Noel Cressie, *Fitting variogram models by weighted least squares*, Journal of the International Association for Mathematical Geology **17** (1985), no. 5, 563–586.

[Cre88] ———, *A graphical procedure for determining nonstationarity in time series*, Journal of the American Statistical Association **83** (1988), no. 404, 1108–1116.

[Cre90] ———, *Correction: A graphical procedure for determining nonstationarity in time series*, Journal of the American Statistical Association **85** (1990), no. 409, 272–272.

[Cre93] Noel AC Cressie, *Spatial prediction and kriging*, Statistics for Spatial Data, Revised Edition (1993), 105–209.

[Cre15] Noel Cressie, *Statistics for spatial data*, John Wiley & Sons, 2015.

[DBM86] David A Dickey, William R Bell, and Robert B Miller, *Unit roots in time series models: Tests and implications*, The American Statistician **40** (1986), no. 1, 12–26.

[EAS11] Ferda Ernawan, Nur Azman Abu, and Nanna Suryana, *Spectrum analysis of speech recognition via discrete tchebichef transform*, International Society for Optics and Photonics, 2011.

[Ein12] Garry A Einicke, *Smoothing, filtering and prediction*, InTech, 2012.

[Fis29] Ronald Aylmer Fisher, *Tests of significance in harmonic analysis*, Proceedings of the Royal Society of London. Series A **125** (1929), no. 796, 54–59.

[GR07] IzrailÊź Solomonovič Gradštejn and Iosif Moiseevič Ryžik, *Table of integrals, series, and products*, Elsevier/Academic Press, 2007.

[GR14] Izrail Solomonovich Gradshteyn and Iosif Moiseevich Ryzhik, *Table of integrals, series, and products.*, Academic press, 2014.

[Han61] EJ Hannan, *Testing for a jump in the spectral function*, Journal of the Royal Statistical Society. Series B (Methodological) (1961), 394–404.

[HHC11] Chunfeng Huang, Tailen Hsing, and Noel Cressie, *Nonparametric estimation of the variogram and its spectrum*, Biometrika **98** (2011), no. 4, 775–789.

[JP57] GM Jenkins and MB Priestley, *The spectral analysis of time-series*, Journal of the Royal Statistical Society. Series B (Methodological) (1957), 1–12.

[JW68] Gwilym M Jenkins and Donald G Watts, *Spectral analysis*.

[Koo95] Lambert H Koopmans, *The spectral analysis of time series*, Elsevier, 1995.

[Mat62] Georges Matheron, *Traité de géostatistique appliquée, tome i: Mémoires du bureau de recherches géologiques et minières*, Editions Technip, Paris **14** (1962).

[Mat73] ———, *The intrinsic random functions and their applications*, Advances in applied probability **5** (1973), no. 3, 439–468.

[MM87] S Lawrence Marple and S Lawrence Marple, *Digital spectral analysis: with applications*, vol. 5, Prentice-Hall Englewood Cliffs, NJ, 1987.

[MM05] Budiman Minasny and Alex B McBratney, *The matérn function as a general model for soil variograms*, Geoderma **128** (2005), no. 3-4, 192–207.

[Nas06] Guy P Nason, *Stationary and non-stationary time series*, Statistics in Volcanology. Special Publications of IAVCEI **1** (2006), 000–000.

[Ols00] Bruno A Olshausen, *Aliasing*, PSC 129–Sensory Processes (2000), 3–4.

[RW06] Carl Edward Rasmussen and Christopher KI Williams, *Gaussian processes for machine learning. 2006*, The MIT Press, Cambridge, MA, USA **38** (2006), 715–719.

[Sch] Arthur Schuster, *The periodogram of magnetic declination as obtained from the records of the greenwich observatory during the years 1871–1895*, Trans. Cambridge Philos. **18**, 107–135.

[Sch98] ———, *On the investigation of hidden periodicities with application to a supposed 26 day period of meteorological phenomena*, Journal of Geophysical Research **3** (1898), no. 1, 13–41.

[Sch38] Isaac J Schoenberg, *Metric spaces and completely monotone functions*, Annals of Mathematics (1938), 811–841.

[Sig07] Milan Sigmund, *Spectral analysis of speech under stress*, IJCSNS International Journal of Computer Science and Network Security **7** (2007), 170–172.

[Sim12] Jeffrey S Simonoff, *Smoothing methods in statistics*, Springer Science & Business Media, 2012.

[SM+05] Petre Stoica, Randolph L Moses, et al., *Spectral analysis of signals*, vol. 1, Pearson Prentice Hall Upper Saddle River, NJ, 2005.

[SM15] Jagriti Saini and Rajesh Mehra, *Power spectral density analysis of speech signal using window techniques*, International Journal of Computer Applications **131** (2015), no. 14, 33–36.

[Sol92] Victor Solo, *Intrinsic random functions and the paradox of 1/f noise*, SIAM Journal on Applied Mathematics **52** (1992), no. 1, 270–291.

[SS11a] Robert H Shumway and David S Stoffer, *Time series analysis and its applications*, Springer, 2011.

[SS11b] Robert H. Shumway and Davis S. Stoffer, *Time series analysis and its applications with r examples*, Springer, 2011.

[Wal14] Sir Gilbert Thomas Walker, *Correlation in seasonal variations of weather, iii: On the criterion for the reality of relationships or periodicities*, Meteorological Office, 1914.

[War98] Rebecca M Warner, *Spectral analysis of time-series data*, Guilford Press, 1998.

[Yag55] Akiva Moiseevich Yaglom, *Correlation theory of processes with random stationary n th increments*, Matematicheskii Sbornik **79** (1955), no. 1, 141–196.

[Yag58] AM Yaglom, *Correlation theory of processes with random stationary nth increments*, Amer. Math. Soc. Transl.(2) **8** (1958), 87–141.

[Yag87] ———, *Introduction*, Correlation Theory of Stationary and Related Random Functions, Springer, 1987, pp. 1–13.

[Yaj85] Yoshihiro Yajima, *Estimation of the degree of differencing of an arima process*, Annals of the Institute of Statistical Mathematics **37** (1985), no. 1, 389–408.

[YZ15] Shu Yang and Zhengyuan Zhu, *Semiparametric estimation of spectral density function for irregular spatial data*, arXiv preprint arXiv:1508.06886 (2015).

[ZH14] Haimeng Zhang and Chunfeng Huang, *A note on processes with random stationary increments*, Statistics & Probability Letters **94** (2014), 153–161.

APPENDIX A

DERIVATION OF SPECTRAL DENSITIES THROUGH STRUCTURE FUNCTION $D_\tau(H)$

We first introduce the following lemma, which will be applied frequently later for the proofs of Propositions 4.2.3 and 4.2.4. Let $\gamma(h)$ be a continuous variogram function with $\gamma(0) = 0$. For all $\tau > 0$, define

$$g(\tau) = \int_0^\tau \gamma(u)du.$$

Hence, $g(0) = 0, g(-\tau) = -g(\tau)$ and $g'(\tau) = \gamma(\tau)$. We have the following lemma.

Lemma 4.1. For each $\tau > 0$, if $g(\tau)$ satisfies

$$\lim_{u\to\infty}(g(u+\tau) + g(u-\tau) - 2g(u)) = \lim_{u\to\infty}\int_0^\tau (\gamma(u+s) - \gamma(u-s))ds = 0,$$

then we have

$$\begin{aligned} & \int_0^\infty \cos(u\omega)\left(\gamma(u+\tau) + \gamma(u-\tau) - 2\gamma(u)\right)du \\ = \;& \omega\int_0^\infty \sin(u\omega)\left(g(u+\tau) + g(u-\tau) - 2g(u)\right)du, \end{aligned}$$

as long as the integral on the left hand side above exists.

PROOF: We first split the integral into two parts.

$$\begin{aligned}
& \int_0^\infty \cos(u\omega)\left(\gamma(u+\tau)+\gamma(u-\tau)-2\gamma(u)\right)du \\
= & \int_\tau^\infty \cos(u\omega)\left(\gamma(u+\tau)+\gamma(u-\tau)-2\gamma(u)\right)du \\
& + \int_0^\tau \cos(u\omega)\left(\gamma(u+\tau)+\gamma(\tau-u)-2\gamma(u)\right)du \\
= & \; I + II.
\end{aligned}$$

We now apply the integration by parts on both integrals.

$$\begin{aligned}
I &= \int_\tau^\infty \cos(u\omega) d\left(g(u+\tau)+g(u-\tau)-2g(u)\right) \\
&= \left[\cos(u\omega)\left(g(u+\tau)+g(u-\tau)-2g(u)\right)\right]_\tau^\infty \\
&\quad +\omega\int_\tau^\infty \sin(u\omega)\left(g(u+\tau)+g(u-\tau)-2g(u)\right)du \\
&= -2\cos(\tau\omega)(g(2\tau)-2g(\tau)) \\
&\quad +\omega\int_\tau^\infty \sin(u\omega)\left(g(u+\tau)+g(u-\tau)-2g(u)\right)du,
\end{aligned}$$

For the second integral,

$$\begin{aligned}
II &= \int_0^\tau \cos(u\omega) d\left(g(u+\tau)-g(\tau-u)-2g(u)\right) \\
&= \left[\cos(u\omega)\left(g(u+\tau)-g(\tau-u)-2g(u)\right)\right]_0^\tau \\
&\quad +\omega\int_0^\tau \sin(u\omega)\left(g(u+\tau)-g(\tau-u)-2g(u)\right)du \\
&= 2\cos(\tau\omega)(g(2\tau)-2g(\tau)) \\
&\quad +\omega\int_0^\tau \sin(u\omega)\left(g(u+\tau)-g(\tau-u)-2g(u)\right)du.
\end{aligned}$$

Then we have the summation of the two parts that concluding the proof.

$$\begin{aligned} I+II &= \omega\left[\int_{\tau}^{\infty}\sin(u\omega)\left(g(u+\tau)+g(u-\tau)-2g(u)\right)du\right. \\ &\quad \left.+\int_{0}^{\tau}\sin(u\omega)\left(g(u+\tau)-g(\tau-u)-2g(u)\right)du\right], \end{aligned}$$

Proof of Proposition 4.3: We first note that

$$\begin{aligned} & \gamma(u+\tau)+\gamma(u-\tau)-2\gamma(u) \\ = \;& c_r\left(\frac{(u+\tau)^2}{1+(u+\tau)^2/a_r}+\frac{(u-\tau)^2}{1+(u-\tau)^2/a_r}-2\frac{u^2}{1+u^2/a_r}\right) \\ = \;& a_rc_r\left(\frac{(u+\tau)^2}{a_r+(u+\tau)^2}+\frac{(u-\tau)^2}{a_r+(u-\tau)^2}-2\frac{u^2}{a_r+u^2}\right) \\ = \;& a_rc_r\frac{(a_r+(u-\tau)^2)(a_r+u^2)+(a_r+(u+\tau)^2)(a_r+u^2)}{(a_r+(u-\tau)^2)(a_r+u^2)(a_r+(u+\tau)^2)} \\ & -2a_rc_r\frac{(a_r+(u-\tau)^2)(a_r+(u+\tau)^2)}{(a_r+(u-\tau)^2)(a_r+u^2)(a_r+(u+\tau)^2)} \\ = \;& 2a_rc_r\frac{\tau^2(3u^2-a_r-\tau^2)}{(a_r+(u-\tau)^2)(a_r+u^2)(a_r+(u+\tau)^2)}. \end{aligned}$$

Now for small τ, saying $\tau<1$ (we will take the limit $\tau\to 0$, hence this is feasible), let $\tau_0>0$, such that

$$\frac{1}{a_r+(u-\tau)^2}\le 1, \qquad \text{for } u>\tau_0.$$

Therefore, for $u>\tau_0$,

$$|\gamma(u+\tau)+\gamma(u-\tau)-2\gamma(u)|\le a_rc_r\frac{6\tau^2}{a_r+u^2}.$$

$$\int_{\tau_0}^{\infty}|(\gamma(u+\tau)+\gamma(u-\tau)-2\gamma(u))\cos(u\omega)|du\le 6\tau^2a_rc_r\int_{\tau_0}^{\infty}\frac{1}{a_r+u^2}du<\infty,$$

which implies the existence of the integral $\int_0^{\infty}(\gamma(u+\tau)+\gamma(u-\tau)-2\gamma(u))\cos(u\omega)du$.

We first notice that, for each fixed $\tau > 0$, we may assume $u > \tau$ since we take $u \to \infty$,

$$\begin{aligned}
& \lim_{u\to\infty} (g(u+\tau) + g(u-\tau) - 2g(u)) \\
= & \lim_{u\to\infty} \int_0^\tau (\gamma(u+s) - \gamma(u-s))ds \\
= & \lim_{u\to\infty} \int_0^\tau c_r \left(\frac{(u+s)^2}{1+(u+s)^2/a_r} - \frac{(u-s)^2}{1+(u-s)^2/a_r} \right) ds \\
= & \lim_{u\to\infty} \int_0^\tau c_r \left(\frac{(u+s)^2 - (u-s)^2}{(1+(u+s)^2/a_r)(1+(u-s)^2/a_r)} \right) ds \\
= & \lim_{u\to\infty} \int_0^\tau c_r \left(\frac{4us}{(1+(u+s)^2/a_r)(1+(u-s)^2/a_r)} \right) ds = 0,
\end{aligned}$$

by the dominated convergence theorem. Hence, from Lemma 4.1,

$$\begin{aligned}
& \int_0^\infty (\gamma(u+\tau) + \gamma(u-\tau) - 2\gamma(u)) \cos(u\omega)du \\
= & \ \omega \int_0^\infty (g(u+\tau) + g(u-\tau) - 2g(u)) \sin(u\omega)du.
\end{aligned}$$

Now we consider the following limit

$$\lim_{\tau\to 0} \int_0^\infty (g(u+\tau) + g(u-\tau) - 2g(u)) \sin(u\omega)du \frac{1}{1-\cos(\omega\tau)}.$$

Note that for $x > 0$,

$$\begin{aligned}
g(x) &= \int_0^x \gamma(u)du = \int_0^x c_r \frac{u^2}{1+u^2/a_r} du \\
&= c_r a_r x - c_r a_r^{3/2} \tan^{-1}(x/\sqrt{a_r}).
\end{aligned}$$

Then we have

$$\begin{aligned}
& g(u+\tau)+g(u-\tau)-2g(u) \\
= \;& c_r a_r(u+\tau) - c_r a_r^{3/2}\tan^{-1}((u+\tau)/\sqrt{a_r})) + c_r a_r(u-\tau) \\
& -c_r a_r^{3/2}\tan^{-1}((u-\tau)/\sqrt{a_r})) - 2c_r a_r u - c_r a_r^{3/2}\tan^{-1}(u/\sqrt{a_r})) \\
= \;& c_r a_r^{3/2}\left(2\tan^{-1}(u/\sqrt{a_r}) - \tan^{-1}((u+\tau)/\sqrt{a_r}) - \tan^{-1}((u-\tau)/\sqrt{a_r})\right)
\end{aligned}$$

For the $\tan^{-1}$ function, we have the following identity.

$$\tan^{-1}(x)-\tan^{-1}(y) \;=\; \begin{cases} \tan^{-1}\frac{x-y}{1+xy}, & xy > -1, \\ \pi + \tan^{-1}\frac{x-y}{1+xy}, & x>0, xy<-1, \\ -\pi + \tan^{-1}\frac{x-y}{1+xy}, & x<0, xy<-1, \end{cases}$$

When u is big, $\left(u/\sqrt{a_r}\times(u\pm\tau)/\sqrt{a_r}\right) > -1$, hence,

$$\begin{aligned}
& 2\tan^{-1}(u/\sqrt{a_r}) - \tan^{-1}((u+\tau)/\sqrt{a_r}) - \tan^{-1}((u-\tau)/\sqrt{a_r}) \\
= \;& -\tan^{-1}\left(\frac{(u+\tau)-u)/\sqrt{a_r}}{1+(u/\sqrt{a_r})((u+\tau)/\sqrt{a_r})}\right) + \tan^{-1}\left(\frac{(u-(u-\tau))/\sqrt{a_r}}{1+(u/\sqrt{a_r})((u-\tau)/\sqrt{a_r})}\right) \\
= \;& \tan^{-1}\left(\frac{\tau/\sqrt{a_r}}{1+u(u-\tau)/a_r}\right) - \tan^{-1}\left(\frac{\tau/\sqrt{a_r}}{1+u(u+\tau)/a_r}\right) \\
= \;& \tan^{-1}\left(\left(\frac{\tau/\sqrt{a_r}}{1+u(u-\tau)/a_r} - \frac{\tau/\sqrt{a_r}}{1+u(u+\tau)/a_r}\right)\right. \\
& \qquad\qquad \left.\times\left(1+\frac{\tau/\sqrt{a_r}}{1+u(u-\tau)/a_r}\times\frac{\tau/\sqrt{a_r}}{1+u(u+\tau)/a_r}\right)^{-1}\right) \\
= \;& \tan^{-1}\left(\frac{2u\tau^2}{a_r^{3/2}(1+u(u+\tau)/a_r)(1+u(u-\tau)/a_r)}\right. \\
& \qquad\qquad \left.\times\left(1+\frac{\tau/\sqrt{a_r}}{1+u(u-\tau)/a_r}\times\frac{\tau/\sqrt{a_r}}{1+u(u+\tau)/a_r}\right)^{-1}\right).
\end{aligned}$$

Now we use Taylor's expansion to approximate $\tan^{-1}(x)$.

$$\tan^{-1}(x) = x + R_2(x)$$

where x is close to zero and the remainder $R_2(x) = \frac{1}{2}\tan^{-1\prime\prime}(\xi)x^2$ with $0 < \xi < x$. Note that

$$\tan^{-1\prime\prime}(x) = -\frac{-2x}{(1+x^2)^2}, \qquad \Rightarrow \qquad |\tan^{-1\prime\prime}(\xi)| \leq 1.$$

Therefore, $|R_2(x)| \leq \frac{x^2}{2}$, and

$$\begin{aligned}
&\left|\tan^{-1}\left(\frac{2u\tau^2}{a_r^{3/2}(1+u(u+\tau)/a_r)(1+u(u-\tau)/a_r)}\right.\right. \\
&\qquad\qquad\left.\left.\times\left(1+\frac{\tau/\sqrt{a_r}}{1+u(u-\tau)/a_r}\times\frac{\tau/\sqrt{a_r}}{1+u(u+\tau)/a_r}\right)^{-1}\right)\right| \\
\leq\ &\left|\frac{2u\tau^2}{a_r^{3/2}(1+u(u+\tau)/a_r)(1+u(u-\tau)/a_r)}\right. \\
&\qquad\qquad\left.\times\left(1+\frac{\tau/\sqrt{a_r}}{1+u(u-\tau)/a_r}\times\frac{\tau/\sqrt{a_r}}{1+u(u+\tau)/a_r}\right)^{-1}\right| \\
&+\frac{1}{2}\left|\frac{2u\tau^2}{a_r^{3/2}(1+u(u+\tau)/a_r)(1+u(u-\tau)/a_r)}\right. \\
&\qquad\qquad\left.\times\left(1+\frac{\tau/\sqrt{a_r}}{1+u(u-\tau)/a_r}\times\frac{\tau/\sqrt{a_r}}{1+u(u+\tau)/a_r}\right)^{-1}\right|^2 \\
\leq\ &\frac{2\tau^2}{a_r^{3/2}}\left|\frac{u}{(1+u(u+\tau)/a_r)(1+u(u-\tau)/a_r)}\right| \\
&\qquad\qquad+\frac{2\tau^4}{a_r^3}\left|\frac{u}{(1+u(u+\tau)/a_r)(1+u(u-\tau)/a_r)}\right|^2.
\end{aligned}$$

When u is big and τ is small, we can have $|u-\tau|>1$. Therefore, the first term above is given as follows,

$$\frac{u}{(1+u(u+\tau)/a_r)(1+u(u-\tau)/a_r)} \leq \frac{a_r^2}{u^2},$$

and so is the second term, implying

$$\int_\tau^\infty (g(u+\tau)+g(u-\tau)-2g(u))\sin(u\omega)du < \infty,$$

and it is also further dominated by an absolutely converging integral. By the dominated convergence theorem, we can take the limit $\tau \to 0$ inside the integral to have

$$c_r a_r^{3/2}\int_0^\infty \frac{2\tau^2}{a_r^{3/2}}\frac{u}{(1+u^2/a_r)^2}\sin(u\omega)du\frac{1}{1-\cos(\tau\omega)} = \frac{4a_r^{1/2}}{\omega^2}\int_0^\infty \frac{u\sin(u\omega)}{(a_r+u^2)^2}du$$

But

$$\int_0^\infty \frac{u\sin(u\omega)}{(a_r+u^2)^2}du = \frac{\omega\pi e^{-\sqrt{a_r}\omega}}{4\sqrt{a_r}},$$

implying

$$\begin{aligned}
& \lim_{\tau\to 0}\int_0^\infty (g(u+\tau)+g(u-\tau)-2g(u))\sin(u\omega)du\frac{1}{1-\cos(\omega\tau)} \\
= \;& c_r a_r^{3/2}\frac{4a_r^{1/2}}{\omega^2}\frac{\omega\pi e^{-\sqrt{a_r}\omega}}{4\sqrt{a_r}} \\
= \;& \frac{c_r a_r^{3/2}\pi}{\omega}e^{-\sqrt{a_r}\omega},
\end{aligned}$$

after repeatedly applying L'Hopital Rule and tedious calculations. Therefore, the spectral density for the rational quadratic variogram is given by

$$f(\omega) = \frac{c_r a_r^{3/2}}{2}e^{-\sqrt{a_r}\omega}\left(\frac{\omega^2}{1+\omega^2}\right).$$

Proof of Proposition 4.4: For all $x > 0$, we define

$$g(x) = \int_0^x \gamma(u)du, \text{ that is, } g'(x) = \gamma(x).$$

Hence, $g(0) = 0, g(-x) = -g(x)$. We first notice that, for each fixed $\tau > 0$, and so we may assume $u > \tau$ since we take $u \to \infty$,

$$\begin{aligned}
& \lim_{u\to\infty} (g(u+\tau) + g(u-\tau) - 2g(u)) \\
= & \lim_{u\to\infty} \int_0^\tau (\gamma(u+s) - \gamma(u-s))ds \\
= & c_e \lim_{u\to\infty} \int_0^\tau \left(\exp(-(u-s)/a_e) - \exp(-(u+s)/a_e)\right) ds \\
= & c_e \lim_{u\to\infty} \int_0^\tau e^{-u} \left(\exp(s/a_e) - \exp(-s)/a_e)\right) ds = 0.
\end{aligned}$$

Hence,

$$\begin{aligned}
& \int_0^\infty (\gamma(u+\tau) + \gamma(u-\tau) - 2\gamma(u)) \cos(u\omega)du \\
= & \omega \int_0^\infty (g(u+\tau) + g(u-\tau) - 2g(u)) \sin(u\omega)du.
\end{aligned}$$

Now we consider the following limit.

$$\lim_{\tau\to 0} \int_0^\infty (g(u+\tau) + g(u-\tau) - 2g(u)) \sin(u\omega)du \frac{1}{1-\cos(\omega\tau)}.$$

Note that for $x > 0$,

$$\begin{aligned}
g(x) &= \int_0^x \gamma(u)du = \int_0^x (c_e(1 - \exp(-u/a_e)))\, du \\
&= c_0 x - c_e a_e + c_e a_e \exp(-x/a_e).
\end{aligned}$$

We have

$$\begin{aligned}
& g(u+\tau)+g(u-\tau)-2g(u) \\
= \;& ((c_0+c_e)(u+\tau)-c_e a_e + c_e a_e \exp(-(u+\tau)/a_e)) \\
& +((c_0+c_e)(u-\tau)-c_e a_e + c_e a_e \exp(-(u-\tau)/a_e)) \\
& -2((c_0+c_e)u - c_e a_e + c_e a_e \exp(-u/a_e)) \\
= \;& c_e a_e \left(\exp(-(u+\tau)/a_e)+\exp(-(u-\tau)/a_e)-2\exp(-u/a_e)\right) \\
= \;& c_e a_e \exp(-u/a_e)\left(\exp(-\tau/a_e)+\exp(\tau/a_e)-2\right).
\end{aligned}$$

Hence,

$$\begin{aligned}
& \int_0^\infty (g(u+\tau)+g(u-\tau)-2g(u))\sin(u\omega)du \\
= \;& a_e c_e \left(\exp(-\tau/a_e)+\exp(\tau/a_e)-2\right)\int_0^\infty e^{-u/a_e}\sin(u\omega)du \\
= \;& a_e c_e \left(\exp(-\tau/a_e)+\exp(\tau/a_e)-2\right)\frac{\omega}{(1/a_e)^2+\omega^2}.
\end{aligned}$$

Now take the limit $\tau \to 0$, we have

$$\begin{aligned}
& \lim_{\tau\to 0}\int_0^\infty (g(u+\tau)+g(u-\tau)-2g(u))\sin(u\omega)du\frac{1}{1-\cos(\omega\tau)} \\
= \;& a_e c_e \lim_{\tau\to 0}\frac{\exp(-\tau/a_e)+\exp(\tau/a_e)-2}{1-\cos(\omega\tau)}\frac{\omega}{(1/a_e)^2+\omega^2} \\
= \;& a_e c_e \frac{2}{a_e^2\omega^2}\frac{\omega}{(1/a_e)^2+\omega^2} = \frac{a_e c_e}{\omega}\frac{2}{1+a_e^2\omega^2}.
\end{aligned}$$

Hence we have,

$$\begin{aligned} & f(\omega) \\ = & \lim_{\tau\to 0}\left(\frac{1}{2\pi}\left(\int_0^\infty (\gamma(u+\tau)+\gamma(u-\tau)-2\gamma(u))\cos(u\omega)du\right)\right. \\ & \qquad\qquad \left.\times\frac{1}{1-\cos(\tau\omega)}\right)\left(\frac{\omega^2}{1+\omega^2}\right) \\ = & \frac{2}{2\pi}\omega\frac{a_e c_e}{\omega}\frac{1}{1+a_e^2\omega^2}\left(\frac{\omega^2}{1+\omega^2}\right) \\ = & \frac{a_e c_e}{\pi}\frac{1}{1+a_e^2\omega^2}\left(\frac{\omega^2}{1+\omega^2}\right). \end{aligned}$$

Proof of Lemma 4.2. Obviously,

$$\begin{aligned} S &= \sum_{k=3}^{\infty}(\sqrt{k+2}+\sqrt{k-2}-2\sqrt{k})\cos(k\omega) \\ &= \sum_{k=3}^{\infty}((\sqrt{k+2}-\sqrt{k})+(\sqrt{k-2}-\sqrt{k}))\cos(k\omega) \\ &= \sum_{k=3}^{\infty}\left(\frac{2}{\sqrt{k+2}+\sqrt{k}}+\frac{-2}{\sqrt{k-2}+\sqrt{k}}\right)\cos(k\omega) \\ &= 2\cdot\sum_{k=3}^{\infty}\left(\frac{\sqrt{k-2}-\sqrt{k+2}}{(\sqrt{k+2}+\sqrt{k})(\sqrt{k-2}+\sqrt{k})}\right)\cos(k\omega) \\ &= 2\cdot\sum_{k=3}^{\infty}\left(\frac{-4}{(\sqrt{k-2}+\sqrt{k+2})(\sqrt{k+2}+\sqrt{k})(\sqrt{k-2}+\sqrt{k})}\right)\cos(k\omega) \\ &= -8\cdot\sum_{k=3}^{\infty}\left(\frac{1}{(\sqrt{k-2}+\sqrt{k+2})(\sqrt{k+2}+\sqrt{k})(\sqrt{k-2}+\sqrt{k})}\right)\cos(k\omega). \end{aligned}$$

Note that the denominator has $O(k^{3/2})$, and so the above summation $S \sim \sum_{k=3}^{\infty}\frac{\cos(k\omega)}{k^{3/2}}$ is absolutely convergent since

$$\sum_{k=3}^{\infty}\left|\frac{\cos(k\omega)}{k^{3/2}}\right| \le \sum_{k=3}^{\infty}\frac{1}{k^{3/2}} < \infty \implies S < \infty.$$